Proceedings of the I·R·E

JUNE 1941

VOLUME 29 NUMBER 6

Institute of Radio Engineers

5000 NEW DESIGNS

U T C

It is surprising to most people to find out that by far the bulk of U.T.C. production is on special units not normally catalogued. It is impossible to describe all these thousands of special designs as they become available.
The solutions to three typical customers' problems are shown below.

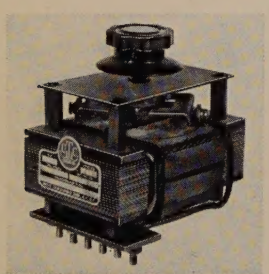

FULL WAVE VARITRAN

● In one full wave rectifier application, our customer was employing a standard varitran with a step-down transformer having a center tapped secondary. The U.T.C. design division simplified this construction by developing a special varitran unit with an insulated secondary and a double contact structure, permitting a continuous variable voltage to be obtained each side of center. The step-down transformer is now entirely eliminated.

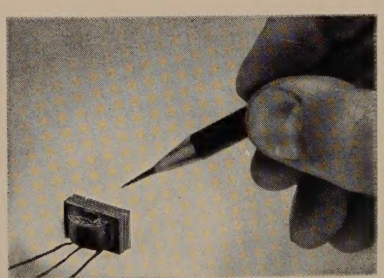

THE SMALLEST

● In one special application the requirements call for the smallest output transformer possible, size and weight being of paramount importance. The design developed by U.T.C. has dimensions only 7/16" square by ¾" high. Almost ten thousand turns are employed in the coil of this unit. Ten of these transformers weigh only three ounces.

600 AMP. VARITRAN

● In bending some types of tubing, it is desirable to heat the tubing to a highly ductile point, thus preventing kinking. A special U.T.C. varitran was developed for this application. This unit combines a standard varitran with a step-down transformer. The output current, for any type of load normally encountered, can be varied continuously from zero to 600 Amps. with direct meter calibration.

MAY WE ASSIST YOU IN YOUR PROBLEMS?

The design ingenuity used in these applications has helped many users in other problems. The cumulative experience acquired in such development makes U.T.C. an ideal source for transformers to specifications.

UNITED TRANSFORMER CORP.

150 VARICK STREET ★ NEW YORK, N. Y.

Proceedings of the I·R·E

Published Monthly by

The Institute of Radio Engineers, Inc.

VOLUME 29 — *June, 1941* — NUMBER 6

Entered as second-class matter October 26, 1927, at the post office at Menasha, Wisconsin, under the Act of February 28, 1925, embodied in Paragraph 4, Section 538 of the Postal Laws and Regulations. Publication office, 450 Ahnaip Street, Menasha, Wisconsin. Editorial and advertising offices, 330 West 42nd St., New York, N. Y. Subscription, $10.00 per year; foreign. $11.00.

THE INSTITUTE OF RADIO ENGINEERS

INCORPORATED

Emporium Section—Summer Seminar—August 1 and 2, 1941

Pacific Coast Convention—Seattle, Washington—August 20, 21, and 22, 1941

SECTIONS

ATLANTA—Chairman, A. W. Shropshire, Secretary, G. M. Howard, 856 St. Charles Ave., N. E., Atlanta, Ga.

BALTIMORE—Chairman, Ferdinand Hamburger, Jr.; Secretary, G. J. Gross, Pennsylvania Water and Power Co., 1611 Lexington Bldg., Baltimore, Md.

BOSTON—Chairman, J. M. Henry; Secretary, R. O. Oberg, Northeastern University, Boston, Mass.

BUENOS AIRES—Chairman, P. J. Noizeux; Secretary, L. C. Simpson, RCA Victor Argentina, Bartolome Mitre, 1961, Buenos Aires, Argentina.

BUFFALO-NIAGARA—Chairman, E. H. Roy; Secretary, Leroy Fiedler, 53 Rosedale Ave., Hamburg, N. Y.

CHICAGO—Chairman, G. I. Martin; Secretary, R. A. Kay, RCA Institutes, Inc., 1154 Merchandise Mart, Chicago, Ill.

CINCINNATI—Chairman, J. M. McDonald; Secretary, W. L. Schwesinger, Crosley Corp., Cincinnati, Ohio.

CLEVELAND—Chairman, C. E. Smith; Secretary, W. G. Hutton, 7314 Dorothy Ave., Parma, Ohio.

CONNECTICUT VALLEY—Chairman, K. A. McLeod; Secretary, W. M. Smith, 250 Main St., Suffield, Conn.

DALLAS-FORT WORTH—Chairman, D. A. Peterson; Secretary, P. C. Barnes, WFAA-WBAP, Grapevine, Tex.

DETROIT—Chairman, M. Cottrell; Secretary, Paul Frincke, WJBK, 6559 Hamilton Ave., Detroit, Mich.

EMPORIUM—Chairman, R. K. Gessford; Secretary, C. W. Reash, Hygrade Sylvania Corp., Emporium, Pa.

INDIANAPOLIS—Chairman, Arthur Curtiss; Secretary, T. N. Rosser, P. R. Mallory & Co., E. Washington St., Indianapolis, Ind.

KANSAS CITY—Chairman, Harner Selvidge; Secretary, G. L. Taylor, Midland Radio School, Power and Light Bldg., Kansas City, Mo.

LOS ANGELES—Chairman, W. W. Lindsay, Jr.; Secretary, C. F. Wolcott, 1609 S. Western Ave., Los Angeles, Calif.

MONTREAL—Chairman, E. A. Laport; Secretary, W. A. Nichols, Canadian Broadcasting Corp., 1012 Keefer Bldg., Montreal, Que.

NEW ORLEANS—Chairman, G. H. Peirce; Secretary, D. W. Bowman, 8327 Sycamore St., New Orleans, La.

PHILADELPHIA—Chairman, C. C. Chambers; Secretary, R. L. Snyder, 103 Franklin Rd., Glassboro, N. J.

PITTSBURGH—Chairman, P. N. Bossart; Secretary, Ralph Overholt, Jr., 7211 Thomas Blvd., Pittsburgh, Pa.

PORTLAND—Chairman, E. R. Meissner; Secretary, L. M. Belleville, 361 N. E. 75th Ave., Portland, Ore.

ROCHESTER—Chairman, H. J. Klumb; Secretary, O. L. Angevine, Jr., Stromberg-Carlson Telephone Manufacturing Co., Rochester, N. Y.

SAN FRANCISCO—Chairman, L. J. Black; Secretary, Karl Spangenberg, Electrical Engineering Dept., Stanford University, Calif.

SEATTLE—Chairman, K. H. Ellerbeck; Secretary, R. J. Gleason, Pacific Alaska Airways, Inc., 3314 White Bldg., Seattle, Wash.

TORONTO—Chairman, R. H. Klingelhoeffer; Secretary, L. C. Simmonds, 301 King St., E., Toronto, Ont.

TWIN CITIES—Chairman, C. A. Culver; Secretary, N. B. Coil, 1664 Thomas St., St. Paul, Minn.

WASHINGTON—Chairman, M. H. Biser; Secretary, C. M. Hunt, WJSV, 817 Earle Bldg., Washington, D. C.

Scott High-Fidelity Receivers*

E. H. SCOTT†, MEMBER, I.R.E.

Summary—*The problem of high-fidelity reception is simplified to some extent because only local-station service is feasible due to the congested condition in the standard broadcast band. However, all of the general receiver problems are encountered in sets designed for both high-fidelity and weak-signal operation. A receiver suitable for both types of service is described here.*

In the design of a high-fidelity receiving system four sections of the system are of primary importance: 1. the loud speaker, 2. the audio amplifier, 3. the intermediate-frequency tuner and second detector, and 4. the radio-frequency tuner. Each of these sections is discussed and their relationship to high-quality performance is considered.

Data applying to certain sections of the receiving system are presented and certain over-all data related to high-fidelity performance are included.

DURING the past few years several high-fidelity receivers designed for operation in only the broadcast band have been introduced by those whose main objective was the production of equipment for listeners interested solely in tone quality. Obviously the scope and appeal of such receivers have been limited; consequently the problems associated with them have been somewhat different than those encountered in sets suitable for short-wave reception as well as high-fidelity broadcast-band performance. In the single-band high-quality receiver the most important consideration is that the radio-frequency sidebands up to a reasonably high audio frequency must be accepted without attenuation and means must be provided for balancing the high- and low-frequency response levels to produce a characteristic form most pleasing to the particular listener for a given program. Sensitivity is relatively unimportant in this special case because usually high fidelity can be obtained only from near-by local stations capable of furnishing a high field-strength level. Selectivity is also of secondary importance, although a rather sharp attenuation beyond the 10-kilocycle sidebands is desirable. Undoubtedly one of the most important elements in such a receiver is the audio amplifier and loud-speaker system, which must supply and handle an electrical power output of at least 15 to 25 watts with very low distortion and must provide audio fidelity at least flat between 30 and 10,000 cycles, preferably with some rise in response below 100 cycles and above 5000 cycles to allow adequate tone control of both the bass and treble regions.

In the Scott receivers the high-fidelity characteristics for the amplitude-modulated broadcast band are maintained and in addition adequate provision is made for the reception of weak signals in this band and in the high-frequency foreign broadcast bands extending up to approximately 23 megacycles. Therefore, both the broadest and the sharpest degrees of selectivity are necessary. Sensitivity levels must be quite high with a good signal-to-noise ratio on weak signals. Image and spurious-signal attenuation must be adequate and in general the features of communication equipment must be combined with the high-fidelity feature to satisfy the requirements of those who are interested in considerably more than "just tone quality."

The chassis of a typical Scott 20-tube receiver is shown in Fig. 1 and a block diagram of the circuit arrangement is shown in Fig. 2. Several of the stages are standard and their functions need not be discussed in detail here. Some of the unusual features are separate automatic radio-frequency gain control, a noise limiter for the reduction of impulse and ignition-noise interference in the high-frequency bands, and a "record-scratch" suppressor employing a circuit similar to that of an automatic tone control to reduce the effects of needle scratch and surface noise from phonograph records. The intermediate-frequency amplifier is somewhat more elaborate than usual for a broadcast receiver and the audio amplifier presents several features found only in high-fidelity receiving equipment. Four stages and 6 tubes are used in the latter to provide high audio sensitivity, high power output, and a degree of audio gain control at the bass and treble frequencies essential for proper tone-control operation. Since there is not sufficient space here to deal with all of the characteristics and circuit arrangements of such a large receiver, the major portion of this paper will deal chiefly with the high-fidelity aspect.

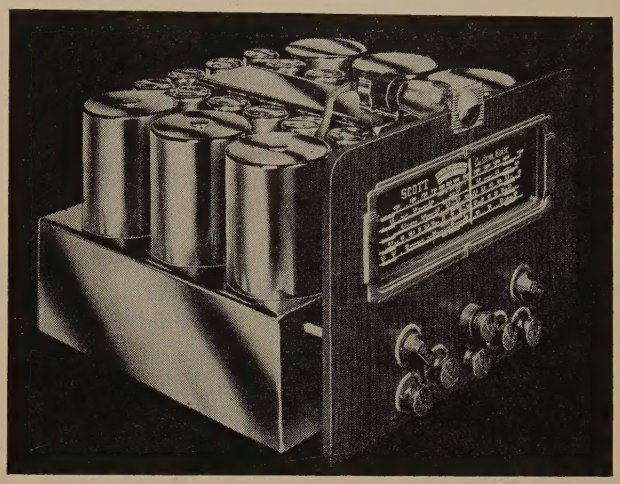

Fig. 1—Tuning chassis of Scott Phantom Deluxe (standard) receiver.

In an analysis of any high-fidelity receiver the following sections of the complete receiving system are of primary importance: 1. the loud speaker, 2. the audio amplifier, 3. the intermediate-frequency tuner and second detector, and 4. the radio-frequency tuner. Since the loud speaker is usually the one point at which all of the efforts toward high fidelity either can be

* Decimal classification: R361.2. The original manuscript of this invited paper was received by the Institute, April 24, 1941.

† President, E. H. Scott Radio Laboratories, Inc., Chicago, Ill.

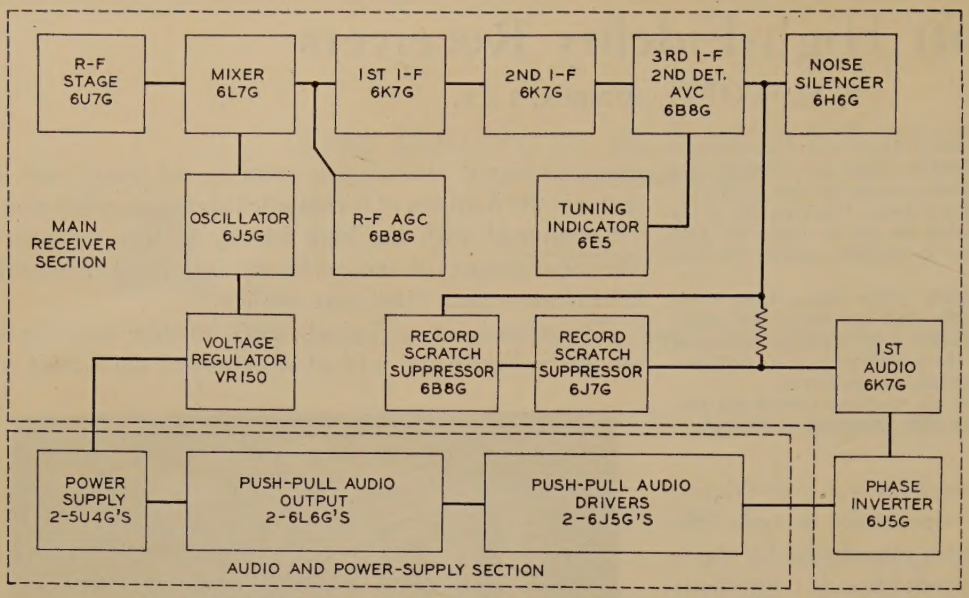

Fig. 2—Block diagram of Scott 20-tube amplitude-modulation receiver.

nullified or enhanced independent of the receiver characteristics, this discussion begins at that point and progresses toward the antenna end of the receiver.

The Loud-Speaker System

While rapid advances have been made recently in the development of single-cone speakers which can reproduce with good fidelity up to 10,000 cycles, this extended high-frequency range is usually obtained at the expense of the bass response, which is affected adversely by the cone materials and other constructions

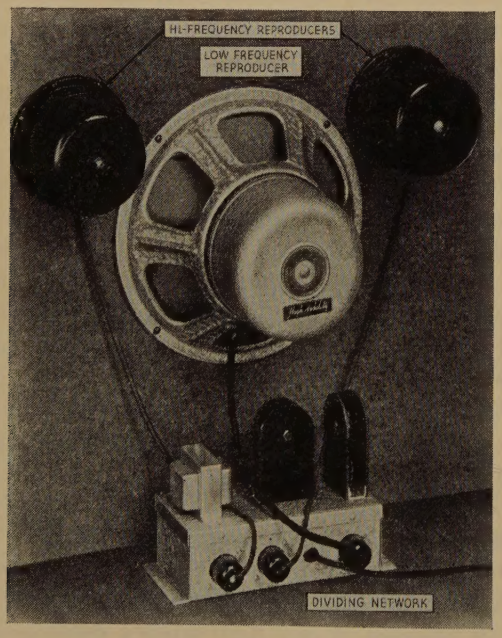

Fig. 3

necessary to extend the high-frequency end. There is little doubt that the most desirable system is one in which the amplifier output is handled by a large cone speaker functioning below 1000 cycles or less and a "power tweeter," high-frequency speaker carrying the output above that point. The separation of the high- and low-frequency energy for the respective speakers is provided by an inductance-capacitance dividing network having a constant input-impedance—frequency characteristic.

Since a practical limitation to this loud speaker is the cost of the high-frequency power unit, only those able to spend large amounts for their receiving systems can afford the elaborate system mentioned here. To provide high-fidelity reproduction in a less expensive form the systems shown in Figs. 3 or 4 may be employed. The high-frequency speakers used

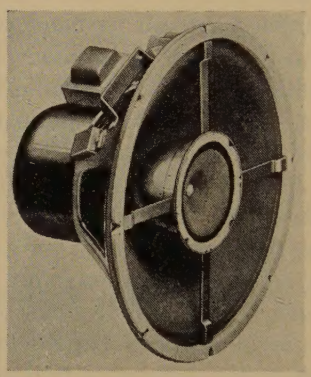

Fig. 4

in these arrangements are somewhat smaller than that mentioned above and, therefore, their power-handling capacity is rather limited. Hence, it is preferable to use two of them in parallel, or where one is used it is preferable to attenuate the high-frequency channel from 3 to 6 decibels to prevent overloading. As a further precaution it is necessary to set the crossover frequency at 4000 cycles or above to limit the amount of power entering the high-frequency units. When these precautions are observed excellent fidelity characteristics may be obtained.

A comparison of the sound-pressure curves for both a single 12-inch speaker with no dividing network and a 3-speaker combination using a 12-inch intermediate-frequency speaker and two 5-inch high-frequency units is shown in Fig. 5. It is interesting to note that we find the characteristic of the single 12-inch speaker to be adequate for amplitude-modulation broadcast programs and shellac-record reproduction provided a suitable degree of audio high-frequency compensation is

provided. In fact, the characteristic of the 3-speaker combination may result in certain unpleasant effects because of the noise generally accompanying any

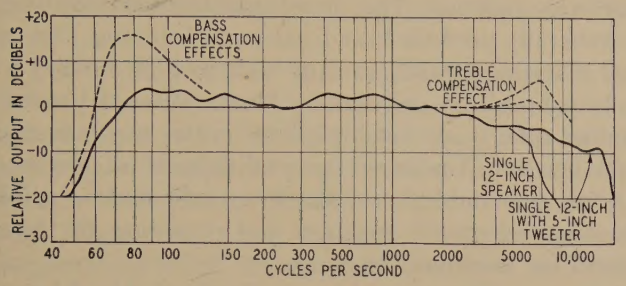

Fig. 5—Sound-pressure data and the effect of audio compensation in the receiver. Measurements were made in an open-back cabinet. This curve is not shown to present the limits of fidelity of a Scott receiver, but rather to present the fidelity for a given set of conditions. They are of the mean-energy type.

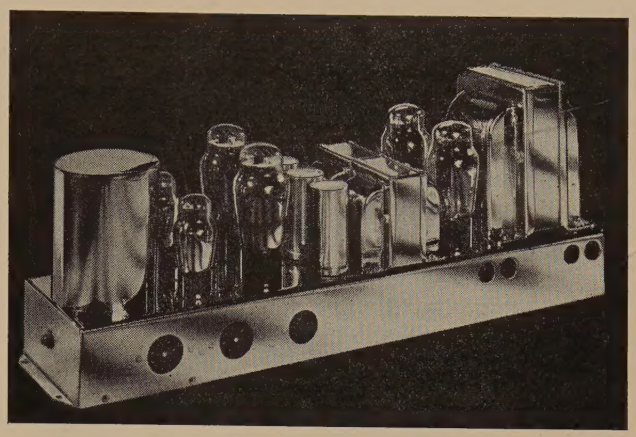

Fig. 6—Power amplifier for new custom-built Scott Phantom Deluxe receiver.

amplitude-modulation programs except those of local origin and the high "scratch" level usually present in the average recording. Hence, in all of the Scott speaker and receiver systems provision is made for automatically switching from the 3-speaker characteristic to that of a single speaker in all ranges, except the frequency-modulation band. When connected for phonograph operation either the 3-speaker or single-speaker system may be used by turning the wave-band switch either to frequency-modulation or to one of the amplitude-modulation ranges, respectively.

The Audio Amplifier

The ability of the audio system to deliver high power output levels with virtual freedom from distortion is a prerequisite for high-fidelity operation. It is well known that the volume range of a large symphony orchestra may extend up to 60 or 70 decibels, thus requiring that the output of the receiver must vary from a few milliwatts to several watts without distortion, if the program is transmitted without volume compression. It is also important that the degree of distortion shall not increase for certain audio frequencies such as the extreme bass or the middle register.

The chassis of the audio amplifier used with the Scott 20-tube amplitude-modulation receiver and the 28-tube frequency-modulation—amplitude-modulation receiver is shown in Fig. 6. The audio and phase-inverter stages are located in the main receiver chassis, while the push-pull driver, the push-pull output stage, and the power supply are located on the power-amplifier chassis. This arrangement minimizes hum pickup by separating the most sensitive section of the amplifier from the main sources of 60- to 120-cycle hum radiation. The heat of the output tubes and rectifiers is also removed from the main receiver chassis by this procedure and the temperature rise is lowered in the region of the oscillator and the radio-frequency and intermediate-frequency tuning components, thus minimizing any tendency toward frequency or tuning drift.

A circuit of the amplifier is shown in Fig. 7. Many of the circuits are self-explanatory. The method of obtaining bass and treble compensation independent of the volume-control setting is that of using a plate load for the first tube, which consists of a 10,000-ohm resistor in series with an iron-core choke shunted by a 0.15-microfarad condenser and an air-core choke shunted by a 2000-micromicrofarad condenser. The effects on audio fidelity due to this arrangement are apparent from the curves of Fig. 8. Bass control is produced by varying the shunting effect on those elements

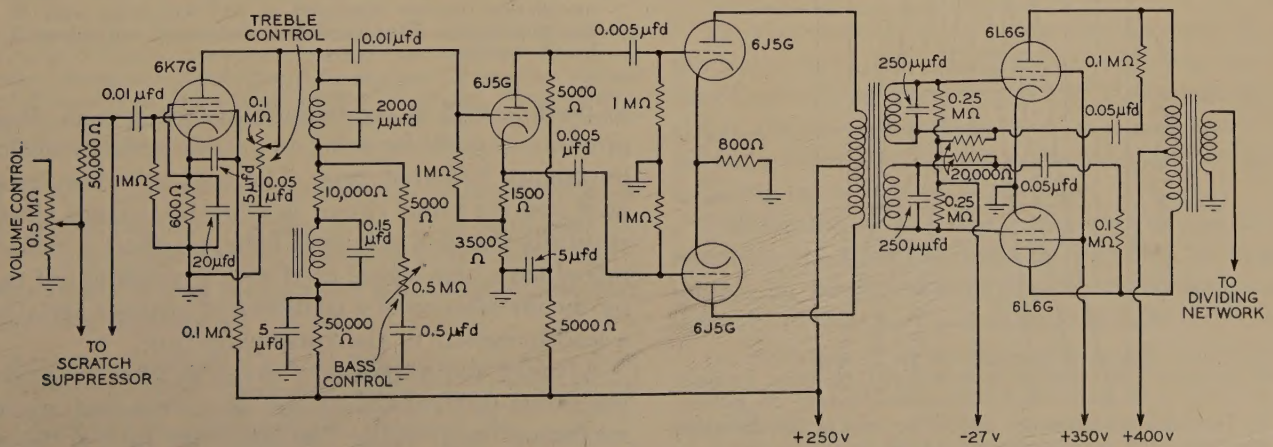

Fig. 7—Audio amplifier circuit.

which contribute to that response, while treble control is accomplished by varying the shunting effect of a condenser across the entire plate-load circuit.

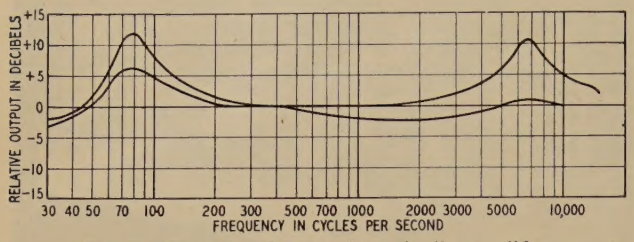

Fig. 8—Electrical fidelity data. Audio amplifier of 20-tube receiver.

It will be noted that a certain amount of negative feedback is present in the inverter stage as well as the audio driver and the output stages. The combined effect of these circuits and the general arrangement of the audio amplifier is reflected in the over-all harmonic distortion data included in the section on over-all performance characteristics. The maximum power output is 40 watts and the undistorted output may be considered to be 25 watts.

The Intermediate-Frequency Tuner and Second Detector

The chief functions of this section are to provide adequate adjacent-channel selectivity with a degree of selectivity variation permitting high-fidelity reception and an adequate gain for proper automatic-volume-control operation. The gain is also such that high sensitivity levels are realized on all of the short-wave bands. The functions of the second detector and the third intermediate-frequency stage are combined in a single 6B8G tube. Alternating-current—direct-current load ratio conditions in the detector circuit are such that low distortion levels are maintained at high modulation percentages.

The selectivity curves for the three positions of variable selectivity on the 20-tube receiver are shown in Fig. 9. The sharp position is usually preferred for

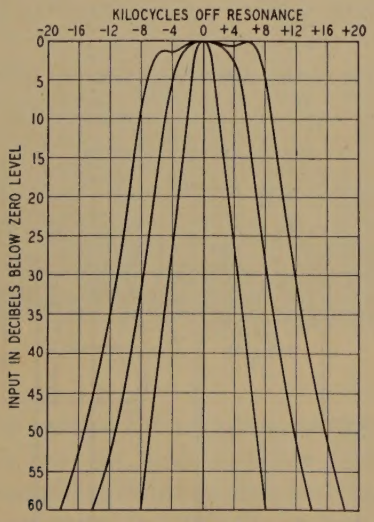

Fig. 9—Intermediate-frequency selectivity data of 20-tube amplitude-modulation receiver measured from modulator grid to signal diodes.

short-wave listening, although the quality of strong signals can be greatly improved without the introduction of appreciable noise by switching into the medium selectivity position. The broad and medium positions are generally used for broadcast-band listening. Strong local stations provide an approach to high fidelity in the broad position and signals of lower strength provide average quality or intelligibility in the medium and sharp position. Under severe conditions of interference or noise reasonable intelligibility can be had by using the sharp-selectivity position and retarding the bass control for minimum response.

Automatic bias control for the first and second intermediate-frequency stages is obtained from the direct-current voltage across the load resistor in the second-detector circuit.

The Radio-Frequency Tuner

This section consists of a tuned radio-frequency stage, converter, separate oscillator, voltage regulator, and a radio-frequency automatic-gain-control stage. On the short-wave bands the circuits of this section contribute maximum sensitivity, as well as the reduction of spurious and image-frequency signals. In addition, in the broadcast band the radio-frequency tuned circuits must be broad enough to pass radio-frequency sidebands up to at least ± 9 kilocycles from the desired carrier if high fidelity is not to be impaired.

Another important consideration is signal-to-noise ratio. If any degree of high fidelity is to be expected, the maximum possible signal level must be delivered

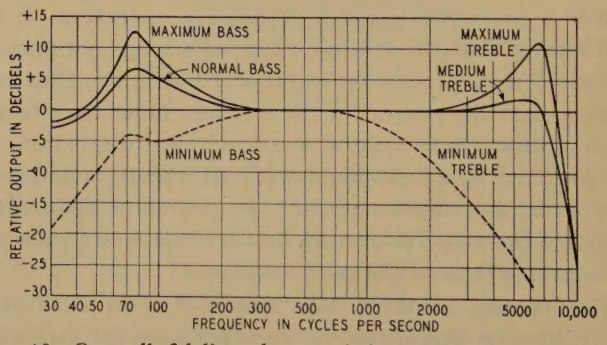

Fig. 10—Over-all fidelity characteristics of 20-tube amplitude-modulation receiver measured at 1000 kilocycles with 30 per cent modulation. The intermediate-frequency switch is set in the broad position.

to the first grid of the radio-frequency system. Hence provision is made for using an outside aerial of the low-impedance balanced type. The lead-in is low impedance and the input circuit is a low-impedance electrostatically shielded primary. Thus, an effort is made to introduce a high signal level with a minimum of noise by the installation of a well-located outdoor aerial and a lead-in system of the low-pickup type.

A tuned radio-frequency stage is used to provide maximum gain ahead of the converter and also for maximum image ratio. The converter tube is the well known 6L7G type which allows oscillator voltage injec-

tion with a minimum of effect upon the oscillator circuit from signal-circuit conditions. The oscillator is a triode whose plate voltage is controlled by a voltage regulator. The design of its circuit and associated components is such that there is negligible frequency drift in all bands.

The radio-frequency automatic-gain-control system serves to provide a delayed automatic-volume-control action on the radio-frequency and mixer tubes and also provides a broader automatic-volume-control characteristic than that of the intermediate-frequency system. Thus, the heavy sideband "splatter" normally encountered when tuning highly selective receivers is considerably reduced.

Over-All Performance Characteristics

In Figs. 10, 11, and 12 the over-all fidelity, sensitivity, and automatic-volume-control characteristics are shown.

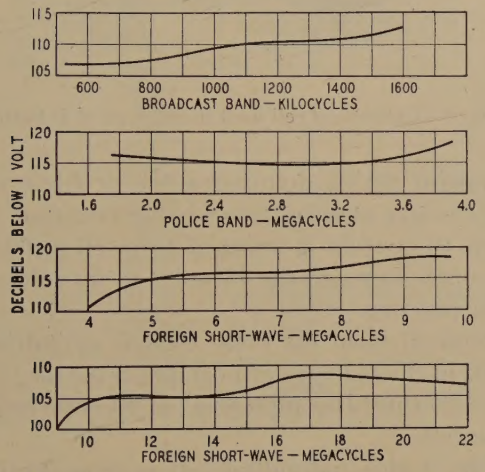

Fig. 11—Over-all sensitivity of 20-tube amplitude-modulation receiver in four frequency ranges.

The following over-all distortion characteristics have been measured with a radio-frequency signal of 5000 microvolts at 1000 kilocycles, 30 per cent modulated at 400 cycles:

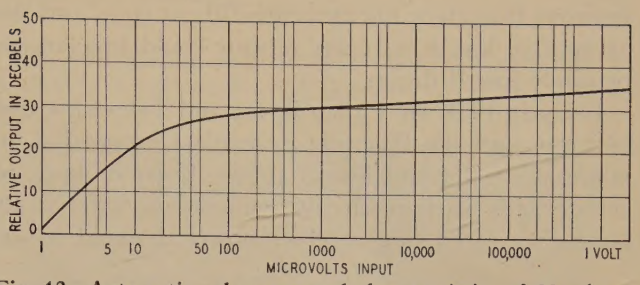

Fig. 12—Automatic-volume-control characteristics of 20-tube receiver measured at 1000 kilocycles with 30 per cent modulation.

TABLE I

Output (Watts)	Harmonic Per Cent		
	2nd	3rd	4th
0.5	1.0	0.5	—
1.0	1.0	0.5	—
5.0	0.5	1.0	—
10.0	0.5	2.0	—
20.0	2.5	2.4	—
25.0	1.2	2.8	1.8
30.0	0.3	3.6	0.6

Also, to show the effects of high percentages of modulation the following measurements were made with an input of 5000 microvolts at 1000 kilocycles, 400-cycle modulation, output, 0.5 watt.

Modulation Per Cent	Harmonic Per Cent		
	2nd	3rd	total
10	1.0	0.5	1.0
30	1.0	0.5	1.0
50	1.0	0.5	1.0
100	0.5	0.75	1.0

Acknowledgment

The author wishes to acknowledge the assistance of Mr. Hobbs of the Scott Radio Laboratories in the preparation of this paper and to acknowledge the use of certain data and photographs furnished by the Jensen Manufacturing Company and the Hazeltine Service Corporation.

Improvements in B-Battery Portability*

H. F. FRENCH†, NONMEMBER, I.R.E.

Summary—*Some marked advances in the reduction of size and weight of B batteries for portable receivers are discussed. By volume savings effected through new design developments, the package size per unit of capacity has been lowered by about 50 per cent. These improvements enhance portability and are reflected in such developments as the personal receiver.*

BATTERY power and battery characteristics are deriving greatly increased importance and interest from the popularity of portable receivers, particularly that of the personal models which recently have been introduced.

The real obstacle to an earlier development of commerically successful portable receivers was the fact that available receiver circuits had a power demand of about 3 watts. Adequate service life at this power level necessitated B batteries which were too heavy and too cumbersome to be readily portable.

The significance of power requirements in battery receivers has been discussed by Temple,[1] in terms of improving power efficiency by better tubes, and by selective overbias. It was shown that the latter might

* Decimal classification: 621.353. Original manuscript received by the Institute, February 14, 1941. Presented, Sixteenth Annual Convention, New York, N. Y., January 9, 1941.

† National Carbon Company, Inc., Cleveland, Ohio.

[1] L. M. Temple, "The importance of power efficiency in battery-operated receivers." Summarized in report of Emporium Section meeting for June 25, 1937, Proc. I.R.E., vol. 25, p. 1098; September, 1937.

improve B-battery life by nearly 70 per cent, and that acceptable levels of power output could involve surprisingly low B drains.

Early in 1938 the Philco Radio and Television Corporation and the Hygrade Sylvania Corporation announced the 1.4-volt line of tubes. These designs, together with various circuit refinements, offered the possibility of cutting receiver power demand to one

Fig. 1—Relative sizes of old and new types of B batteries.

half, or even one third, of its prior value, and portable receivers appeared in considerable quantities in 1939.

The battery industry promptly contributed a large reduction in the size of B batteries, and a description of this development is our present subject.

The magnitude of this reduction in the size of batteries is illustrated in Fig. 1. An old type 45-volt B battery is shown on the left, and its new type replacement on the right. Per unit of capacity the new battery has one half the volume and two thirds the weight of the old battery. These batteries have a suitable capacity for service in the usual portable, and the new smaller type can save upwards of 25 per cent in receiver volume.

Fig. 2 shows a B battery of the new construction, in the size which has contributed vitally to the development of personal receivers. It is a 67.5-volt unit, and its capacity is sufficient for several months' service under normal operating conditions. Its small dimensions are indicated by comparison with the accompanying tubes. Its size per unit of capacity again is about half of that which heretofore has been available. Nevertheless this battery may still amount to 20 per cent of the weight and volume of a typical personal receiver.

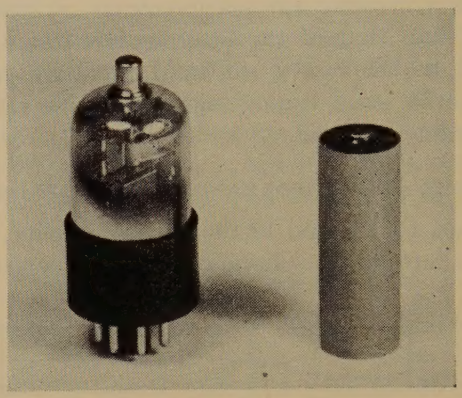

Fig. 3—Cylindrical cell used in old type of B battery.

The point which dominates the problem of minimizing the size of B batteries is the fact that the battery has to contain a series of from 30 to 60 1.5-volt cells in order to reach the 45 volts to 90 volts encountered in practice.

A common form for these cells is cylindrical. The cell used in the old type of portable B battery is shown in Fig. 3. A total B complement of 90 volts requires 60 of these cells.

In Fig. 4 this individual cell is cross-sectioned to show its structure. The shaded area shows items the functions of which are nonchemical; their volume, therefore, does not contribute to cell capacity. The items in this group, and their respective purposes, are as follows: the positive electrode which collects and carries current, the cover which closes the cell against

Fig. 2—New type 67.5-volt B battery for personal receivers.

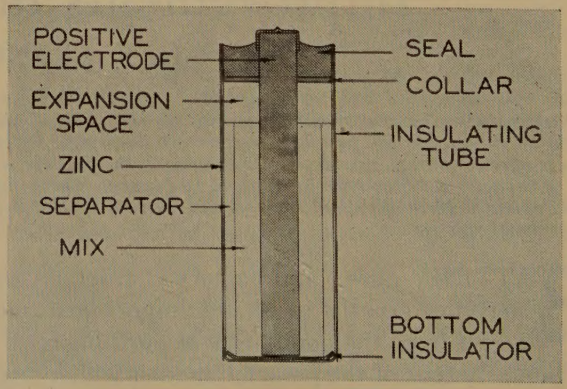

Fig. 4—Structure of cylindrical-type B-battery cell.

leakage, the collar which is a structural member, and a tube and bottom which act as insulators. The

aggregate volume of these nonactive materials is about 30 per cent of the total cell volume.

The remaining 70 per cent of this cell volume comprises items that are dimensioned by the chemical reactions which control the electrical capacity. The zinc is oxidized to furnish electrical energy. The separator contains electrolyte which enters the necessary reactions. The mix also contains electrolyte, together with a depolarizer which becomes chemically reduced to yield further electrical energy. An expansion space accommodates new volume arising from the cell reactions, and it constitutes a space where semiliquid exudates can subside and vent their considerable gas contents out the top of the cell. This gas venting usually occurs through the pores of the carbon electrode.

Of these active materials the mix occupies by far the greatest volume, and it constitutes a convenient meas-

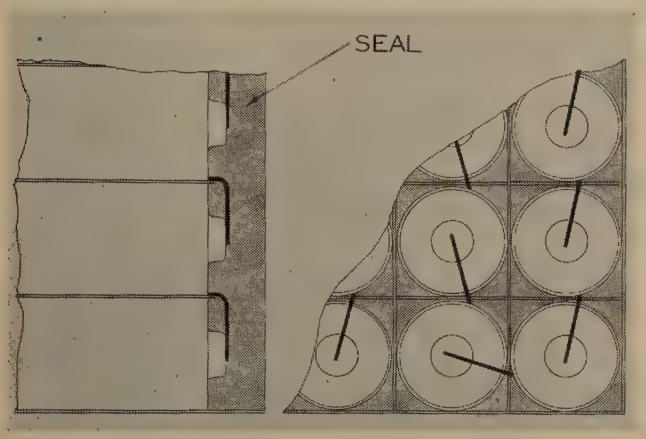

Fig. 5—Space occupied by sealing material and cylindrical cells in old type of B battery.

ure of relative electrical capacity. In the case just examined 35 per cent of the cell volume consists of mix.

Packing these conventional cylindrical cells into a rectangular container was the first and obvious construction for B batteries. When this is done, however, a 35 to 40 per cent relative mix volume in the cells becomes only about 25 per cent of the volume in the total battery. As indicated in Fig. 5, the greatest increase in idle volume is the space left between the circular contours of the cells. The remainder comprises an insulating seal around the intercell connecting wires, assembling clearances, and actual volume of outer-case material.

The first step in improving this condition occurred about 15 years ago, when the flat-cell type of B battery was introduced. In this construction (Fig. 6) the conventional zinc can is replaced by a flat sheet. The usual cylindrical positive electrode becomes a thin carbon layer coated on one side of this sheet. This forms a duplex electrode which serves as the series connection between adjacent cells, the separator of one cell contacting the zinc, while the mix of the next cell contacts the carbon layer.

The assembling of 15 of these flat cells in series, to form a 22.5-volt section of B battery, is described in

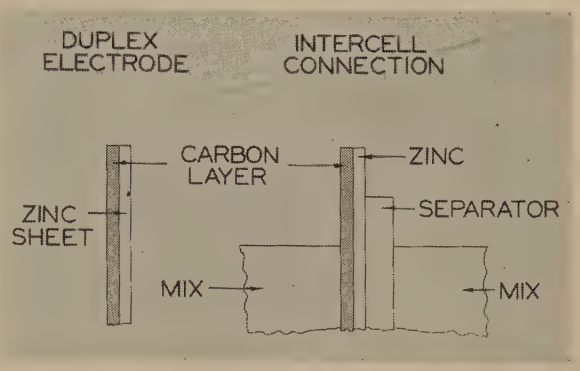

Fig. 6—Elements of flat-cell type of B battery.

Fig. 7. The elements start with a plain negative zinc, followed by a separator and a mix cake. A duplex electrode completes the first cell, and starts the second. A separator follows, and the established order of arrangement continues, until the addition of a duplex electrode completes the 15th cell and serves as the positive terminal for the series. The stack is placed under pressure through the agency of fiber members at each end, and tied with adhesive paper tape.

The mix cake carries two features. Depressions molded into the mix constitute the expansion space, while a carbon rod from each cake serves as a gas vent.

The assembly is finally completed in a container by the introduction of a sealing material, which fills the space peripheral to the mix cakes, and which adheres to the exposed edges of the duplex electrodes.

This construction has various advantages in simplicity and output.[2] Its relative mix content is higher, and its service capacity per unit of volume is about 25

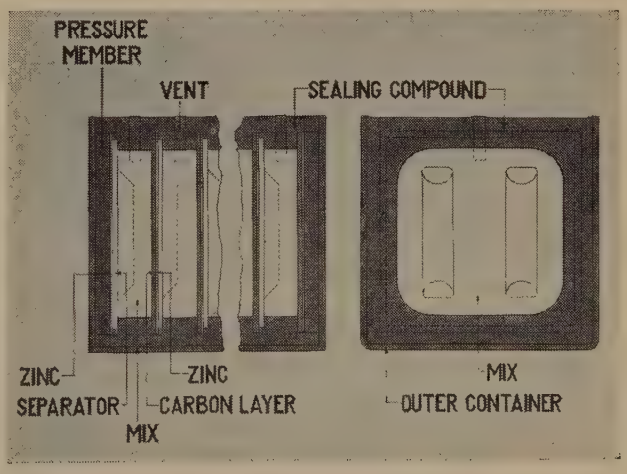

Fig. 7—Structure of flat-cell type of B battery.

per cent greater than in batteries assembled from cylindrical cells. It still carries, however, considerable

[2] A. Karl Huntley, "A radio 'B' battery of flat type construction," *Trans. Electrochem. Soc.*, vol. 68, pp. 219–229; 1935.

proportions of idle volume, chiefly concentrated in the peripheral sealing material. In the example illustrated the mix volume of the cell would be increased by about 60 per cent if the mix cake could be extended to the edges of the duplex electrode. Furthermore these sealing losses are proportionately greater as the battery size decreases, since practically constant sealing margins must be maintained. This fact has prevented advantageous extension of this construction to batteries sufficiently small for the portable field.

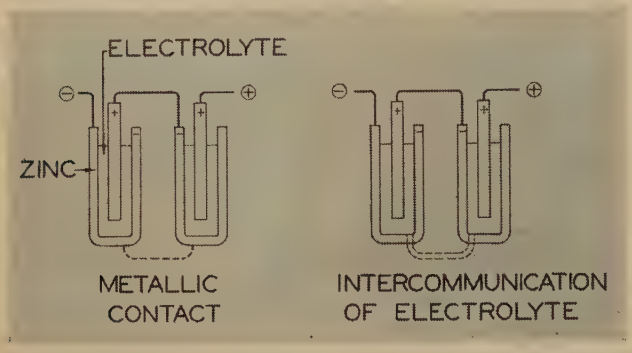

Fig. 8—Short-circuiting of B-battery cells by electrolyte intercommunication.

A conversion of this seal volume to mix is clearly the best possibility for further improvements in volumetric efficiency, and the fundamental consideration at this point is the isolation of the electrolyte. If the electrolyte from different cells in a series-connected group intercommunicates, it constitutes a short circuit. This behavior is analogous to short-circuiting by metallic contact between cells.

The two cases are diagrammed in Fig. 8. In the first pair the downstream cell is short-circuited by a metallic connection between the zinc elements. In the second pair the two electrolytes intercommunicate through leakage. This forms a short circuit consisting of the positive element of the downstream cell, the normal intercell series connection, the negative element of the upstream cell, and the electrolyte which, by intercommunication, has become common to the two cells.

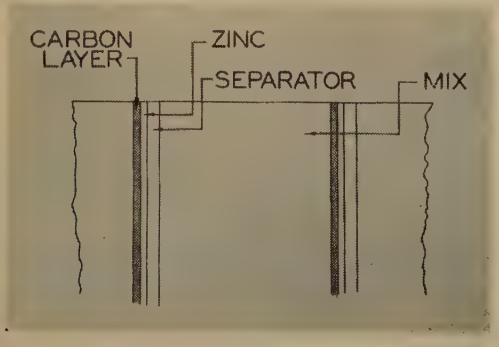

Fig. 9—Elements of flat-cell type of B battery.

The necessity for rigid confinement of the electrolyte to individual cells is the major problem in attempting to extend the mix cake to the edges of the electrode in flat-cell batteries as shown in Fig. 9. Both the separator and the mix contain electrolyte, and only the duplex plates, having a thickness of perhaps 1/32 of an inch or less, are nonabsorbent.

The problem was solved by the application of thin rubber or plastic wrappings around the edges of individual cell groups, as indicated in Fig. 10. The wrapping is cemented to the face of the carbon layer, extends around the remainder of the cell, and its overhang on the back is maintained in pressure contact with the next wrapping.

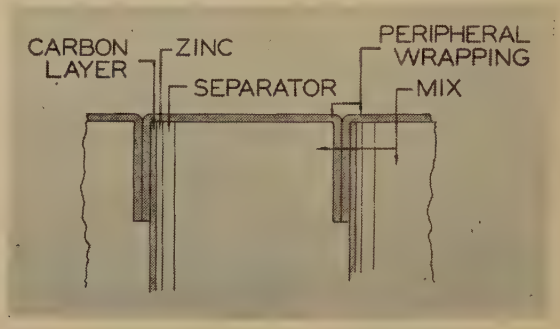

Fig. 10—Cell wrappings in new type of B-battery construction.

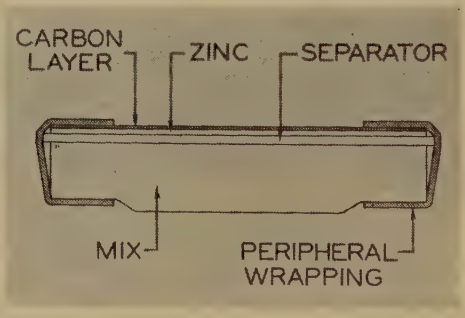

Fig. 11—Individual cell of new wrapped type.

Fig. 11 shows the design of an individual cell which embodies the new construction. It is seen that the major part of the mix cake extends to the full area of the duplex electrode, while on the back the cake protrudes through the wrapping to make contact with the

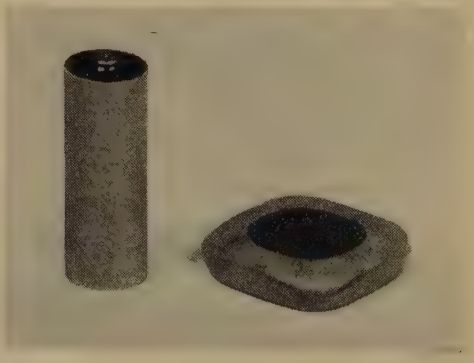

Fig. 12—Comparison between cylindrical and new wrapped type of flat cell.

duplex electrode of the adjacent cell. The separator is slightly extended to insure adequate partition between the mix and the zinc.

Fig. 12 is a photograph of this cell in comparison with a cylindrical cell of similar capacity.

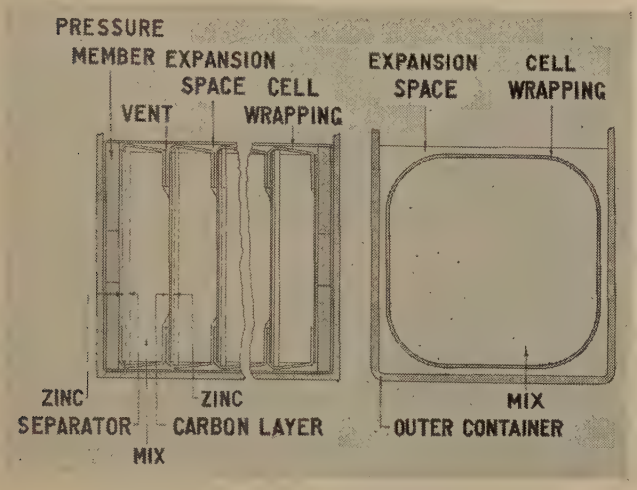

Fig. 13—Structure of wrapped-cell type of B battery.

An assembly constructed from this new type of cell is diagrammed in Fig. 13. The desired number of cells is stacked, a duplex electrode added to complete the last cell and to act as the positive terminal. The stack is tied under sufficient pressure to bring adjacent cakes and electrodes into contact, and to seat the faces of the wrappings. The expansion space is afforded by the elasticity of the wrapping material, and it is efficiently located around the edge, where it occupies practically no more room than is necessary for installing the assemblies in an outer container. No seal is used around the assemblies, but they are dipped in molten wax to prevent moisture loss through the pressure joints between cells. Since the dipping bath is hot, escape of expanded air from the cells maintains a sufficient number of minute openings at the joints to serve as subsequent gas vents.

The relative mix volume in a completed battery is about 60 per cent higher than in the old type of flat-cell battery previously described, and twice as great as in a cylindrical-cell battery of similar size.

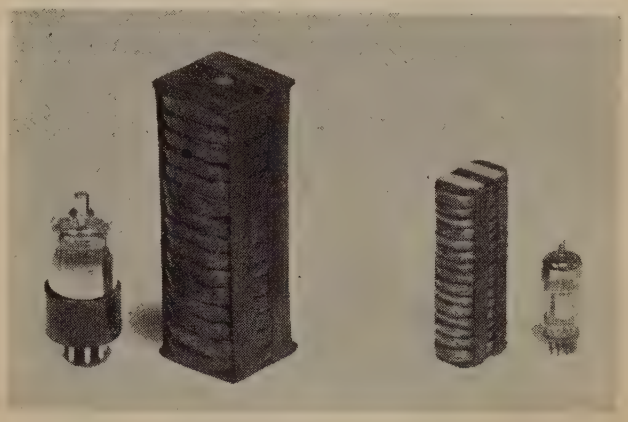

Fig. 14—Typical assemblies of the wrapped-cell type of B-battery construction.

Fig. 14 is a photograph of typical completed assemblies of this new construction. Four units of the size shown on the left are installed in outer containers to make two 45-volt B batteries of the type used in the 90-volt complement of ordinary portables. Three assemblies of the size shown on the right compose a 67.5-volt B battery of the type used for personal receivers.

New Designs of Television Control-Room Equipment*

J. D. SCHANTZ†, ASSOCIATE, I.R.E.

Summary—*This paper deals with what are believed to be novel design and development conceptions which have led to the construction of television control-room equipment for commercial use. Both mechanical and electrical design features of the equipment are considered, and its performance is briefly described.*

Introduction

MODERN television-studio technique places rather stringent demands on the facilities of the associated control room. The equipment described in this paper constitutes an attempt to satisfy these demands. To this end, flexibility and accessibility were stressed in its design. In the following description of this equipment, the numerous features which make for flexibility and accessibility will be considered.

* Decimal classification: R583. Original manuscript received by the Institute, January 27, 1941; revised manuscript received, April 20, 1941. Presented, Sixteenth Annual Convention, New York, N. Y., January 10, 1941.

† Farnsworth Television & Radio Corporation, Fort Wayne, Ind.

General Considerations

The control-room equipment is separated physically into two major parts; namely, the console or control operator's desk and the equipment racks. In accordance with the modern trend, both units have been styled to provide eye appeal, without any sacrifice of flexibility, convenience, or performance.

In keeping with the central theme of flexibility, the console is so designed that it can be used to direct the operation of one to four cameras in an associated

studio, or at other pickup locations. This flexibility is achieved by equipping the console with two picture monitors and two associated cathode-ray oscilloscopes, which can be seen in Fig. 1 where the console is pictured in operating position with the mirrored lid raised.

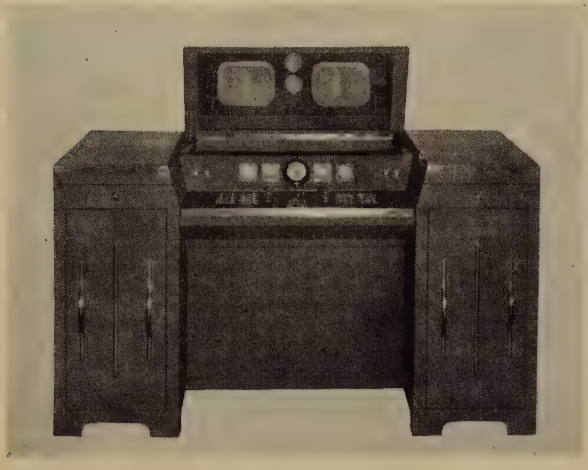

Fig. 1—Console in operating position.

In addition to the two monitors and oscilloscopes, the console also contains the mixing amplifier for injecting suitable synchronizing signals, the fading amplifier and controls, the line amplifier which supplies the composite video signal to the co-axial line leading to the transmitter, and shading-signal generators which provide the necessary shading signals for mosaic-type camera pickup tubes.

The cabinets housing the rack equipment also emphasize the motive of flexibility, Fig. 2. They can be

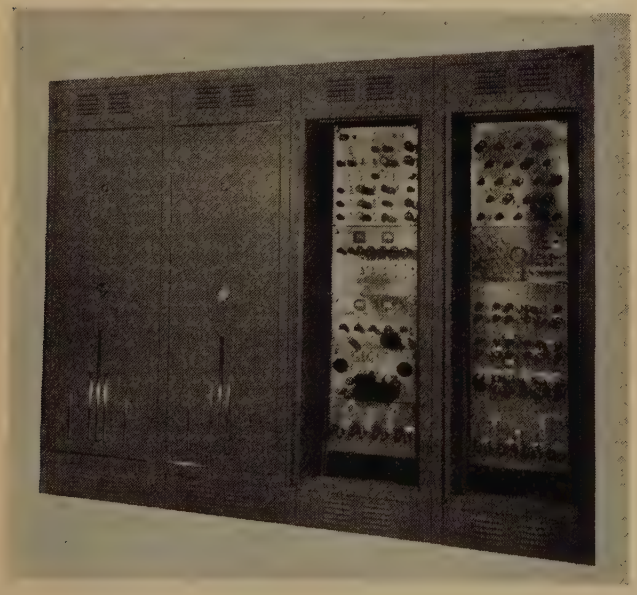

Fig. 2—Cabinets housing rack equipment.

utilized in single units or can be arranged in a row of two or more cabinets so assembled as to give the appearance of a single structure. Thus, control equipment for a television studio of any degree of complexity can be housed by the simple addition of individual racks in the associated cabinets. One cabinet unit serves to house the master timer and synchronizing- and blanking-signal generator equipment with its associated power supplies. Another cabinet unit provides adequate space for the power supplies of the console and for the audio amplifiers for a single studio. One camera channel requires the rack space contained in a single cabinet unit for its associated electrical circuits and power supplies.

Mechanical Design

A. Cabinets and Racks

Mechanical construction of the racks is such as to provide a maximum of serviceability. The racks are patterned after standard relay racks insofar as spacing of the channels and the drilling and tapping of the holes in them is concerned. The enclosing cabinets are

Fig. 3—Individual chassis (closed position).

of formed sheet steel finished on the outside in a grey wrinkle finish with a chrome trim. The front of the cabinet contains a large door, which is somewhat wider than a standard relay rack, and which extends almost the entire length of the cabinet. The door catch is released by turning a recessed handle located in the center of the door. It is opened by swinging it out to a right-angle position, after which it may be slid back into the cabinet itself so as to provide maximum accessibility to the equipment housed in the cabinet. The chassis can be removed from the cabinets through a large rear door.

Ventilation is provided by louvre panels at the top and bottom of the front door, and by louvres punched in the top and bottom of the rear door. The side panels likewise are provided with louvres at the top and bottom. The top of each cabinet is fitted with panels of expanded metal under which dust deflectors are placed. Exhaust fans are provided at the top of each cabinet to aid in ventilation.

The individual chassis are of unique mechanical design which provides a maximum of accessibility for servicing and a chimney structure, which serves as an additional aid in proper ventilation when the several units are mounted one above the other in the rack. Power supplies and filters are mounted on the rear panel while active circuits are located on the hinged front panel (Fig. 3). Tubes may be removed from the front when the panel is closed. When the front panel is opened and dropped to a horizontal position, all of the circuit components and the tube-socket connections are accessible for servicing or adjustment. The front panel may be opened while the equipment is in operation without in any way disturbing its performance (Fig. 4).

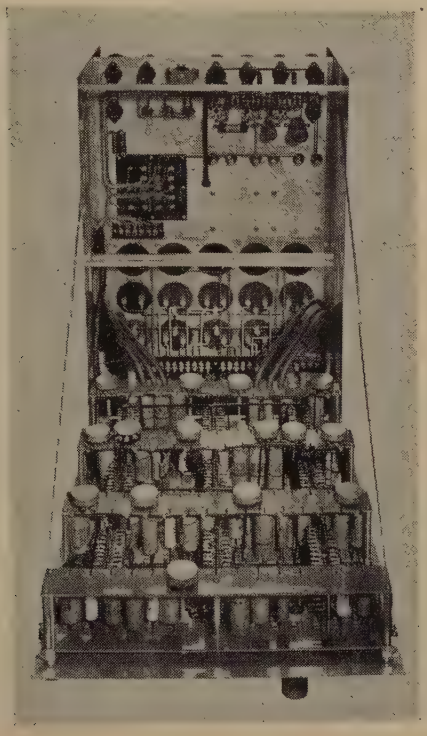

Fig. 4—Open chassis showing details of construction.

B. Console

The console is designed to provide maximum accessibility and ease in operation by an operator seated in a comfortable position before it (Fig. 1). To this end, the normal operating controls are placed on a horizontal panel slightly lower than normal desk height. The control panel is hinged so that it may be raised to provide accessibility to the equipment mounted underneath it (Fig. 5). The images on the monitor tubes are viewed in a mirror placed inside a hinged lid, which is adjustable by a touch, to provide for different eye levels. The monitor tubes, the oscilloscope tubes, and the associated scanning circuits and video amplifiers are all located in the central portion of the console and constitute a complete unit which is connected to the other equipment in the console by means of flexible shielded leads. This complete unit weighs approximately 185 pounds. In order to provide for ease of servicing, it is placed on a motor-driven elevator

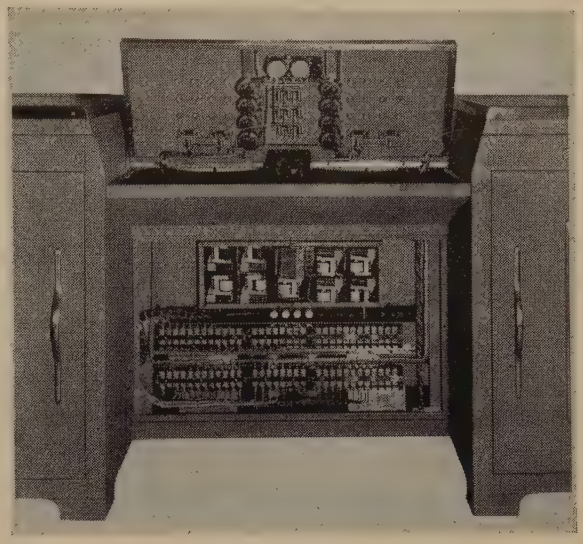

Fig. 5—Terminal wiring, relay panel, and control details of console.

(Fig. 6). Thus it can be raised out of its well and tipped forward for convenient servicing, without moving the console as a whole, and with a minimum of effort (Fig. 7). The elevator is controlled by means of a push-button switch located on the instrument panel. An interlock is provided on the mirrored lid so that the elevator cannot be operated until the lid is raised to a vertical position. Another interlock on the lid cuts off all power to the console when the lid is closed.

On each side of the operator are large drawers. The drawer on the left houses the mixing amplifier, in which the synchronizing signal is mixed with the video signal, and the fading and line amplifiers. The right-

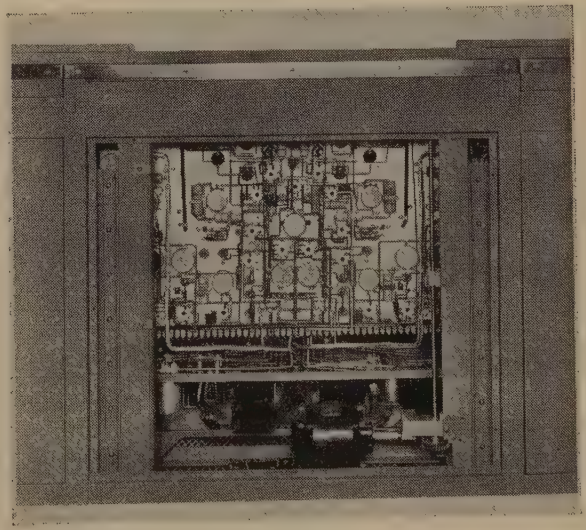

Fig. 6—Rear view of console showing elevator arrangement.

hand drawer provides space for shading-signal-generating equipment used in the adjustment of the signal produced by a mosaic-type camera tube. The top

panels above these drawers are hinged to provide further accessibility to the equipment located in the console. Access to the terminal strips and to the relays

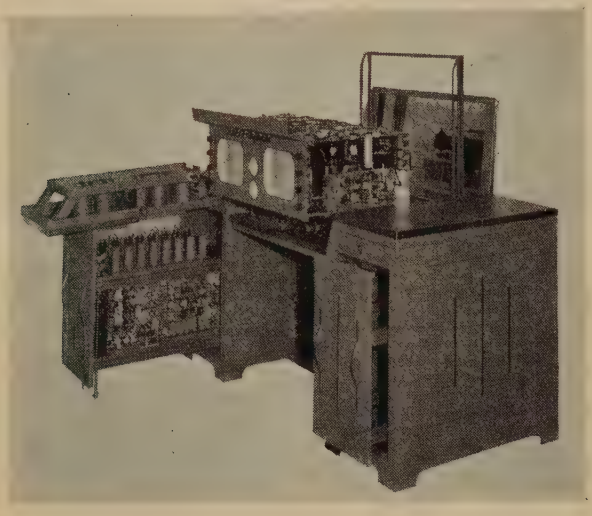

Fig. 7—Console opened for servicing.

contained in the console is provided by removing the front panel of the console desk.

Electrical Design

A. Master Timer and Synchronizing-Pulse-Generating Equipment

Since this unit of equipment is common to a studio control room of any degree of complexity, its design will be considered first. The equipment is divided into four component units, each mounted on a separate chassis.

The uppermost chassis in the rack contains the master timing generator (Fig. 2). It contains 22 receiving-type vacuum tubes which serve variously as oscillators, frequency dividers, pulse generators, clippers, and amplifier and buffer stages.

The circuit arrangement of the timing generator (Fig. 8), is the following: A sine-wave oscillator of conventional design is tuned to operate at a frequency equal to twice the line-scanning frequency, i.e., at 26,460 cycles per second. (The equipment here described was designed to operate according to the system of standards suggested by the Radio Manufacturers Association.) Operating through a suitable buffer tube, this oscillator drives a frequency divider which operates at one third of the synchronizing frequency. Successive frequency-dividing stages step down the frequency in the ratio 7, 7, 3, providing a final frequency of approximately 60 cycles per second. The pulses generated by the final frequency-dividing stage are supplied to a circuit which compares their phase relation to the 60-cycle line voltage. The output of the phase comparator circuit is integrated, or filtered, to provide a varying direct voltage that varies in accordance with the phase difference between the 60-cycle pulse and the 60-cycle line voltage. This varying direct voltage is applied as a grid bias to an automatic-frequency-control tube, the plate circuit of which provides a simulated capacitance across the tuned circuit of the master sine-wave oscillator. The phase-comparing and automatic-frequency-control circuits provide a positive tie between the frequency of the timing generator and that of the 60-cycle line.

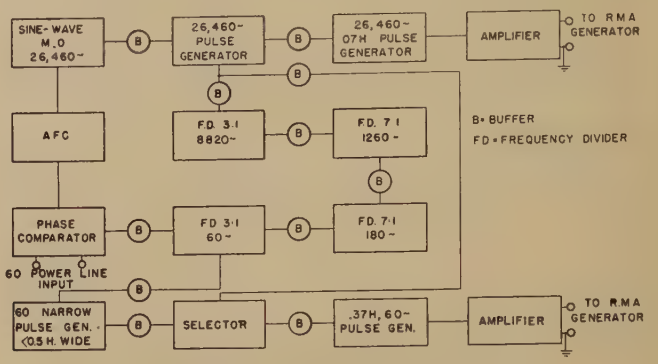

Fig. 8—Functional diagram of timing generator.

The frequency-dividing circuits are variations of the well-known Abraham-Bloch multivibrator circuit which has frequently been used in frequency-dividing apparatus. They differ in one important respect from their prototype, namely that they are stable and will not relax or oscillate except under the stimulus of an externally applied impulse. These circuits have been found to be extremely stable and reliable for this type of operation. They have been operated at dividing ratios greater than 20:1, though naturally greater stability is realized at the lower dividing ratios.

The master timing generator provides two series of electrical impulses at its output terminals. One of these is a series of impulses occurring at the rate of 26,460 per second. Each impulse has a duration of $0.07H$; that is, 7 per cent of the time required to scan one line. This series of impulses synchronizes all of the high-frequency generators in the synchronizing and blanking-pulse-generating unit.

The other series of pulses, provided at the output of the timing generator, is a series occurring at the rate of 60 per second. The width of each impulse is less than $0.5H$. These 60-cycle pulses are very accurately timed since they are initiated by a series of master 60-cycle pulses, each of which is one of the master 26,460-cycle pulses appearing at the high-frequency output terminal. This is accomplished by means of a pulse selection circuit utilizing a pentode.

B. Cathode-Ray Oscilloscope for Timing Rack

Immediately below the master timing generator in the timing-equipment rack, appears an oscilloscope for observing the rates, shapes, and phase relations of the various impulses generated by the timing generator and the synchronizing and blanking-pulse generator. In nearly all respects it is a conventional cathode-ray

oscilloscope employing the well-known sweep and accelerating circuits and amplifiers. However, it provides several additional features which make it more useful for the purpose which it serves.

C. Synchronizing and Blanking-Pulse Generator

Directly below the special oscilloscope in the timing rack is the chassis which houses the synchronizing and blanking-pulse generator (Fig. 9). In order to provide the intricate series of signals specified in the proposed Radio Manufacturers Association standards for 441-line, 60-field, 30-frame television images this unit comprises a total of 34 tubes and associated circuits. The incoming 0.07H, 26,460-cycle pulses from the timing generator are fed to a series of amplifier stages which serve to isolate the succeeding circuits from the input as well as to increase the magnitude of the incoming pulses. Several pulse generators are synchronized by the incoming pulses. They produce the following series of 26,460-cycle pulses:

(1) Delay pulses, 0.06H wide.
(2) Master synchronizing pulses, 0.08H wide.
(3) Equalizing pulses, 0.04H wide.

The first-named pulses are synchronized on the leading edge of the 0.07H pulses; the other two, on the trailing edge. The 0.07H pulses are also used as the serrations in the field-synchronizing pulse.

The line-blanking pulses are 0.15H wide. They occur at the rate of 13,230 per second and are synchronized on the trailing edge of the 0.06H pulse. These blanking pulses are also used to select alternate 0.08H pulses for use as line-synchronizing pulses. The difference between 0.06H and 0.07H, namely 1 per cent of H, is the "front porch" of the pedestal. The timing of the line-synchronizing pulses is extremely accurate because of the selection of alternate 26-kilocycle pulses.

The series of narrow 60-cycle pulses supplied by the master timing generator also synchronizes a number of different pulse generators. These pulse generators provide the following pulses, all occurring at the rate of 60 per second:

(1) Field-blanking pulses, variable in width from 0.08 to 0.12V (V is the duration of one field).
(2) Keying pulses, 9.4H wide.
(3) Keying pulses, 3.2H wide.

Another series of pulses, each 3H wide, and synchronized on the trailing edge of the 3.2H pulses, are also generated. These pulses, together with the 9.4H pulses and 3.2H pulses, are used to key in the equalizing and serration pulses, forming the field-frequency synchronizing pulses of the Radio Manufacturers Association signal. A series of pulses each approximately 12H wide, used for controlling the field-scanning generators in the local equipment, are synchronized on the trailing edge of the 3.2H pulses. (Line-frequency synchronizing pulses are also brought out separately to synchronize local equipment.) The field-frequency blanking pulses are combined with the line-frequency blanking pulses to form the mixed blanking pulses specified by the Radio Manufacturers Association standards.

The pulse generators utilized in the synchronizing and blanking-pulse generator are also variations of

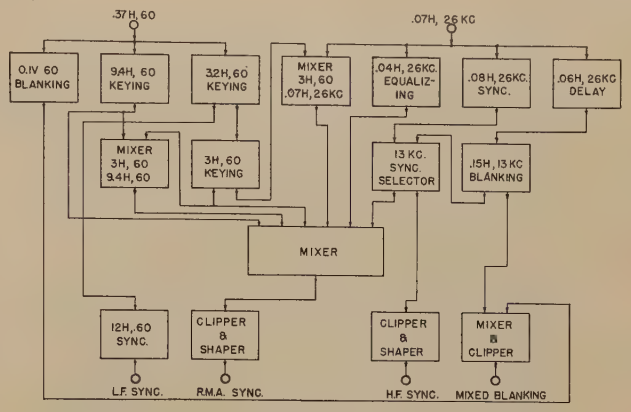

Fig. 9—Functional diagram of synchronizing and blanking-pulse generator.

the familiar Abraham-Bloch multivibrator mentioned previously. These generators are ideally suited to the task of generating the components of the composite Radio Manufacturers Association synchronizing signal because the phase and width of the output of the generator is very readily controlled and because they possess the desirable property of stability.

D. Pulse Line Amplifiers

The lowermost chassis in the timing rack contains four identical amplifiers which amplify the pulses supplied by the synchronizing and blanking-pulse generator and apply them to low-impedance coaxial lines. The pulses are negative in polarity and have an amplitude of approximately 5 volts.

Dissector Camera Channel

A. Rack Video Amplifier

The uppermost chassis in the cabinet housing the camera equipment contains a video amplifier. It receives a video signal having a peak amplitude of 50 millivolts from the camera preamplifier. The polarity of this signal is negative. In addition to providing amplification of the video signal, means are also provided for gamma correction, pedestal insertion, and reestablishment of the background level at the grid of the cathode-follower output stage. Gamma correction and gain are controlled from the console through the medium of motor drives.

B. Line-Frequency Camera Scanning Generator

The chassis immediately below the intermediate amplifier contains the line-frequency camera scanning generator. All of the scanning generators employed in this line of studio-control-room equipment are of the driven type; that is, no oscillators are contained in the

generators themselves. Instead the synchronizing pulses are amplified and then shaped to provide the correct scanning current wave for the linear scanning of the camera and monitor tubes. This type of scanning generator has been employed to insure the greatest possible accuracy of interlace.

C. Field-Frequency Camera Scanning Generator

The principle of operation of this circuit is identical with that of the line-frequency, camera scanning generator. It differs only insofar as the frequency of operation and the impedance of the scanning coils which it energizes differ from the previous case.

D. Camera High-Voltage and Focus Supply

Three separate direct-current power supplies are located on one chassis located below the field-frequency camera scanning generator. On the front panel are located the several controls and an electronically regulated power supply which furnishes the direct current used in the camera focusing-coil system. The focusing current is controlled by a motor-driven rheostat in series with the coil. The full-wave, single-phase rectifier circuits located on the rear panel supply the high voltages (up to 1000 volts) required to accelerate the electron stream and to operate the multiplier in a dissector-type camera. The output voltages of these rectifiers are continuously variable by means of Variacs mounted on the front panel. The output voltage of these rectifiers is rendered independent of line-voltage variations by means of a regulating transformer housed in the bottom of the cabinet.

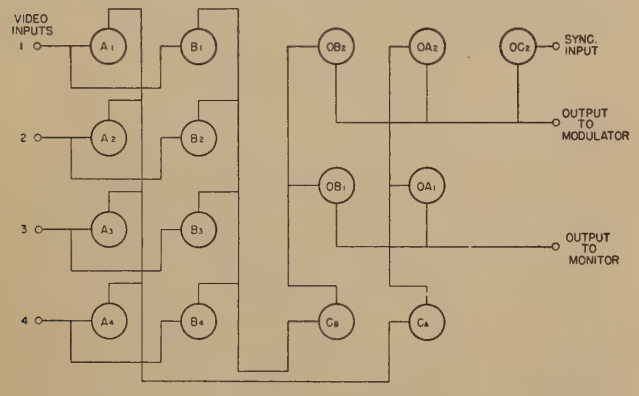

Fig. 10—Functional diagram of mixing and line amplifier.

The Console

A. Mixing and Line Amplifier

The video signal, after amplification in the rack video amplifier, is applied to the input of the mixing and line amplifier located in the left-hand drawer of the console. This amplifier has four separate inputs to receive the signal generated by four different cameras (Fig. 10). Each input is connected to the grids of two separate amplifier tubes. Thus, the signal from channel No. 1 is applied to the grids of tubes A_1 and B_1. Likewise the signal from channel No. 2 is applied to the grids of tubes A_2 and B_2, etc. The plates of tubes A_1, A_2, A_3, and A_4 are connected in parallel to a common load impedance. Similarly, tubes B_1, B_2, B_3, and B_4 supply a common load impedance. Each of the eight tubes just enumerated, has a separate gain control which permits its gain to be adjusted from zero to a maximum value. The output of the A group of tubes is applied to the grid of an amplifier C_A. In similar fashion, the signal from the B group of tubes is applied to amplifier C_B.

The signal after amplification by tube C_A is then applied to the grids of two separate cathode-follower output tubes which we may designate as OA_1 and OA_2. Likewise, the amplified signal from C_B is applied separately to the grids of output tubes OB_1 and OB_2. The cathodes of OA_1 and OB_1 are connected in parallel and constitute one output which supplies a video signal to the stand-by monitor while the cathodes of OA_2 and OB_2 connected in parallel deliver the video signal to the transmitter line and to the other monitor. The synchronizing signal is added to this output by means of an additional tube in parallel with OA_2 and OB_2. Direct-current reinsertion is provided at the grids of each of the four video output tubes.

Fading is accomplished in the following manner: The grid returns of OA_1 and OB_2 are brought to one variable contact on the fader potentiometer while the grid returns of OA_2 and OB_1 are brought to the other. Mechanically, the potentiometer is so arranged that when the fader knob is rotated the bias on OA_1 and OB_2 is increased while that on OA_2 and OB_1 is decreased, and vice versa. Thus it is possible to observe the signal produced by any camera on either monitor, and if desirable the outputs from two or more cameras can be blended for additional effects. All gain controls and the fading control are direct-current devices and may accordingly be located remote from the circuits which they control.

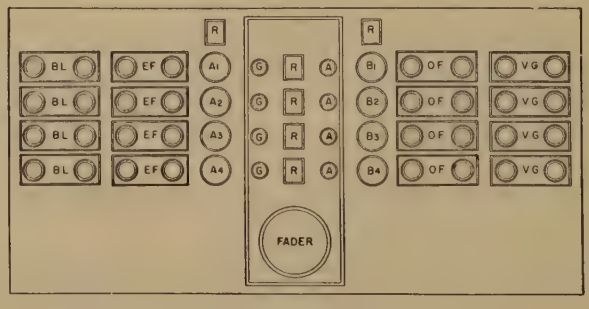

Fig. 11—Layout of control panel on console.

Associated with the gain controls and the fading control on the console, is a system of indicator lights which reveal the status of each camera channel. Fig. 11 is a diagram of the arrangement of the several lights and gain controls and the fader knob on the control panel of the console. The four rows of knobs and lights are the controls and indicators for the four different

channels. The knobs in the left-hand column are the gain controls for the amplifiers in the *A* group of the previous diagram, while the knobs on the right are the gain controls for the amplifiers in the *B* group. The larger knob below the column of lights is the fader control.

The operation of the control knobs and indicator lights can be summarized as follows: Red lights indicate that the control in the row or column containing them may not be touched because the circuits associated with the controls are "on the air." Amber lights indicate that the associated circuits are in a stand-by condition, while green lights show that the associated channels are not being used. These indicator lights or "cue" lights are duplicated at other positions such as the equipment rack and the cameras themselves, to convey the necessary information to the operators.

B. Monitor and Oscilloscope

The mixing and line amplifier has two separate output circuits. The one output is connected to the input circuit of the right-hand monitor in the console (the stand-by monitor). The other output supplies the composite video signal to a coaxial line which transfers the signal to the transmitter. The input circuit of the left-hand monitor is bridged across the input to the transmitter line. The two monitor circuits are identical in every respect; accordingly, it will be necessary to consider only one of them. The video signal is amplified by a single amplifying stage and is then applied to the

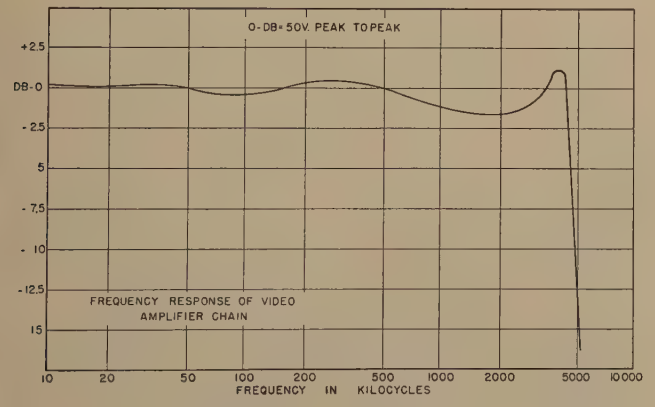

Fig. 12—Frequency-response curve of video amplifiers.

grid of the monitor tube. The scanning generators for the monitor tube are similar in principle to those employed to energize the camera scanning coils, with only such modifications as are dictated by the difference in scanning energy requirements. The accelerating voltage supply for the monitor tube is contained on the monitor chassis in the console. The electrically regulated power supply for the deflecting and video circuits is housed in the racks.

The video signal is also applied to the vertical deflecting plates of the monitor oscilloscope which permits visual observation of the composite video wave form. The horizontal-deflection plates are supplied with a linear sweep voltage. Two separate sweep frequencies are employed, one of 60 cycles per second and the other of 6615 cycles per second.

The oscilloscope also affords a means of determining accurately the amplitude as well as the wave form of

Fig. 13—Photograph of television image on monitor tube.

the video signal. This is accomplished by providing means for calibrating the oscilloscope. To this end a gain control on the video amplifier and a switch for connecting a source of 60-cycle sine-wave voltage across the input of the amplifier are provided. The amount of calibrating voltage applied to the oscilloscope is read on a voltmeter located to the left of the clock on the instrument panel of the console.

All of the power supplies for the oscilloscope are contained in the monitor chassis.

Conclusion

A consideration of equipment of the type described in this paper would not be complete without a word about performance. The performance of the timing and pulse-generating equipment may be judged from the fact that over a period of some months it has performed satisfactorily without any need of servicing and only very occasional minor adjustment of the master oscillator. When the equipment is operated intermittently a warm-up period of approximately ten minutes suffices. After the warm-up period the timing signals generated are of such accuracy as to provide excellent interlace of the television image over any period of operation.

The over-all performance of the equipment can be judged from the following figures: Fig. 12 shows the over-all frequency response of the video amplifiers from the input of the preamplifier to the grid of the monitor tube. Fig. 13 is a photograph of an image appearing on the monitor tube when a "still" picture is projected on the cathode of a dissector-type camera tube.

Acknowledgment

The author wishes to acknowledge the assistance and contributions of all the members of the Farnsworth television development and engineering staff.

Brightness Distortion in Television*

DONALD G. FINK†, ASSOCIATE, I.R.E.

Summary—*Brightness distortion, a term analogous to harmonic distortion in sound transmission, refers to nonlinearity of the brightness transfer characteristic of a television system. This characteristic is the curve relating the brightness values in the televised object to the corresponding brightness values in the received image. Brightness distortion is defined as occurring whenever the brightness transfer characteristic departs from a straight line passing through the origin corresponding to black in object and image. This paper offers a unified theory of brightness distortion, suggests a rational terminology, and presents a graphical method of evaluating the visual effects of the distortion.*

THE TERM brightness distortion is intended to describe the condition which exists when the brightnesses of the various parts of a television reproduction are not directly proportional to the brightnesses of the corresponding parts of the original scene. Early in the television art it was found that such disparity between the tonal values at the sending and receiving ends of the system was not a very serious matter compared with the lack of pictorial detail exhibited by the early images. But as the detail of television images has improved, the problem of brightness distortion has assumed a correspondingly greater importance. Today it is hardly an exaggeration to say that the most pressing technical problem in television engineering, within the limitations of the 6-megacycle channel, is that of bringing the effects of brightness distortion under control.

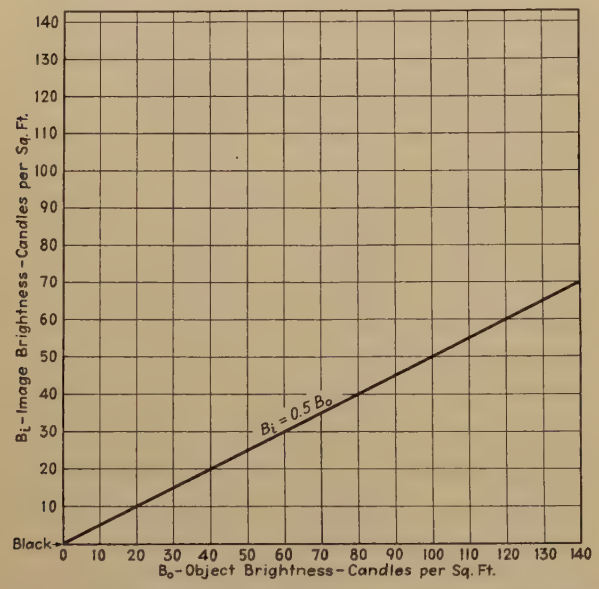

Fig. 1—Typical distortionless brightness transfer characteristic.

The control of brightness distortion assumes particular importance because it offers one of the very few ways in which television images may be improved without change in the standards of transmission. The width of the television channel, for example, does not impose any limitation on the tonal range reproduced in television images. The limitation in this respect is imposed by the signal-to-noise ratio and apparatus limitations, all of which can be improved as the art progresses without recourse to a change in the standards.

The purpose of this paper is to consider the limitations imposed by brightness distortion, and to explore the possibilities of improvement. Similar work has already been reported by such workers as Maloff,[1] Kallmann,[2] and Goldmark and Dyer[3] in papers already published, but there is as yet no uniform terminology or straightforward method of representing the effects of brightness distortion. This paper, therefore, suggests a rigorous definition for brightness distortion, develops a rational terminology, and presents a simple graphical method of measuring its effects.

The Definition of Brightness Distortion

Brightness distortion is defined, qualitatively, as a lack of proportionality between the brightness values in the television image and those in the televised object. For a more quantitative definition it is convenient to use the graphical representation shown in Fig. 1. This curve, known as a brightness transfer characteristic, relates the brightness scale in the television object, i.e., the scene before the camera, to the brightness scale of the television image, on the receiver screen. The horizontal scale is marked in linear physical units, candles per square foot, over a typical range of brightnesses. The vertical scale is marked, likewise linearly in candles per square foot, with the corresponding brightness scale in the image. The origin of each scale corresponds to complete absence of light, or black, while the maximum values represent the high lights of the scene.

The curve relating the two sets of brightnesses may have almost any shape, depending on the camera and picture tubes employed, as well as on all the intermediate transducers in the system. *Brightness distortion is defined as occurring whenever this curve, plotted in linear co-ordinates, departs from a straight line passing through the origin.* The brightness transfer characteristic shown in Fig. 1 is linear, and it passes through the origin, hence it is free of brightness distortion. Such a substantially straight-line characteristic is seldom attained in practice, but an approximation to it may be obtained, provided the over-all ranges of brightness are not too extensive.

* Decimal classification: R583. Original manuscript received by the Institute, February 3, 1941. Presented, Sixteenth Annual Convention, New York, N. Y., January 11, 1941.

† Managing Editor, *Electronics*, McGraw-Hill Publishing Company, New York, N. Y.

[1] I. G. Maloff, "Gamma and range in television," *RCA Rev.*, vol. 3, pp. 409–417; April, 1939.

[2] Heinz E. Kallmann, "The gradation of television pictures," Proc. I.R.E., vol. 28, pp. 170–175; April, 1940.

[3] P. C. Goldmark and J. N. Dyer, "Quality in television pictures," Proc. I.R.E., vol. 28, pp. 343–351; August, 1940.

The brightness transfer curves shown in Fig. 2, on the other hand, display several common forms of brightness distortion, two being nonlinear but passing through the origin, the others being linear but not passing through the origin. Curve *A* has a convex-downward shape, curve *B* a convex-upward shape. In curve *C* the image has a finite brightness where the object is black, whereas in curve *D* the object has a finite brightness where the image is black. The characteristics shown are simple analytic functions, as indicated, the nonlinear curves being power functions and the straight lines being displaced linear functions.

While the distortion exhibited by these curves is obvious, so far as the shape of the curves is concerned, it would be very misleading to attempt to draw conclusions from these curves regarding the *appearance* of the television image relative to the object. The reason is that the curves are plotted in linear co-ordinates. The eye, on the other hand, displays a substantially logarithmic response to changes in brightness. Hence a linearly plotted function gives only a limited indication of the visual effect of the brightness distortion.

The fact that the eye displays a substantially logarithmic response suggests that the brightness transfer curves, shown in Figs. 1 and 2, should be replotted on log-log co-ordinates if the visual effect is to be apparent. This replotting has been done in Fig. 3. In this logarithmic representation of the curves, equal distances along the horizontal scale indicate equal changes in visual sensation for an observer in the studio, whereas equal distances along the vertical scale indicate equal changes in visual sensation for an observer at the receiver. Hence if we consider the linearity or curvature of the curves plotted on these log-log co-ordinates, we obtain a direct indication of the relative visual effect of the brightness distortion on the appearance of the image, relative to that of the object, If the brightness transfer curve, plotted on log-log co-ordinates, is a straight line, then the visual sensation of the image observer has a linear correspondence to the visual sensation of an observer in the studio.

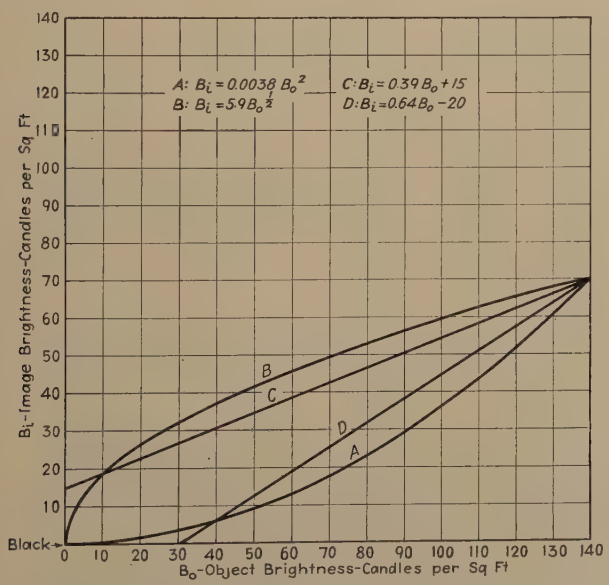

Fig. 2—Forms of brightness distortion resulting from nonlinearity (*A* and *B*) and from displacement from the black origin (*C* and *D*).

Examining the log-log curves in Fig. 3, we note that the distortionless curve of Fig. 1 retains its linear form. The convex-upward and downward curves of Figs. 2*A* and 2*B* now become linear. However, the off-origin linear curves, Figs. 2*C* and 2*D*, become nonlinear in the log-log plots, producing compression of the tones in the shadows in Fig. 2*C* and compression of tones in the high lights in Fig. 2*D*.

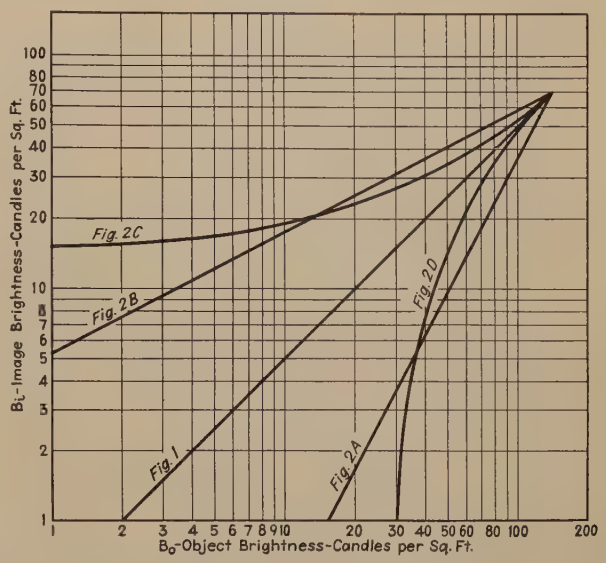

Fig. 3—The curves of Figs. 1 and 2 replotted on log-log co-ordinates to reveal the visual effect of the distortion.

Since the log-log plots reveal the visual effect of the distortion, it is instructive to consider the plots in pairs, one plotted linearly, the other doubly logarithmically. We consider first the pair of plots shown in Fig. 4. The linear curves at the left are distortionless, but they have different slopes, corresponding to different values of over-all gain in the system. The same curves, plotted in log-log co-ordinates at the right, reveal the fact that such changes in gain merely displace the log-log plots vertically, producing an effect on the eye merely of brightening or darkening the picture. These plots illustrate the fact that the so-called "contrast" control in a television receiver, which varies the gain of the system, is in reality a brightness control, and that it has no effect on contrast whatever, provided that the system is linear and the black level remains at the origin.

Since the term "contrast" has been used, it is desirable to define it. One commonly used definition of "contrast" is the ratio of the brightness of the brightest portion to that of the darkest portion of the scene in linear units. However, since contrast means little except in terms of visual sensation, it is desirable to express the ratio logarithmically. Accordingly, the

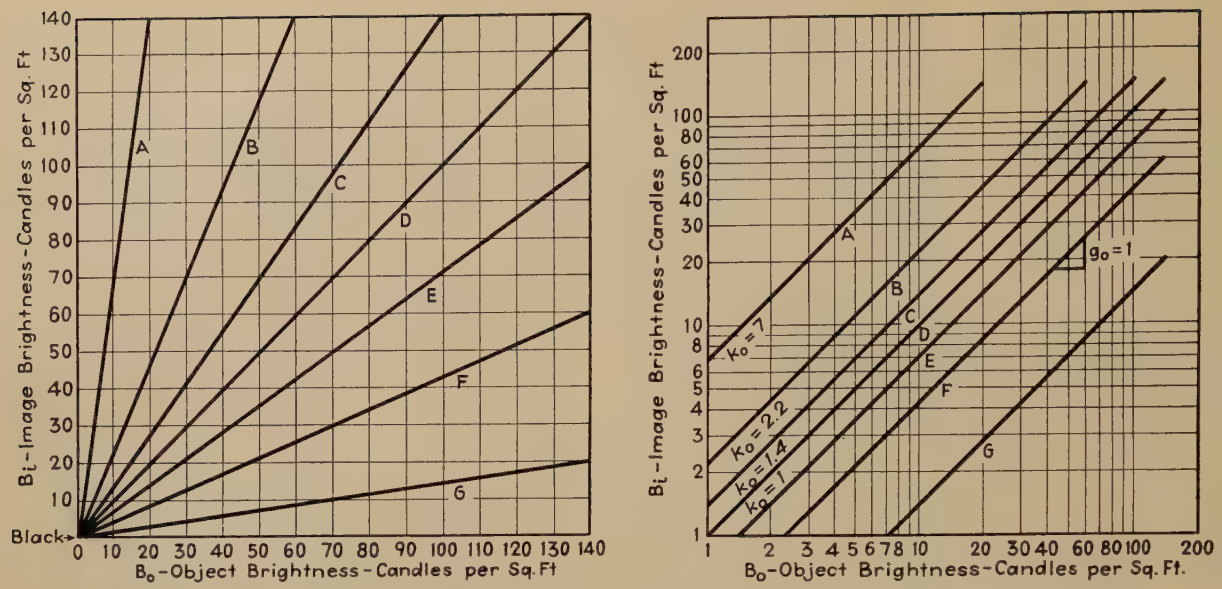

Fig. 4—Distortionless characteristics illustrating the effect of changing the over-all gain of the system.

definition of contrast used here is the difference between the maximum and minimum brightnesses expressed in logarithmic units. Thus contrast is indicated graphically by the distance occupied by the brightness range on the brightness scales of the log-log plots. Image contrast is the distance occupied on the image brightness scale, whereas object contrast is the distance on the object brightness scale.

In view of this concept, we may define another term, *contrast distortion*, as occurring whenever the log-log plot of the brightness transfer characteristic displays curvature. When the log-log plot of the brightness transfer curve is not straight, i.e., when contrast distortion is present, the effects of the brightness distortion are usually detrimental. The absence of contrast distortion does not mean that brightness distortion, as previously defined, is necessarily absent. The log-log plots of certain types of brightness distortion assume a straight-line shape. These forms of brightness distortion are admissible, and may serve a useful purpose.

The concept of contrast is useful in characterizing a reproduction entirely aside from any consideration of the original scene. Usually, however, we wish to relate the contrast of a reproduction to that of its original. This relationship is expressed by the slope of the log-log brightness transfer characteristic. Accordingly, this slope is defined as the *contrast gradient* and is given the symbol g_o.

In the plots of Fig. 4, the contrast gradient of each log-log plot is a constant and its value is unity. Moreover changing the slope of the linear plots does not change the value of the contrast gradient. Hence a true gain control by itself cannot affect the contrast of a television image relative to that of the original object,

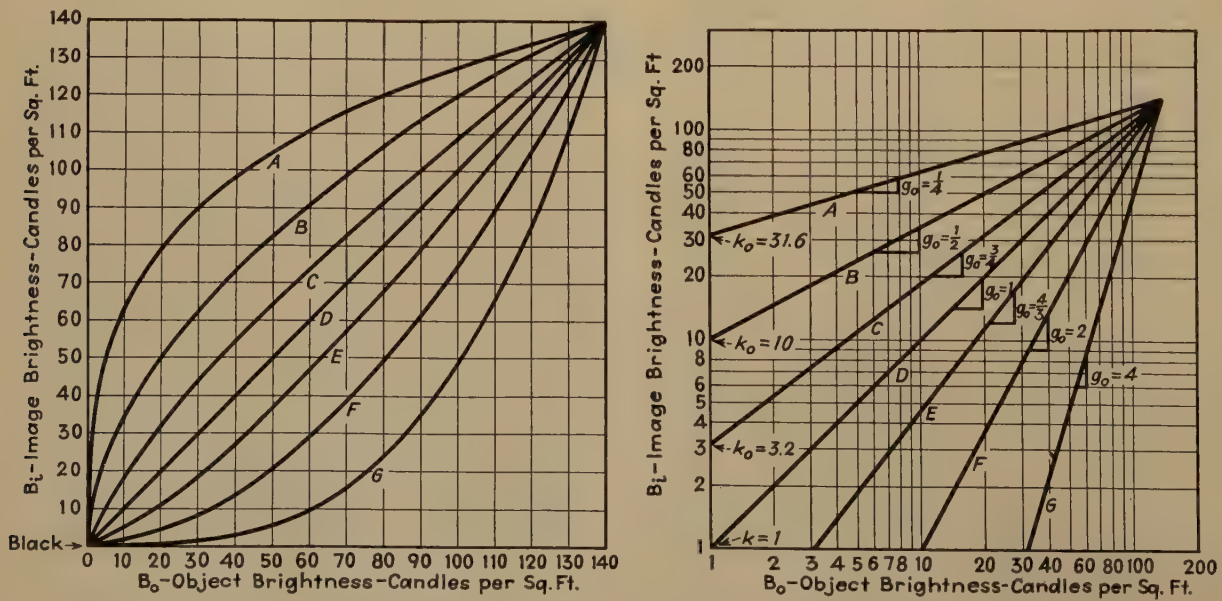

Fig. 5—Power functions displaying brightness distortion, but free of any corresponding contrast distortion.

unless other effects come into play.

The pair of plots shown in Fig. 5 illustrate the means by which the contrast gradient may be altered. At the left are the linear plots of several power functions, at the right, the corresponding log-log plots.

All of the curves shown in the right-hand figure are of the form

$$\text{image brightness} = k_0\,(\text{object brightness})^{g_0}.$$

The parameter g_0, the contrast gradient, is readily identified on the log-log plots as the slope of the curve. The parameter k_0, the scale factor, is likewise readily found as the intercept of the log-log plot with the unity abscissa. All of the curves except D display brightness distortion, but none of them display contrast distortion, since the contrast gradient of each log-log curve is constant. The higher the value of the contrast gradient, the higher is the contrast of the image relative to that of the object.

Since none of the curves display contrast distortion, the types of brightness distortion shown do not necessarily have an adverse effect on the appearance of the image, so long as the observer does not know the brightness range of the original object. Thus a given range of brightnesses in the received image may arise from a long range of brightnesses in the transmitted object reproduced with a low contrast gradient, or it may equally well arise from a short range of brightnesses in the object, reproduced with a high value of contrast gradient. Unless the observer has information concerning the brightness range actually present in the object, he may find it difficult to distinguish which mode of reproduction is the more "natural." However, in many cases the observer may have information concerning the actual appearance of the object. Such information may arise from direct observation, as in the case of an operator in a monitor room who has a direct view of the object. More generally the "information" is an intuitive conception of how the scene should look in the context under which it is presented. Thus the range of brightness in a brightly sunlit scene is considerably greater than that of the same scene under a cloudy sky. If the context is clear, reproduction with too low a contrast gradient will destroy the crispness of the sunlit scene. But if the source of illumination is not obvious, and if the conditions under which the scene is viewed are not familiar to the observer, a considerable variation in the value of over-all contrast gradient is permissible before an obviously unnatural rendition of the tones may be said to exist. Moreover such variations may serve a useful purpose in making it possible to utilize the full image brightness range under the variety of ranges of brightness encountered in picking up various objects.

The value of the over-all contrast gradient currently adopted in processing motion-picture film is about 1.4. So far as the film and its processing are concerned, the image contrast therefore exceeds the object contrast by 40 per cent. However, all of this additional contrast is not effective when viewed by the observer due to halation, scattered light in the projection system, and scattering at the surface of the projection screen. Part of this excess contrast has the effect also of compensating for the lack of color contrasts, inherent in monochromatic reproduction.

It will be noted that thus far we avoided the use of the term "gamma," used in photographic work to represent the slope of the log-log plots between exposure and film opacity. This word has been used by television engineers, but its utility in television work is open to question. The word gamma as used in photography refers only to the straight-line portion of the log-log plots. In television work, the log-log plots commonly encountered have a straight-line portion conspicuous

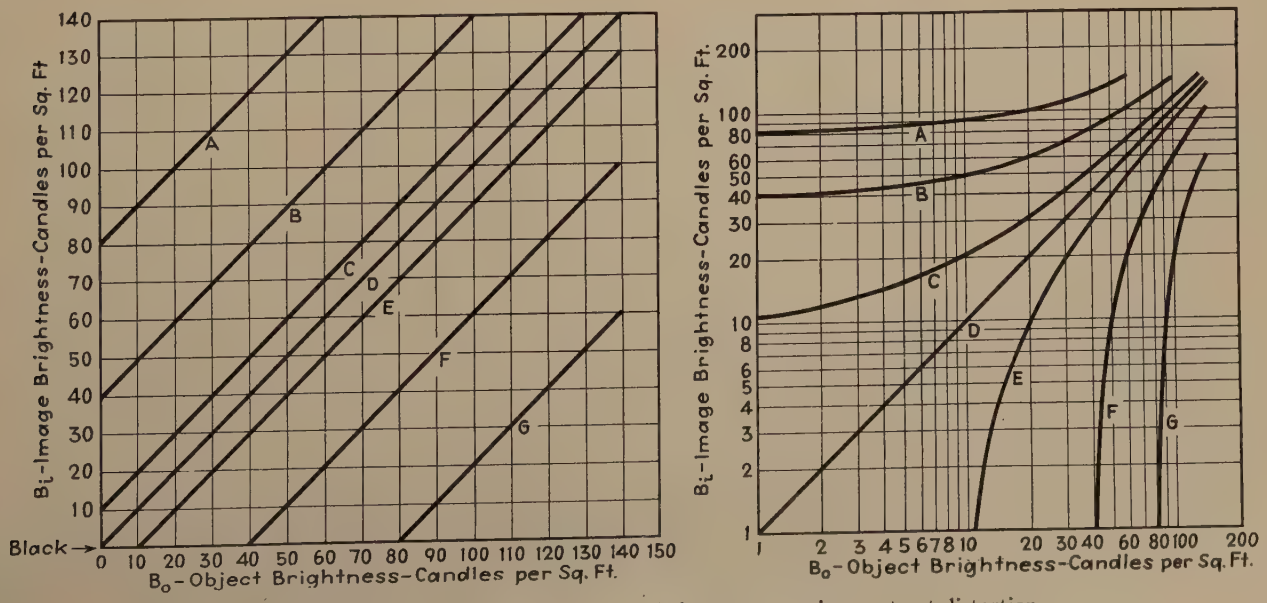

Fig. 6—Off-origin brightness distortion and the accompanying contrast distortion.

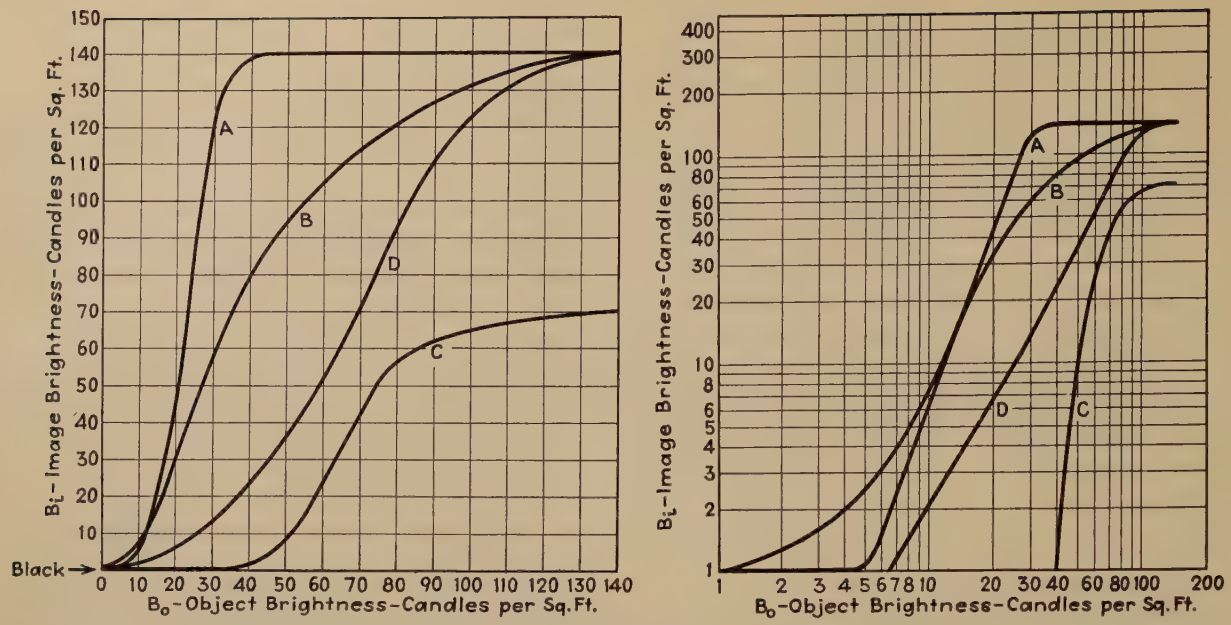

Fig. 7—General nonlinear saturation curves, showing brightness and contrast distortions typical of practical television systems.

by its absence. In such cases a localized slope or gradient serves a better purpose. When, as in Fig. 5, the contrast gradient has a constant value, it may properly be termed the "gamma" of the system. Otherwise it seems desirable to forsake the use of the term "gamma" and to employ the more general concept of a gradient.

We examine next another type of brightness distortion which, in contrast to the forms just shown, does have an adverse effect on the appearance of the reproduced image. Fig. 6 shows at the left linear plots which are distorted because they do not pass through the origin representing black in the object and image. When these curves are plotted on log-log co-ordinates, curvature appears. In other words, the contrast gradient changes along the length of each log-log curve. In curve *B*, for example, the high-light portions of the scene are reproduced with high contrast gradient, whereas the shadow portions of the scene are reproduced with low gradient. In other words, the high-light detail of the image is reproduced over a greater range than the shadow detail. In curve *F* the situation is just reversed. The shadow portions display a higher contrast gradient, hence are reproduced with a wider range than the high-light portions.

This type of brightness distortion produces contrast distortion, and in general this effect is undesirable. But it should be remarked in passing that such contrast distortion may have value in enhancing the appearance of an object inadequately or improperly illuminated. The effect is obtained by shifting the black level of the transmitted signal relative to that of the received image. Such shifts have been used by television broadcasters as well as by members of the viewing audience to improve an otherwise inadequate pickup. As other limitations of the system are overcome off-origin brightness distortion will probably cease to serve a useful purpose.

These plots illustrate the importance of operating the television system so that the black level in the studio scene corresponds exactly with the black level on the receiver screen. Two requirements must be satisfied to meet this condition of operation. In the first place the operator monitoring the picture signal should see to it that blanking level, or pedestal, of the video signal corresponds to the output of the television camera when the light is completely cut off from the mosaic of the camera tube, and he must see to it that this adjustment remains in effect throughout the performance. If it is desired to change the brightness of the image without changing the illumination entering the camera tube, such changes in apparent brightness should be produced by variation in gain, not by variation in the direct-current component of the signal. The second requirement to be satisfied is that the receiver operator must set the brightness control of his receiver so that the blanking level, or pedestal, of the video signal produces a substantially black level of illumination on the receiver screen. The easiest way of assuring this condition is to increase the brightness control until the return lines (formed by the scanning spot between the individual fields and frames) just become visible, and then back off the control until they just disappear. If this point of operation is not established, and maintained, then the types of contrast distortion illustrated in Fig. 6 come into play. As previously noted, some such contrast distortion may be tolerated or even desirable, but it should not be inadvertently introduced.

In Fig. 7 another pair of plots is shown which display brightness distortion as well as contrast distortion. These curves approximate conditions met in practical television systems of the present day. The log-log plot of curve *A* displays sharp saturation of the high-light and shadow portions of the scene. This curve produces

a "whitewash and lampblack" effect (loss of high-light and shadow detail) whenever the brightness range in the object exceeds the straight-line portion of the curve. The linear plot of curve *A* shows that a comparatively small saturation occurs at the origin, and that the saturation in the brighter portions is sharper and more extensive. Curve *B* in the linear plots illustrates a more symmetrical and gradual saturation, which does not produce so serious an effect on the appearance of the image as shown at the right. Curve *C* is very similar but the image brightness range, as shown most clearly in the linear plots, is reduced. This type of brightness distortion produces the high image contrast and sharp high-light saturation shown in the log-log plots, Finally, curve *D* displays, in the linear plots, an equal degree of saturation at the origin and at the bright end of the scale. This type of distortion limits the shadow detail but does not seriously affect the high-light detail as shown in the log-log plots. These curves illustrate the varieties of brightness distortion which may be encountered in practice. They also show how readily the corresponding contrast distortion may be identified by replotting on log-log co-ordinates.

The Influence of Television Transducers on Brightness Distortion

In a self-contained televison system, such as a television studio and its associated picture-monitoring apparatus, it is a relatively simple matter to measure the brightness transfer characteristic and to determine therefrom the extent of the brightness distortion and its concomitant contrast distortion. One simple method of so doing is to transmit the image of a standard photographic gray scale, measuring the brightness of the various steps with a photographic exposure meter in the studio, and with a sufficiently sensitive photometer on the monitor screen.

When the brightness and contrast distortions have thus been revealed, the question of isolating the sources

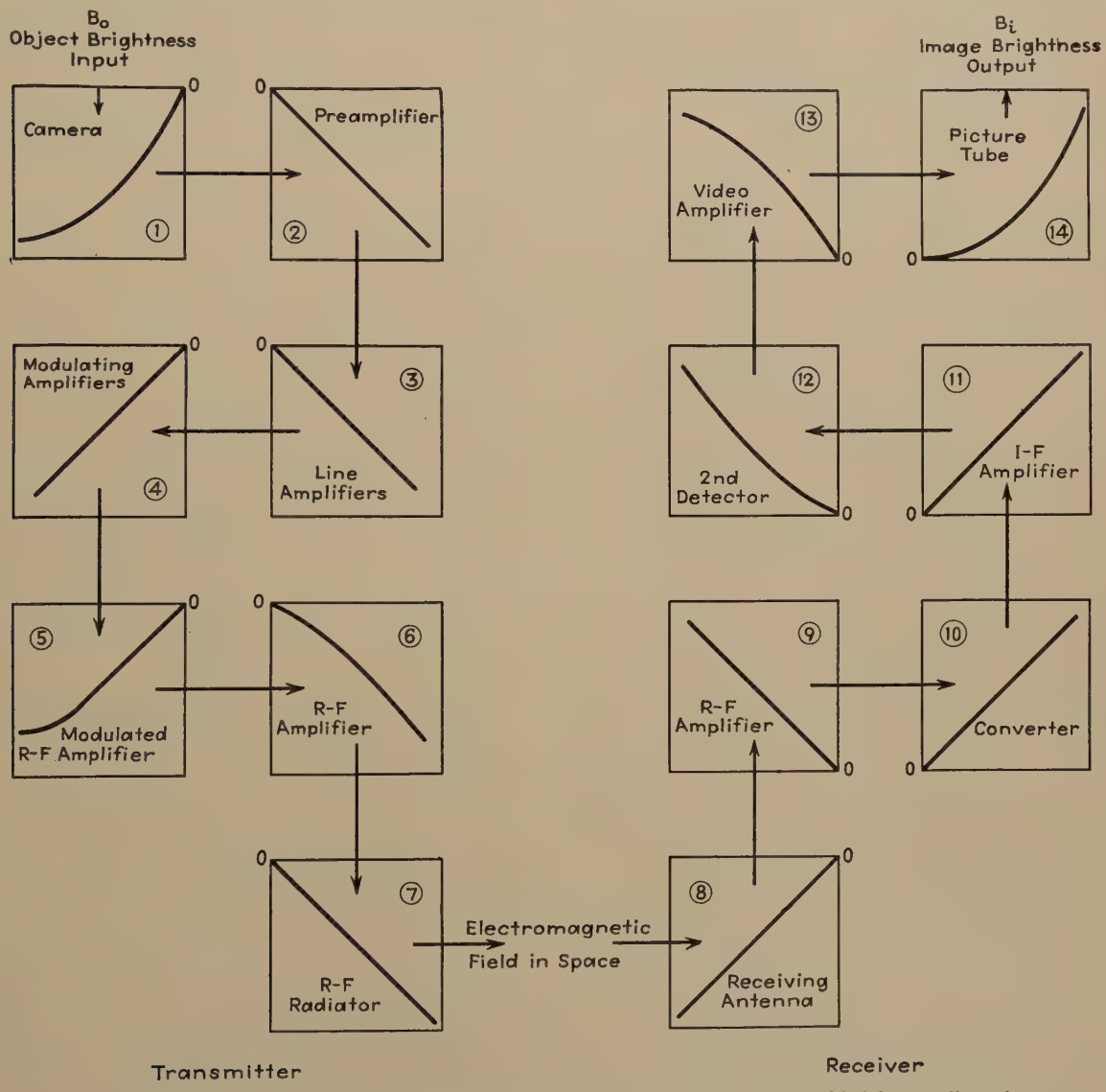

Fig. 8—Analysis of the brightness transfer characteristic to reveal the sources of brightness distortion.

of the distortion then presents itself. This is an important and difficult technical problem. In fact, so far as is known to the writer, no complete analysis of the sources of brightness distortion has ever been undertaken in any television broadcasting system.

One of the reasons for this rather remarkable lack of information is revealed in Fig. 8, which shows how brightness distortion must be analyzed in terms of the individual transducers of the system. Here we have brought together the "transfer characteristics" of all the important transducers in a television system, starting with the camera, the video preamplifiers and line amplifiers, the modulator, modulated radio-frequency amplifier, radio-frequency amplifier, transmitter antenna, propagation path, receiving antenna, receiver radio-frequency amplifier, converter, intermediate-frequency amplifier, second detector, demodulator, video amplifier, and picture tube. The input-versus-output relationships of each of these elements of the transmission system have been shown in typical form. Note that we have returned to linear co-ordinates here because such plots are the commonly accepted engineering usage. The significant input quantity is the brightness of the object (strictly, the illumination falling on the sensitive plate of the camera). The corresponding output quantity is the voltage across the camera-tube coupling resistor, measured in millivolts. This output is applied to the input of the preamplifier whose input scale, in millivolts, is shown directly opposite. The corresponding output, in volts, is applied to the line amplifiers, including a mixing amplifier with its clipping stages, etc., thence to the input of the modulator, whose output in turn is applied to the input of the modulated radio-frequency amplifier, and so on through the system, following the arrows. The units in the scale of each output quantity correspond exactly to the units of the succeeding input quantity. The extent of each characteristic is taken over a sufficient range to accommodate the full range of brightness over which the system is intended to operate and the characteristics are plotted so that they have a common origin, corresponding to the black level. All these input-output characteristics must be measured, or accurately estimated, before the sources of the brightness distortion can be isolated. Thus, in this figure the principal contributors to the distortion (whose characteristics exhibit the greatest curvature) are the camera tube and the picture tube.

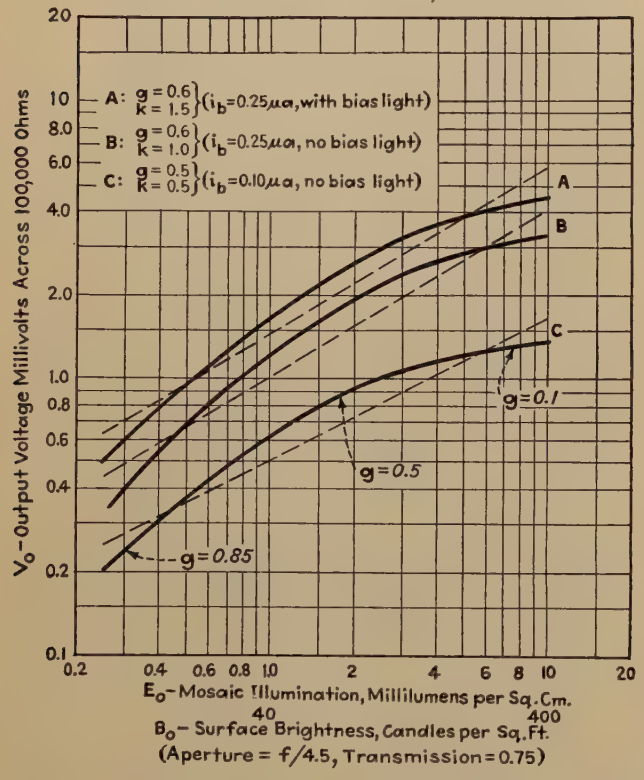

Fig. 9—Transfer characteristics of a typical iconoscope camera tube.

The only universal method of analyzing the brightness distortion involves the measurement of these subsidiary transfer characteristics, and this may be a very tedious and difficult task. However, a simplified analytic approach may be used as a basis for discussion. If the subsidiary transfer characteristics are plotted on log-log paper it will be found that many of them approximate straight lines. When the approximation is a good one, a value of scale factor k, and a gradient g can be found for that particular transducer. On the assumption that all the transducers are found to have scale factors k_1, k_2, k_3, etc., and corresponding gradients g_1, g_2, g_3, etc., the over-all scale factor k_0 and over-all contrast gradient g_0 may be determined by the following theorem:

Cascaded Transducer Theorem

If n transducers, whose outputs and inputs are related by the expression

$$(\text{output}) = k(\text{input})^g,$$

are connected in cascade, the output of one forming the input of the next, then the output of the final transducer is related to the input of the initial transducer by the expression

$$(\text{output}) = k_0(\text{input})^{g_0},$$

where

$$k_0 = (k_1^{g_2 g_3 g_4 \cdots g_n})(k_2^{g_3 g_4 g_5 \cdots g_n}) \cdots (k_{n-1}^{g_n})(k_n),$$

and

$$g_0 = g_1 g_2 g_3 g_4 g_5 \cdots g_n.$$

(The subscripts 1, 2, 3, 4, 5 . . . n refer to the individual transducers, 1 referring to the initial and n to the final transducer.)

The expression for k_1 is very cumbersome, but since

it sets only the scale of brightness, a matter apart from the main consideration of distortion, we may disregard it. The over-all contrast gradient on the other hand assumes a very simple form,

$$g_0 = g_1 g_2 g_3 g_4 \cdots g_n.$$

Thus if we know the gradients of all the transducers, we may obtain the over-all contrast gradient simply by forming their product. Suppose we assume, in line with established motion-picture practice that the over-all contrast gradient g_0 should have a value of 1.4. If the camera g_1 is 0.6 (typical of iconoscopes) and the picture tube g_n is 2.0 (typical of commercial picture tubes) the product of the gradients of all the other transducers must be

$$g_2 g_3 g_4 \cdots g_{n-1} = \frac{1.4}{0.6 \times 2.0} = 1.17.$$

If this condition is not satisfied, we may modify the gradient value of one of the transducers to make it so, or more directly, we may add a transducer having a gradient which, when combined in the product, forms the required value.

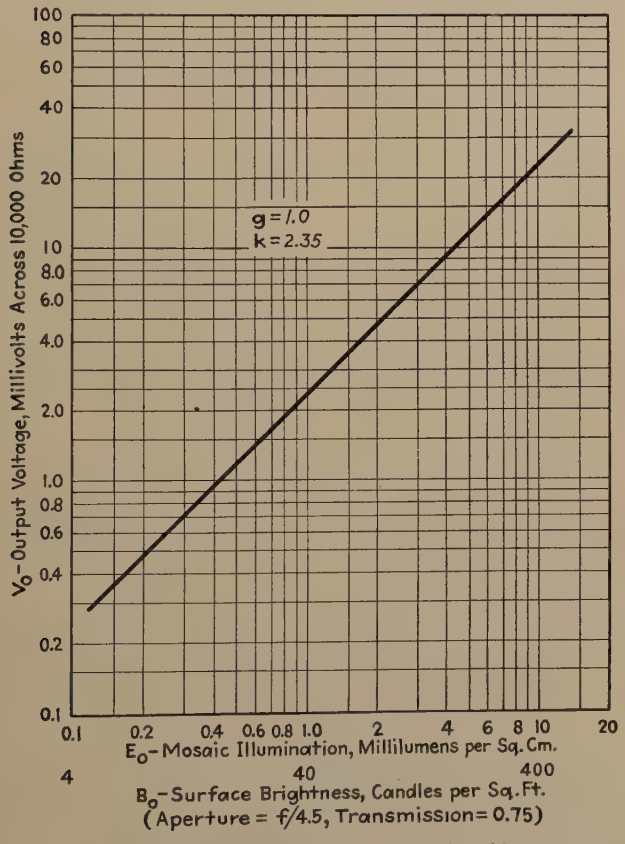

Fig. 10—Transfer characteristic of a typical orthiconoscope.

If the subsidiary-transducer characteristics do not yield straight lines when plotted on log-log paper, the above analysis does not apply, and in fact there is no simple analytic approach.

Typical Transducer Characteristics

To illustrate the process of isolating the sources of brightness distortion we consider next several input-output curves of typical television transducers. In Fig. 9 are shown several such curves of a typical iconoscope camera tube. In order to determine the value of gradient and scale factor, the curves are plotted on log-log co-ordinates. It will be noted that the iconoscope does not operate on a power-function curve, since the log-log curves are not straight lines. The gradient describing the curves varies from about 0.1 to 0.85 with 0.6 as an average. The straight lines are arbitrarily drawn to obtain values of g and k descriptive of the tube operation, but these values have no great significance compared with the basic characteristics. The point to be noted is that the iconoscope has a variable gradient lower than unity. The effect of the iconoscope characteristic on the reproduction of the image depends, of course, not only on these curves but on the curves of the rest of the system.

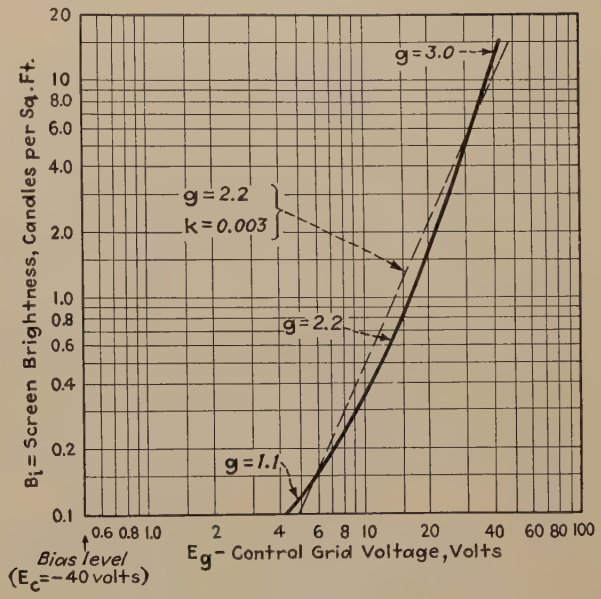

Fig. 11—Transfer characteristic of a typical picture tube (Type 12AP4).

Fig. 10 shows a similar log-log plot of the input-versus-output characteristic of another television camera tube, the orthicon. This device displays a gradient of unity, i.e., it is a linear device. If a given television system is used first with an iconoscope camera tube, then with an orthicon, the contrast of the image is increased in the second case, other factors being equal, because the gradient of the orthicon tube has the constant value unity, while that of the iconoscope is a variable quantity between 0.1 and 0.85.

Fig. 11 shows a log-log plot of the input-versus-output curve of the transducer at the other end of the system, the picture tube. The data are taken from the published curves of the type 12AP4 kinescope. Here,

as in the iconoscope, no single value of gradient is found, but a range from about 1.1 to 3.0 appears. An average value of about 2.2 may be obtained by selecting the straight line shown as representative of the tube operation, but such a single value has no significance except as a very rough approximation.

Since the average values of g and k shown in the figures are of doubtful significance, it is desirable to combine the iconoscope and picture-tube curves point by point. This has been done in Fig. 12. Here we find

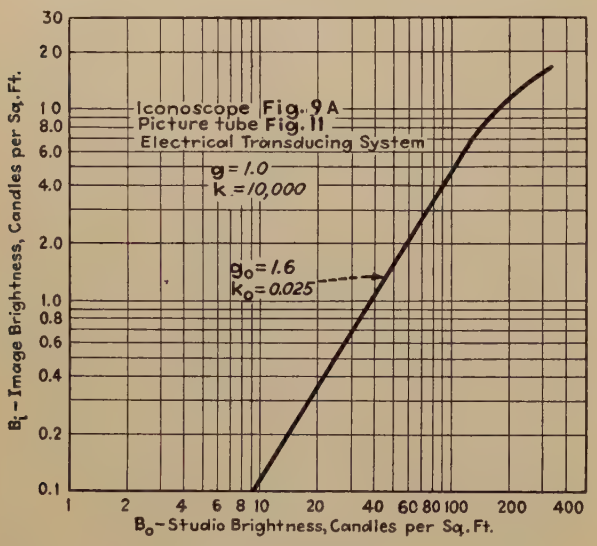

Fig. 12—Point-by-point combination of the transfer characteristics of Fig. 9 and Fig. 11.

the rather remarkable fact that although neither the iconoscope nor the picture tube display constant values of gradient over the operating range, the combination of the two tubes does display a constant value of contrast gradient, equal to 1.6, over most of the operating range. This is, insofar as the writer is aware, a matter of coincidence rather than predetermined design. It is however, a fortunate situation since the contrast gradient of the two tubes corresponds closely to that adopted for motion pictures.

The image contrast of the television system is accordingly greater by 60 per cent than the object contrast, assuming the electrical transducing system between the iconoscope and the picture tube is linear. As in motion pictures, this excess image contrast is useful, partly in compensating for the lack of color contrast, and partly in overcoming the effects of halation, noise, and scattered light which are visible on the receiver screen, and which degrade the over-all contrast. (It should be noted that the measurement of the picture-tube characteristic is made with uniform flat fields of light, and thus neglects entirely the loss of contrast due to the spreading of light between adjacent picture areas.)

Contrast Modulation—A Combination of Logarithmic and Exponential Nonlinear Functions

Thus far all the transfer characteristics we have considered are power functions, since this is the simplest form to use in analytic discussion. Two other very important types of transfer characteristics, which apply to the transmitter as a unit and the receiver as a unit, are illustrated in Fig. 13. The transfer characteristic at the left is a *logarithmic* function whereas the receiver characteristic at the right is an antilogarithmic or *exponential* function. Since the second function is the obverse of the first, the brightness distortion introduced by the first may be compensated by the second. This compensation is illustrated by the dashed lines, which represent linear modulation.

It will be noted that the percentage modulation produced by the logarithmic characteristic in the dark portions of the picture is very much greater than that produced by the linear characteristic, whereas the reverse is true in the bright portions of the picture. This type of modulation, which has been called "contrast modulation" by Kallmann, serves the purpose of improving the signal-to-noise ratio when the noise is introduced between the output of the camera circuits and the picture tube.

The explanation of the gain in signal-to-noise ratio lies in the fact that with linear modulation a given amplitude of interfering voltage produces a very large visual effect in the dark portions of the picture, whereas the same amplitude of noise produces a much smaller effect in the bright portions of the picture. By devoting a larger portion of the carrier amplitude to the dark portions of the signal and a correspondingly smaller portion in the bright portions, the effect of the noise is evenly distributed over the half-tone scale, and the

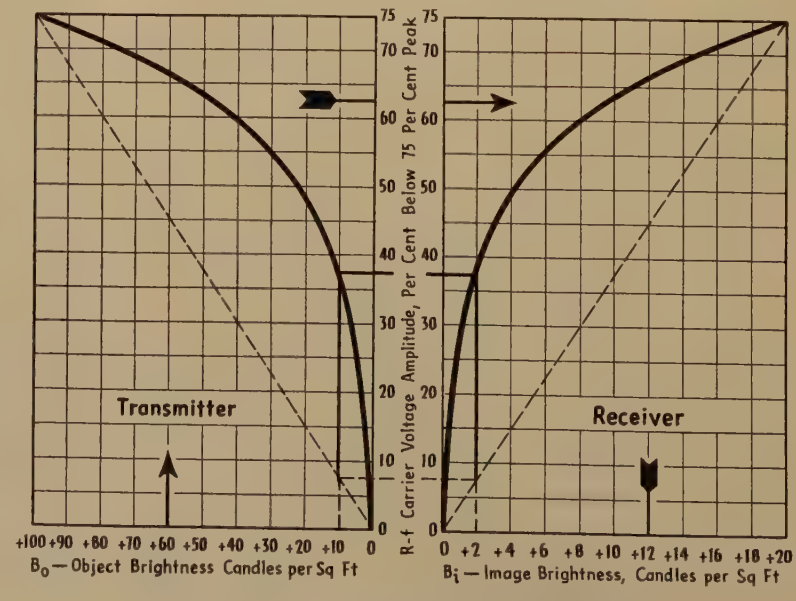

Fig. 13—Contrast modulation employing logarithmic modulation and antilogarithmic demodulation.

noise does not become visible until a much higher level of interference is reached.

When contrast modulation is used, an antilogarithmic characteristic is required at the receiver, of course, to remove the brightness distortion and contrast distortion which have been introduced. The question then arises whether an antilogarithmic characteristic at the receiver may be so chosen as to allow any desired value of over-all contrast gradient for the system as a whole. Fig. 13 illustrates that unity contrast gradient is readily obtained, but it is not clear that a contrast gradient of, say, 1.4 could be readily obtained.

A simple analysis shows that any contrast gradient may be obtained by combining logarithmic and antilogarithmic characteristics, provided that the coefficients and bases of the logarithms in each case are properly chosen with respect to the desired values of contrast gradient and scale factor. The theorem relating these quantities is as follows:

Intermediate Compensation Theorem

If the final output of a series of cascaded transducers is related to the initial input by the expression

$$\text{output}_0 = k_0\,(\text{input}_0)^{g_0}, \tag{1}$$

and if the output of an intermediate transducer is related to the initial input by the logarithmic expression (to the base A)

$$\text{output}_i = k_i \log_A (\text{input}_0) \tag{2}$$

then the final output of the series must be related to the input of the next following intermediate transducer by the exponential (antilogarithmic) expression

$$\text{output}_0 = k_0 \operatorname{antilog}_B (\text{input}_{i+1}) \tag{3}$$

where the base B of the antilogarithm is the base A raised to the g_0/k_i power:

$$B = A^{g_0/k_i}. \tag{4}$$

Conversely, if two groups of cascaded transducers are characterized by (2) and (3) respectively, then the two groups in cascade are characterized by expression (1), where

$$g_0 = k_i \log_A B. \tag{5}$$

The logarithmic and antilogarithmic characteristics required in transmitter and receiver are very closely approximated by the transfer characteristics of the iconoscope and picture tubes whose characteristics are shown in Figs. 9 and 11. It thus happens that, more by chance than by design, the transmitters of the present day may take advantage of a substantial improvement in signal-to-noise ratio, provided merely that the electrical transducing system between the iconoscope and the picture tube is linear.

When contrast modulation is applied to other types of camera tubes, however, difficulties may ensue. If an orthicon is used, for example, the logarithmic characteristic must be imposed by an additional transducer, since the orthicon is inherently a linear device. When

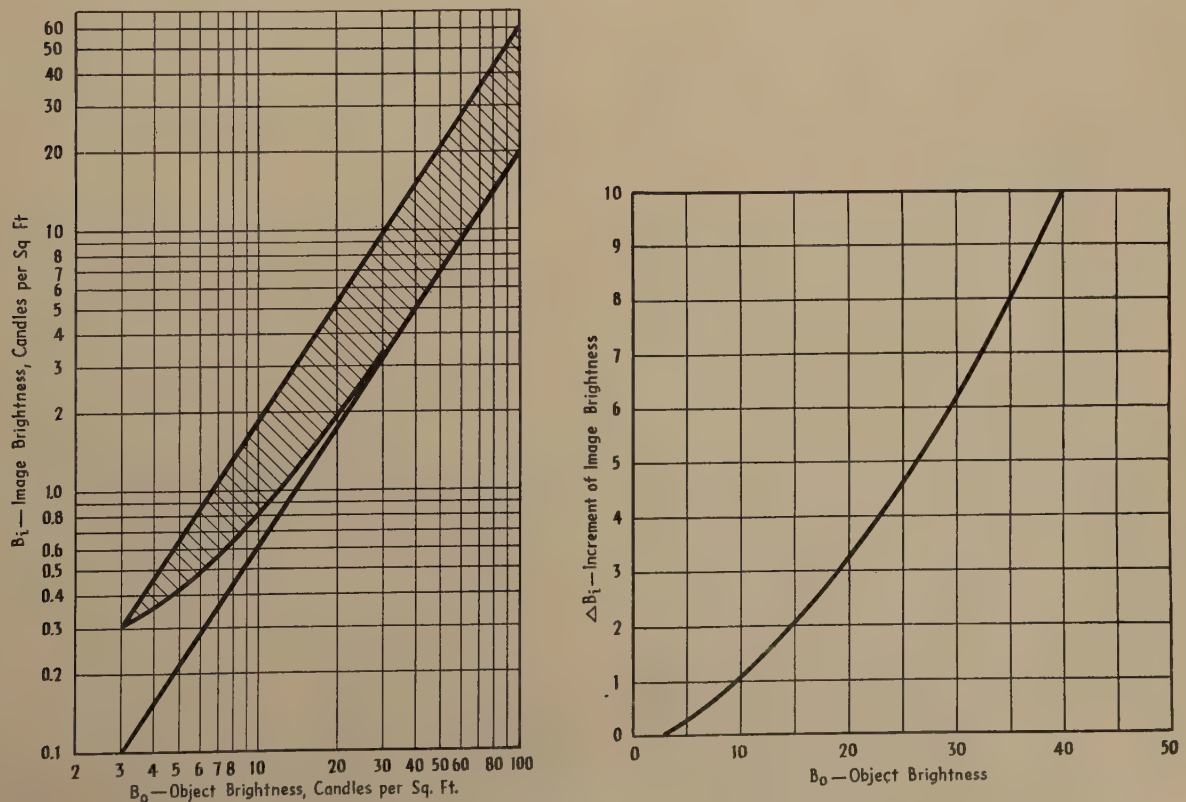

Fig. 14—Compensation of ambient illumination.

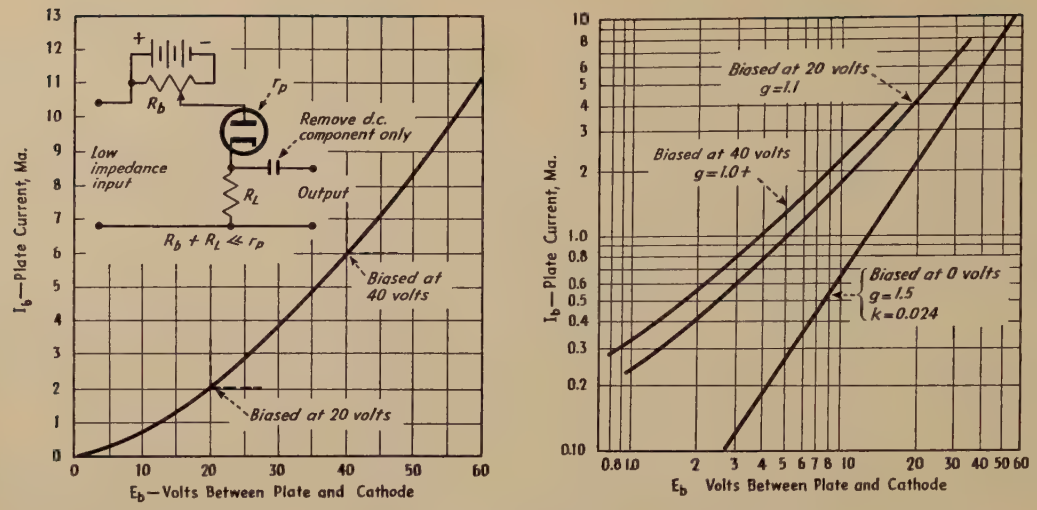

Fig. 15—Use of a diode as a voltage-divider element to introduce controllable nonlinearity.

such a characteristic is added, in a logarithmic amplifier for example, the effect on signal-to-noise ratio is reversed, since the noise generated in the camera circuit is thereby augmented in the shadow portions of the picture, precisely where it will have the most visible effect. Hence contrast modulation can be applied in this case only when the illumination of the subject is sufficiently adequate to avoid noise difficulties in the camera circuits. If this condition is satisfied, contrast modulation has the advantage of suppressing the effect of noise introduced after the camera circuits and before the picture tube.

Compensation of Ambient Illumination

One of the interesting possibilities in the use of controlled brightness distortion is that of compensating for ambient illumination at the receiver. In Fig. 14 there is shown in the lowest curve at the left a typical brightness transfer characteristic in log-log co-ordinates which is linear, i.e., displays no contrast distortion. If ambient illumination produces an additional brightness to the extent of 0.2 candle per square foot, the brightness transfer characteristic is thereby caused to assume the nonlinear shape shown, i.e., the image contrast in the shadow portions is reduced and distorted. One obvious method of correcting for this additional light is to reduce the brightness by an adjustment of the brightness control of the receiver, subtracting from the picture an amount of brightness equal to that due to the ambient illumination. But this procedure is not practical because such a reduction of brightness, if the black level has been previously set at the origin as it should be, places a portion of the shadow detail of the image of the infrablack region of the video signal, and this shadow detail is lost. As an alternative method of correcting for ambient illumination, brightness may be added to the scene by the amount indicated by the shaded area, producing a transfer characteristic free from contrast distortion but having a greater over-all brightness. The difference between the distorted characteristic and the upper linear curve is shown at the right. A transducer planned to add this amount of brightness distortion will accordingly serve to compensate exactly for the ambient illumination, resulting in a picture indistinguishable from the original picture viewed in total darkness, except that the over-all brightness is increased. This analysis serves as an example of the ease with which the problems of tonal representation may be attacked using the log-log brightness transfer characteristic.

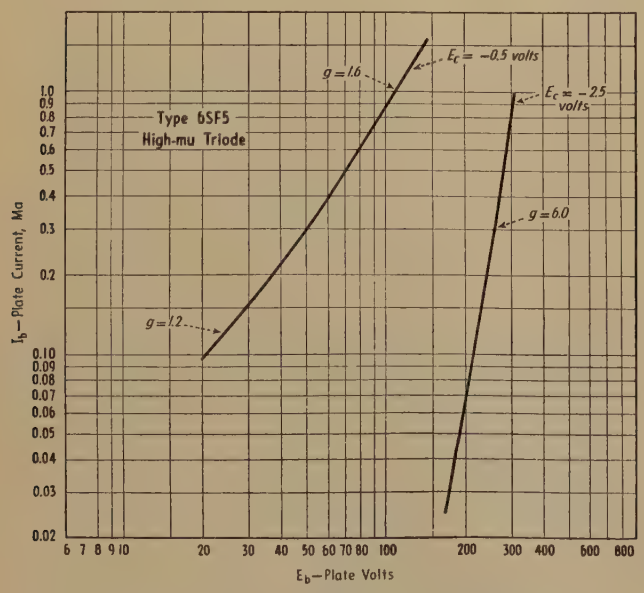

Fig. 16—Gradient characteristics of a triode vacuum tube used as an element in a voltage divider.

Practical Means of Gradient Control

The foregoing discussion has revealed the need for a transducer which will introduce a controllable amount of nonlinearity, particularly of the types represented by power, logarithmic, and antilogarithmic functions. A variety of possible means of so doing are

available. One of the means which has suggested itself to the writer is the use of the internal plate resistance of a vacuum tube as part of a voltage divider. The simplest possible case is that of the diode tube. If the diode follows the Langmuir equation, its plate current will vary as the 3/2 power of the applied voltage, as shown in Fig. 15. This figure is a plot of the plate current versus plate voltage plotted on log-log paper to reveal the gradient, as well as the variations in the gradient, of the associated nonlinearity. The gradient of the plate-current-versus-plate-voltage curve of such a tube is 3/2 or 1.5. If the tube is used as a portion of a voltage divider, as shown in the diagram, and if the external output resistor is small compared with the internal resistance, the output voltage will vary as the 1.5 power of the input voltage. There will be also a loss in the magnitude of the voltage through the transducer, but this loss can be made up in linear amplifiers following the diode. If a biasing battery is placed in series with the anode of the diode, the portion of the 3/2-power curve over which the video voltage varies may be selected with the results shown at the right in the figure. Thus a gradient control having a variable g from 1.0 to 1.5 is readily available.

The triode tube may be used in exactly the same manner, as indicated in Fig. 16. Here the presence of the grid gives the added possibility of control by grid-bias voltage variation. Gradients as low as 1.0 and as high as 6.0 (the latter value is probably outside the useful range) may be obtained by a combination of plate-bias and grid-bias control.

Finally the pentode tube offers possibility of use in a voltage divider with gradients lower than unity, using the upper shoulder of the plate-voltage—plate-current characteristic. Fig. 17 shows that contrast gradients as low as 0.1 and as high as 0.5 may be obtained by grid-bias voltage control alone, and the plate-voltage-bias scheme will extend this range. A combination of the below-unity gradients shown in Fig. 17 with the above-unity gradients shown in Figs. 15 and 16 makes possible a wide variety of over-all gradients.

Other Effects

It is necessary to point out that effects other than the nonlinearity of transducers may have a marked influence on the shape of the brightness transfer characteristic and its associated brightness and contrast distortions. Thus, for example, halation in the picture tube affects the contrast of adjacent areas on the receiver screen, and a spurious signal in the iconoscope likewise has a local effect on relative brightness. The effect of the frequency response on the amplitude of the brightness variations often introduces losses of contrast in portions of the scene depicted by the high- and low-frequency extremes of the video range. These factors must be evaluated when making experimental determinations of the transfer characteristics and in isolating the sources of the brightness distortion.

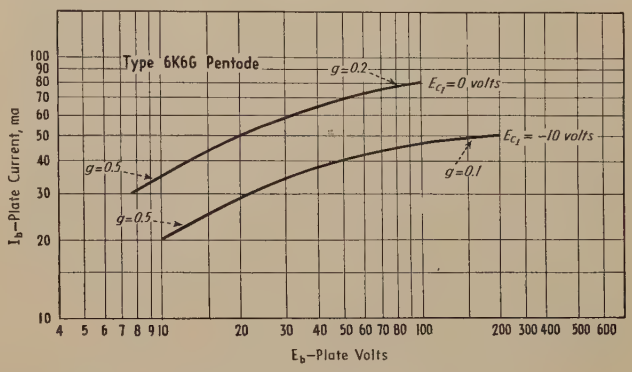

Fig. 17—Gradient characteristics of a pentode vacuum tube, for obtaining gradients lower than unity.

Acknowledgment

The author wishes to express appreciation to Mr. Craig Walsh, Associate Editor of *Electronics*, for a suggestion concerning terminology, and to Mr. Beverly Dudley, Managing Editor of *Photo Technique*, who has contributed greatly to the writer's understanding of photographic tone reproduction, and who suggested the use of log-log plots, from the analogous scheme used to depict the Hurter and Driffield curves of photographic emulsions and processes.

Acknowledgment is also due to Professor John B. Russell of the Marcellus Hartley Research Laboratories of Columbia University, for permission to render this report, which is a part of a graduate research project being conducted under his direction.

Additional References

(1) D. G. Fink, "Principles of Television Engineering," McGraw-Hill Book Company, New York, N. Y., 1940, p. 328.
(2) V. K. Zworykin and G. A. Morton, "Television," John Wiley and Sons, Inc., New York, N. Y., 1940, p. 172.

Measurements of the Delay and Direction of Arrival of Echoes from Near-By Short-Wave Transmitters*

C. F. EDWARDS†, NONMEMBER, I.R.E., AND KARL G. JANSKY†, MEMBER, I.R.E.

Summary—*Observations on pulses radiated by a high-power beam transmitter operating in the short-wave range show that when the receiver is located within the skip zone, echoes are observed having delays of from 1 to 50 milliseconds. These echoes are the result of scattering and three different types may be recognized, each arising from a different source.*

Echoes of the multiple type were found to occur the most frequently and to have many of the characteristics of signals transmitted over long distances. Components were observed from regions up to 4000 miles distant. Direction-of-arrival measurements using steerable arrays operating on the musa principle indicate that these multiple echoes are scattered from regions along the transmitted beam. Vertical angle-of-arrival measurements using a musa receiving system indicate that the surface of the earth may be the source of scattering.

Similarities between multiple echoes and southerly deviated waves from European transmitters have been found which indicate that the same phenomena may be responsible for both.

I. Introduction

THE existence of so-called "short-range" echoes from near-by high-power short-wave transmittors has been known for many years. Echoes of this type were first reported by Taylor and Young,[1,2] in 1928 when they were discovered during the course of studies of around-the-world echoes. Taylor and Young found that these echoes had delays of from 10 to 50 milliseconds and concluded that they were due to scattering, either from the polar regions or from regions where the waves are reflected from the earth's surface. The existence of these echoes was verified by later investigators[3,4] and considerable work has been done on the subject in recent years by T. L. Eckersley.[5]

The existence of these echoes was impressed on the authors' attention in 1930 when it was found that the wobbled carrier then used by the transatlantic short-wave telephone transmitters at Lawrenceville, N. J., had associated with it signal components which were delayed sufficiently to beat with the directly received signal and give rise to a characteristic grumbling sound. This sound was picturesquely referred to as the Lawrenceville "grunt" and was observed at the monitoring station at Netcong, N. J., at all times when transmission conditions were normal. Early investigations made by analyzing oscillograms of the received signal showed the delay of the echo components to be of the order of 10 milliseconds, thus identifying them with those reported by Taylor and Young.

In 1937 measurements were made at Holmdel, N. J., of the direction of arrival of these "grunt" echoes from Lawrenceville using a two-element rotatable direction finder. In the course of these measurements instances were found in which the echo components appeared to return from regions along the transmitted beam, verifying a previous finding by T. L. Eckersley,[6] but in many cases no satisfactory bearings could be obtained. This measuring technique possessed two major defects; first, failure of the null-indicating-type direction finder to give bearings on signal components covering an appreciable range of direction and second, the extremely limited information regarding the number, amplitude, and delay of the echo components provided by wobbled carrier transmission. These tests made it clear that some improvement in equipment and test procedure would be necessary before any new evidence concerning the origin of short-range echoes could be obtained.

II. Equipment

The musa receiving system[7] developed at the Holmdel laboratory has provided the basis for the design of a more effective type of direction-finding system[8] which, when used in conjunction with pulse modulation at the transmitter, constitutes an important improvement in the test procedure. In addition, the use of the musa receiving system with an array of rhombic antennas directed toward England which is capable of quickly determining the vertical angle of arrival of signals within its range has made possible further investigations into the nature of short-range echoes.

The direction-finding system used in determining the direction of arrival of these echoes consists of two linear arrays of vertical antennas having different orientations. In each of these arrays the antennas are spaced 15 meters apart and are connected to the musa receiver through equal-length coaxial transmission lines. One such array is shown in Fig. 1 together with those portions of the musa receiver essential to its use. The fundamental principle of musa operation, viz., that

* Decimal classification: R113.62. Original manuscript received by the Institute, February 5, 1941. Presented, Sixteenth Annual Convention, New York, N. Y., January 9, 1941.

† Bell Telephone Laboratories, Inc., New York, N. Y.

[1] A. Hoyt Taylor and L. C. Young, "Studies of high-frequency radio wave propagation," PROC. I.R.E., vol. 16, pp. 561–578; May, 1928.

[2] A. Hoyt Taylor and L. C. Young, "Studies of echo signals," PROC. I.R.E., vol. 17, pp. 1491–1507; September, 1929.

[3] J. B. Hoag and Victor J. Andrew, "A study of short-time multiple signals," PROC. I.R.E., vol. 16, pp. 1368–1374; October, 1928.

[4] E. Quäck and H. Mögel, "Short range echoes with short waves," PROC. I.R.E., vol. 17, pp. 824–829; May, 1929.

[5] T. L. Eckersley, "Analysis of the effect of scattering in radio transmission," *Jour. I.E.E.* (London), vol. 86, pp. 548–567; June, 1940.

[6] T. L. Eckersley, "Scattering, polarization errors and the accuracy of short wave direction finding," *Marconi Rev.*, no. 53, p. 1–8; March–April, 1935.

[7] H. T. Friis and C. B. Feldman, "A multiple unit steerable antenna for short-wave reception," PROC. I.R.E., vol. 25, pp. 841–917; July, 1937.

[8] C. B. Feldman, "Deviation of short radio waves from the London-New York great-circle path," PROC. I.R.E., vol. 27, pp. 635–645; October, 1939.

of steering the array characteristic by means of rotatable phase changers, is used.

The angle β between the array axis and the direction of maximum reception is given by the relation

$$\cos \beta = \frac{\lambda}{360\, D} \phi \qquad (1)$$

where D is the antenna spacing, λ the wavelength, and ϕ the phase-changer dial setting in degrees. Since β is measured from the array axis, this direction of maximum reception is a cone whose axis is the axis of the array and whose generator is at an angle β with this axis. In the absence of other information concerning the direction of arrival, a determination using a single array is thus inconclusive. When two arrays having different orientations are used, however, a value for β may be determined on each array separately and the

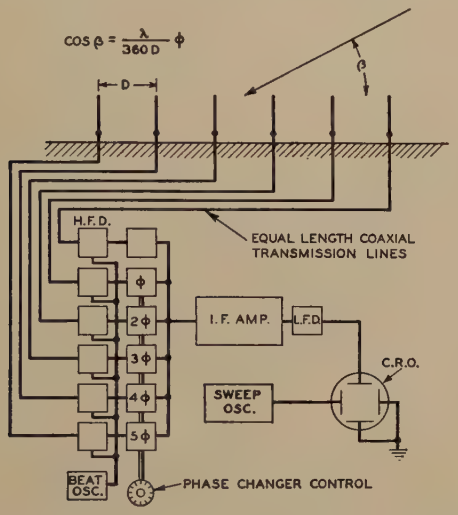

Fig. 1—Musa-type direction-finder-array schematic.

two cones thus established will then intersect along the direction of propagation of the wave which determines both the horizontal direction and the vertical angle of arrival. Considering one array only, the horizontal direction α and the vertical angle of arrival δ are related to β in the equation

$$\cos \beta = \cos (\alpha - \theta) \cos \delta \qquad (2)$$

where θ is the orientation of the array axis. This is shown for the two arrays in Fig. 2 where each curve corresponds to the indicated value of β and α is plotted in degrees clockwise from north.

Since the antenna spacing is fixed at 15 meters it will be seen from (1) that a unique solution is obtained only when the wavelength is greater than 30 meters and β is single valued during a 360-degree change in ϕ. When the wavelength is between 15 and 30 meters, β becomes double valued and the system yields, in general, two solutions for the direction of wave propagation. Frequently one of these solutions can be rejected because its value of δ is unreasonably large but, in general, additional information must be resorted to if a choice is to be made.

The pulse transmissions for these tests were made by the American Telephone and Telegraph Company using the commercial transmitters and their associated arrays located at Lawrenceville, N. J. The receiver is located at Holmdel, N. J., 32 miles distant. The map

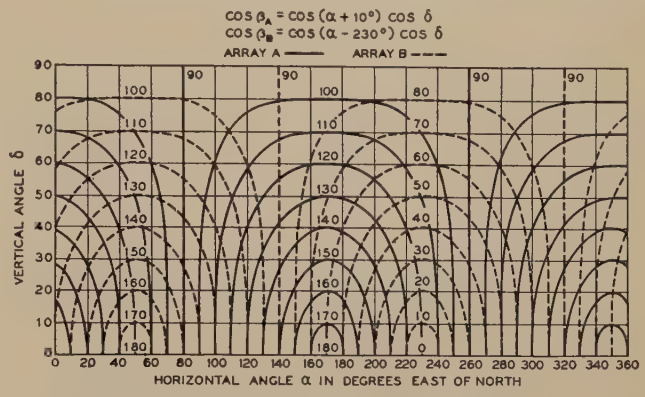

Fig. 2—Curves for converting direction-finder angles into vertical and horizontal directions.

in Fig. 3 shows the location of the two stations and the orientations of the transmitting arrays used. In all of the tests, except one, a transmitting array directed toward London (50 degrees east of north) was used. In the one remaining test an array directed toward Buenos Aires (166 degrees east of north) was used. In both cases the receiver is well off the transmitted beam.

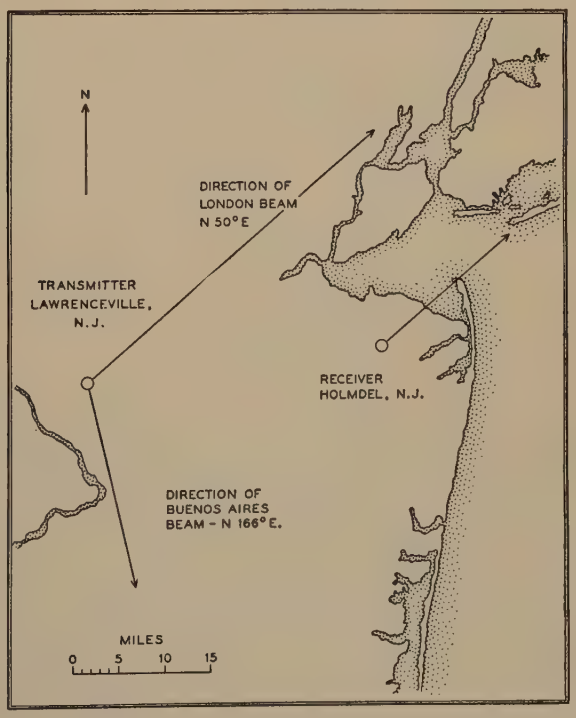

Fig. 3—Transmitter and receiver locations.

Two series of tests were conducted, the first using pulses 125 microseconds in length and the second using pulses 800 microseconds in length. In both cases the pulsing rate was 10 per second. The transmissions were received with the Holmdel experimental musa receiver using the antenna systems described above and the

pulses were observed by means of a cathode-ray oscilloscope in the usual manner. The sweep voltage for the cathode-ray oscilloscope was obtained from a gas-tube oscillator giving 10 sweeps per second which were synchronized with the 60-cycle power supply. Since the transmitting station was supplied by the same power system perfect synchronization was obtained without additional equipment.

The 125-microsecond pulses were generated by means of a Thyratron pulser arranged so that pulses of carrier frequency were delivered by the crystal-controlled oscillator to the transmitter power-amplifier stages. At the receiver, an intermediate-frequency amplifier having a band width of 20 kilocycles was used. This band width is adequate for the reception of 125-microsecond pulses without distortion.

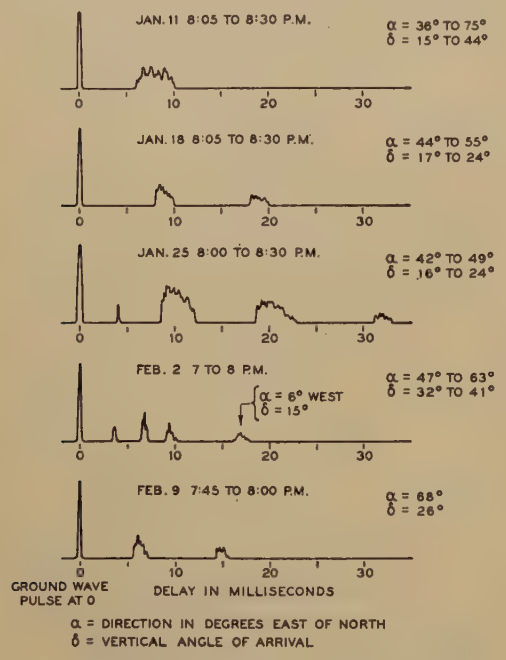

Fig. 4—Echoes observed in the first series of tests. WON, 9870 kilocycles.

The change from 125- to 800-microsecond pulses was made after it was found that the 125-microsecond pulses were unnecessarily short and that the wide receiver band width necessary resulted in an undesirably poor signal-to-noise ratio. These longer pulses were obtained in a somewhat different manner. It was found that by modulating a single-sideband reduced-carrier transmitter with pulses of 5000-cycle tone, satisfactory pulses of carrier could be obtained. The pulses of tone were generated by means of a small motor-driven commutator connected in the output of a 5000-cycle oscillator. This in turn was connected to the speech-input terminals of the transmitter. With reduced carrier at the transmitter and the large carrier rejection provided by the receiver selectivity, this method did not differ materially from the one in which straight carrier pulses were employed. Since the commutator was in contact only for about 4 cycles of the 5000-cycle tone, there was probably some variation in the pulse length but no effects from this cause were observed. At the receiver an intermediate-frequency filter having a band width of 3.2 kilocycles was used and considerable improvement in signal-to-noise ratio was thereby obtained.

III. Results

The first series of tests using 125-microsecond pulses were made between January 11 and February 9, 1939. The pulse transmissions were radiated by WON operating on 9870 kilocycles and using an array directed toward London. This frequency was chosen so that measurements of the direction of arrival made with the vertical-element musas would not yield more than one solution. All observations were made at some time between 7:00 and 8:30 P.M.

Fig. 4 shows sketches of typical echo pulse patterns observed during each test of this series together with the values of α and β obtained with the vertical-element arrays. The relative amplitudes shown approximate those obtained without receiving-array directivity. The intensity of these echoes varied considerably but was generally quite low, observations frequently being prevented by atmospheric noise. The echoes were strongest on January 25 but during a test on February 6 (not indicated) no echoes were observed, presumably because of disturbed transmission conditions.

Twelve measurements of the direction of arrival of the echoes made with the vertical-element arrays are given in Table 1.

TABLE I

Number of Observations	α	β
	Degrees	Degrees
6	44 to 55	22 to 38
5	36 to 75	15 to 44
1	354	15

In the first group α corresponds quite closely to the direction of the transmitted beam while the range of β is somewhat above that commonly observed on 30-meter transatlantic signals. In the second group the general direction of arrival is roughly the same but the spread is greater both horizontally and vertically. The direction of arrival of the third single-echo group appears unrelated to that of the transmitted beam. When received on a rhombic antenna directed 50 degrees east of north the echoes in the first group were of the order of 15 decibels stronger than when received on a vertical antenna.

As seen in Fig. 4, the echoes under consideration are complicated and contain components from more than one source. Three different types of echoes are recognized:

1. "Multiple echoes," observed on January 18, 25, and February 9, in which succeeding echoes have delays which are approximate multiples of the delay of the first echo in the group.

2. Random echoes, observed on January 11 and February 2, whose direction of arrival is not closely associated with that of the transmitted beam and whose delays are not related to those of the multiple echoes.
3. Sharp echoes, observed on January 25 and February 2, which are low in amplitude and of relatively short delay.

Measurements of the vertical angle of arrival of the strong multiple echoes observed on January 25 made with the rhombic-element musa showed that in the first echo group the early part arrived at a higher angle than the later part. The measured angles were 24 and 16 degrees, respectively. The two succeeding echo groups appeared to be mostly at 24 degrees. Thus the maximum vertical angle at which echo components were received was found to be the same in all three echo groups. As shown in the sketch each echo group was found to decrease in amplitude with increasing delay and succeeding echo groups are weaker. These three characteristics were found to be typical of all multiple echoes.

The single-echo group observed on January 11 appeared to be made up of two components having nearly the same delay but different directions of arrival. A bearing of $\alpha=75$ degrees, $\delta=15$ degrees was obtained on the earlier part and $\alpha=36$ degrees, $\delta=44$ degrees on the later part. Whether echo components were received from intermediate directions could not be determined. No satisfactory bearing measurements were obtained on the sharp echoes of January 25 and February 2.

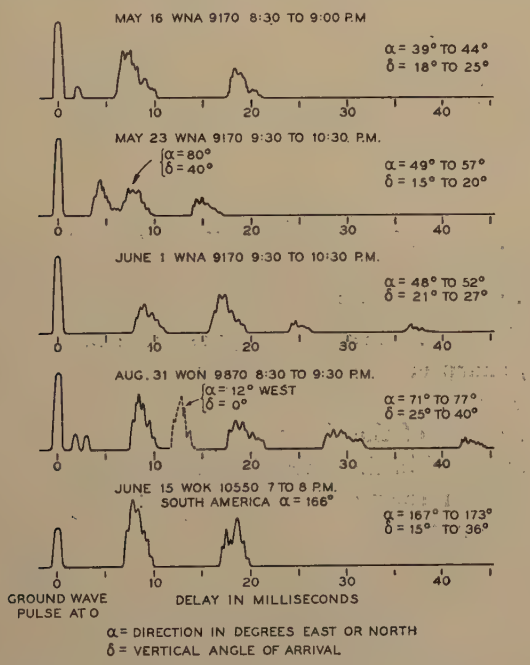

Fig. 5—Echoes observed on 30 meters in the second series of tests.

The second series of tests in which 800-microsecond pulses of single sideband were used were made between May 16 and September 6. Typical echo pulse patterns obtained on 30 meters are shown in Fig. 5 and those obtained on 20 and 16 meters are shown in Fig. 6. The frequency used and the time of each test are also indicated. The transmitting array was directed toward London in all tests except that of June 15 when an array directed toward Buenos Aires was used.

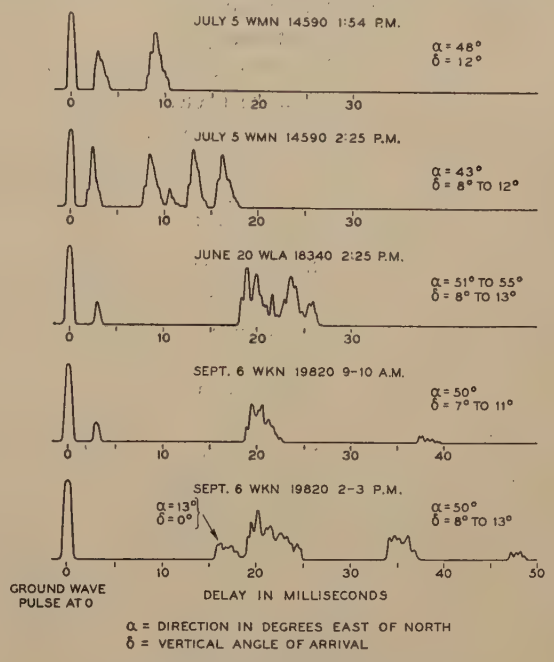

Fig. 6—Echoes observed on 16 and 20 meters in the second series of tests.

Exclusive of the June 15 test, eighteen measurements of the direction of arrival of the echoes were made with the vertical-element arrays. The results are given in Table II.

TABLE II

Number of Observations	α	δ
	Degrees	Degrees
10	45 to 55	7 to 27
6	39 to 80	10 to 40
2	348 and 13	(small)

These are seen to be similar in all respects to the results obtained during the first series of tests. The lower values of δ were obtained during the tests on 16 and 20 meters. Gains in the output of a rhombic antenna over a vertical of between 14 and 18 decibels were obtained on May 16, 23, July 5, and September 6.

The echo pulse patterns in Figs. 5 and 6 show the same three types of echoes as were observed during the first series of tests. The multiple echoes observed on May 16, August 31, and September 6 exhibited the three typical characteristics found before. Some new effects were observed, however. In the pattern obtained on June 1 the second echo group appears stronger than the first. On the basis of past experience it would appear that the second group is a random echo which happened to be from the same direction as the multiple echoes. The random echo from 12 degrees

west of north observed on August 31 was found to fluctuate widely in amplitude. During this same test two sharp echoes were observed instead of one.

The improvement in signal-to-noise ratio obtained with the longer pulses made measurements during disturbed transmission conditions possible. On May 23 and June 20 transmission conditions were moderately disturbed and on July 5 were greatly disturbed. The echo patterns obtained during these tests are seen to be more complicated than usual and do not exhibit the "multiple-echo" characteristics. Furthermore the delay range appears restricted and the echoes in the 2- to 5-millisecond range observed on May 23 and July 5 lack the sharpness usually found. With the exception of the test on May 23, which was made at night, the direction of arrival of the echoes is quite close to that of the transmitted beam.

During the tests on September 6, measurements were made of the field strength and vertical angle of arrival of signals from GAU at Rugby, England, operating on a frequency of 18,620 kilocycles. These were compared with the data obtained on the multiple echoes from WKN. The angles of arrival of the two signals were found to be not very different. For example, during the morning test the angle of arrival of the echoes was from 7 to 11 degrees while GAU showed a strong path at 6 to 10 degrees and a weaker one at 13 degrees. During the afternoon test the angle of arrival of the echoes measured 8 to 13 degrees and GAU measured 11 to 13 degrees. A great difference in intensity was observed, however. During the afternoon test it was estimated that the echoes were of the order of 40 decibels weaker than the signals from GAU.

At 3:05 P.M. on September 6, immediately following the pulse test with WKN, a sudden ionospheric disturbance or fade-out occurred and the strength of signals from Europe dropped to a very low value. At 3:21 pulse transmission was resumed and no echoes were observed. As the disturbance subsided the echoes gradually reappeared until at 3:42 conditions were back to normal and the echo pulse pattern was practically identical to that observed during the 2 to 3 P.M. test.

In the test on June 15 the double-sideband transmitter WOK was used with an array directed toward Buenos Aires ($\alpha = 166$ degrees). It was modulated with 800-microsecond pulses of 5000-cycle tone as before. Only one sideband was received and the use of double-sideband transmission resulted in reduced pulse power but no carrier interference was experienced and a satisfactory signal-to-noise ratio was obtained. As indicated in the bottom sketch of Fig. 5 the bearing of the echoes was 167 to 173 degrees east of north corresponding closely to the bearing of the transmitted beam. Since the rhombic musa could not be used on signals from this direction, precise angle-of-arrival measurements could not be made.

In Table III are listed all of the tests performed and the type of echoes observed during each. Included in the list are the three tests made during disturbed transmission conditions for which the echoes are listed as unclassified. Echoes of the multiple type are seen to occur most frequently and were found during all but two of the tests made during undisturbed conditions. Random echoes were found during about half of the tests and sharp echoes occurred about as often.

TABLE III

Date	Time	Frequency Kilocycles	Type of Echoes Observed
Jan. 11	8:05 to 8:30 P.M.	9870	Random
Jan. 18	8:05 to 8:30 P.M.	9870	Multiple
Jan. 25	8:00 to 8:30 P.M.	9870	Multiple, Sharp
Feb. 2	7:00 to 8:00 P.M.	9870	Random, Sharp
Feb. 9	7:45 to 8:00 P.M.	9870	Multiple
May 16	8:30 to 9:00 P.M.	9170	Multiple, Sharp
May 23	9:30 to 10:30 P.M.	9170	Unclassified
June 1	9:30 to 10:30 P.M.	9170	Multiple, Random
June 15	7:00 to 8:00 P.M.	10550	Multiple
June 20	2:25 P.M.	18340	Sharp, Unclassified
July 5	1:30 to 2:30 P.M.	14590	Unclassified
Aug. 31	8:30 to 9:30 P.M.	9870	Multiple, Random, Sharp
Sept. 6	9:00 to 10:00 A.M.	19820	Multiple, Sharp
Sept. 6	2:00 to 3:00 P.M.	19820	Multiple, Random

The direction of arrival of the multiple echoes was found to be within 8 degrees of the direction of the transmitted beam in all cases except two. On February 9 their direction was about 18 degrees south and on August 31 about 24 degrees south of the direction of the transmitted beam. Both of these tests were made on 30 meters at night which suggests that there might be some similarity between this effect and the moderate southerly deviations (i.e., less than 20 degrees) of transatlantic signals. The direction of arrival of the random echoes was confined to the sector between 12 degrees west and 80 degrees east of north. No satisfactory determinations of the direction of arrival of the sharp echoes were obtained.

IV. Conclusions

The results of these tests indicate that at least three different types of echoes may be received from a high-power beam transmitter by a receiver located within the skip zone. These three types have been described as (1) sharp echoes, (2) random echoes, and (3) multiple echoes.

The origin of the sharp echoes is not clear from the data acquired in these tests since no satisfactory measurements of their direction of arrival were obtained. They are not believed due to normal-incidence reflection in the ordinary sense since they were observed at frequencies as high as 19.82 megacycles and their intensity was always below that of the other echoes.

Random echoes do not occur as frequently as multiple echoes and, since their direction of arrival is not closely associated with the orientation of the transmitted beam, apparently arise from different causes than those responsible for multiple echoes. The maximum delay observed on these echoes was 18 milliseconds. It is believed that they are caused by irregularities in the ionosphere such as sporadic E regions or ionospheric "clouds."

The multiple echoes appear to be the most consistent both in point of frequency of occurrence and direction of arrival. Regarding them the following generalizations may be made:

1. They consist of several echo groups, each succeeding group having a delay which is an approximate multiple of that of the first group. The maximum delay may be as much as 50 milliseconds.
2. Each group is complex and contains components covering a delay range of about 4 milliseconds.
3. When a directional transmitting array is employed, they normally return from regions along the transmitted beam.
4. Their vertical angle of arrival is similar to that of signals received from a distant transmitter via the same transmission path and on a near-by frequency.
5. Their intensity is of the order of 40 decibels below that of signals from such a distant transmitter.
6. The intensity of successive echo groups varies ap-approximately inversely with the delay.
7. In the first echo group at least, components having the shortest delay arrive at the highest vertical angle.
8. In a single echo group, the early or high-angle portion is the strongest.
9. They are adversely affected by ionospheric disturbances, either losing many of the above characteristics or being replaced by echoes of another type during ordinary disturbances and disappearing entirely during "fade-outs."

A possible explanation of the manner in which multiple echoes are produced is that, as the signals radiated by the transmitter are propagated between the ionosphere and the earth as in ordinary long-distance transmission, sufficient roughness in the earth's surface exists to produce scattered radiation and that this scattered energy, returning along its original path from successive regions of reflections from the earth, is received in the immediate vicinity of the transmitter as multiple echoes.

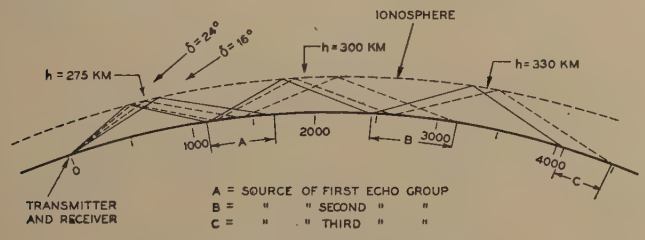

Fig. 7—Paths of multiple echoes on January 25, 1939.

In Figs. 7 and 8 are shown scale drawings of the paths followed by the echoes on January 25 and September 6 following this hypothesis. These drawings were constructed by first plotting path length versus echo group number as shown by the heavy horizontal bars in Fig. 9. Since it was observed that the components in the early portion of each echo group have the same angle of arrival they must have traveled along a single common path. The left end of the bars in Fig. 9 thus give the distances along this path to the reflection points. If we assume these to be at the earth's surface a curve drawn through these ends will, under

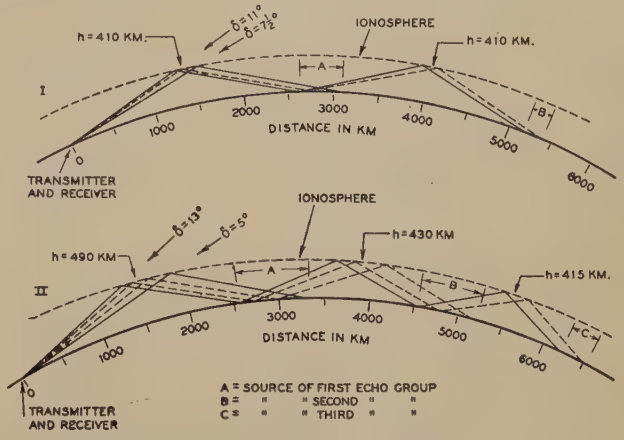

Fig. 8—Paths of multiple echoes on September 6, 1939.

idealized conditions, give the distances to the points of reflection from the ionosphere at ordinate values of $\frac{1}{2}$, $1\frac{1}{2}$, and $2\frac{1}{2}$.

The shape of this curve is determined by the manner in which the height of the ionosphere varies along the path. Thus, a similar curve passing through the origin

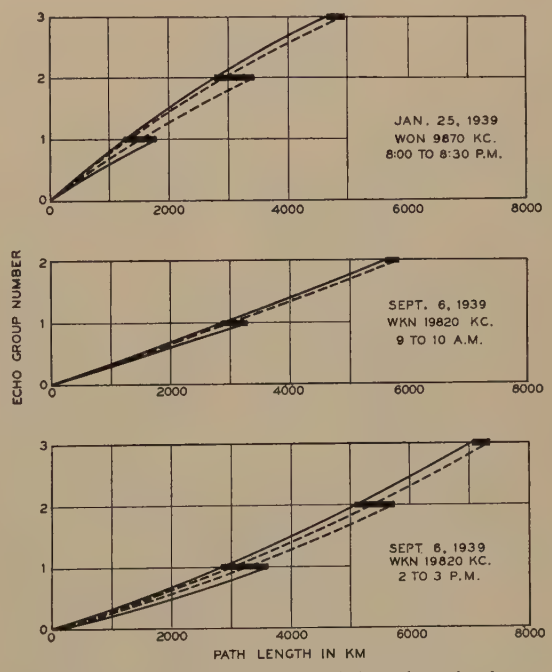

Fig. 9—Relation between path length and echo group number for multiple echoes.

and other measured points gives conditions along other paths having different vertical angles of arrival and reflected from the same ionospheric layer.

The position of the ionosphere in Figs. 7 and 8 was thus determined[9] by the measured angle of arrival and

[9] The layer heights shown are not those for a constant ionic density since rays at different angles penetrate the layer different amounts. The constant-ionic-density height varies along the path in the same manner but to a somewhat greater extent than that shown.

the path length values obtained from Fig. 9 plus the condition that the angles of incidence and reflection are the same at each ground reflection point. In checking the vertical angle of arrival of the later portion of the first echo group determined in this manner against the measured value, good agreement was obtained on January 25 and on the morning of September 6. For the last test, however, the calculated value was 5 degrees while the measured value was 8 degrees.

That these echoes are the result of scattering is at once suggested by their complexity and low intensity. The reason for the assumption that this scattering occurs at the earth's surface and not in some low layer, such as the E layer, is that no echoes were found corresponding to the point where the energy first strikes such a layer. The sharp echoes have about the right delay to fill this role but they do not appear to be necessary accessories to multiple echoes and the relative intensity is much too low. Thus if a low layer is responsible for multiple echoes it must be one which will scatter only the energy striking it from above.[10]

The conditions which must be fulfilled in order that "rough" surfaces act as regular reflectors is given in the relation

$$\frac{2H}{\lambda} \sin \delta \ll 1$$

where H is the difference in elevation, λ the wavelength, and δ the angle of incidence measured from the plane of the surface.[11] Thus as δ decreases, conditions producing scattering are less effective and those favoring regular reflection are improved. This effect operates in a manner which would tend to cause the intensity of a single echo group to decrease with increasing delay and decreasing angle of arrival. Other effects tending to produce this same result are the reduced efficiency of both transmitting and receiving arrays at low angles and the inverse distance loss in intensity. It does not seem unreasonable that these three effects are sufficient to account for the observed tapering in the intensity of a single echo group. However, the issue is seriously confused by such unknown factors as the variation in E-layer absorption and changes in the refracting efficiency of the upper layer with a changing angle of incidence.

The upper limit of angle of arrival at which echo components may be received is sharply restricted by the degree of ionization of the layer while the above-mentioned effects act to limit more or less gradually the lower angle of arrival. It thus appears that energy is being scattered from all regions beyond the first skip zone but only those components within the relatively small angular ranges shown in Figs. 7 and 8 have sufficient intensity to be observed.

The restriction imposed by atmospheric noise on the minimum observable intensity of echo components is the factor responsible for the incomplete appearance of the diagrams in Figs. 7, 8, and 9. Thus in Figs. 7 and 8 it appears that the only reason for not continuing the lowest angle ray beyond zone A is that components scattered from regions beyond zones B and C at this angle were too weak to be observed. If this ray were continued, zones B and C would be greatly extended, and in Fig. 9 the curve joining the origin with the right-hand end of the bar corresponding to the first echo group could be similarly completed. Thus, if sufficient improvement in the signal-to-noise ratio could be effected, succeeding echo groups in the multiple-echo pulse patterns would appear longer and each would cover the same angular range instead of appearing shorter and covering smaller angular ranges as was observed.

V. Additional Tests and Conclusions

In addition to the foregoing tests, observations have been made since September, 1938, on signals from WGEO (formerly W2XAF) at Schenectady, N. Y., operating on 9530 kilocycles. This station is 167 miles distant in a direction 6 degrees east of north and broadcasts to South America during the evening hours on an array directed 13 degrees east of south with a carrier power of 50 kilowatts.

During the few periods when ionization was sufficient to locate the Holmdel receiver beyond the skip zone, signals were observed to arrive from the direction of the transmitter at vertical angles between 55 and 70 degrees corresponding to direct reflections from the ionosphere at heights of 200 to 400 kilometers. At all other times the signals were observed to arrive from the south (13 degrees east of south ± 20 degrees) at vertical angles less than perhaps 30 degrees. Most of these latter observations were made after 7 P.M. when the ionization is less than during daylight hours.

This phenomena appears identical, as far as can be determined, to the multiple echoes observed on the Lawrenceville pulses. The quality and signal-to-noise ratio were always poor but otherwise the signals were intelligible. In addition, fluttery signal components were sometimes observed coming from the northerly regions. These undoubtedly correspond to the random echoes from the north observed during the pulse tests.

The theory given above, describing the manner in which multiple echoes are produced, when extended to include the case in which the transmitter and receiver are widely separated provides an explanation for the large horizontal deviations (20 degrees and more)[12]

[10] In the excellent and extensive treatment of the subject of echoes and scattering by T. L. Eckersley,[6] echoes very much like the first of a series of multiple echoes are described and considerable evidence is presented showing that they are scattered from the E layer. However, no mention whatever is made of multiple echoes. The existence of a layer capable of scattering from one side only (upper or lower) is proposed by Eckersley but only for the purpose of accounting for certain otherwise incompatible types of normal-incidence echoes which are occasionally observed.

[11] See R. W. Wood, "Physical Optics," third edition, Macmillan Company, New York, N. Y., pp. 39–41.

[12] These are to be distinguished from the moderate deviations (less than 20 degrees) which are believed due to a different cause.

observed at times of signals from transmitters in Europe.[8] This case differs from the previous one in that the receiver is no longer within the skip zone. Hence, under normal transmission conditions, it receives the energy propagated along the great circle in the usual manner which, because of its greater intensity, completely obscures any components which reach the receiver as a result of scattering.

If, however, transmission conditions along the great circle become sufficiently poor, the energy scattered from regions along other less affected routes may provide the sole transmission path. Its direction of arrival will, of course, no longer be on the great circle. In the case of signals from European transmitters this requires the further assumption that the disturbing effect of ionospheric storms is most intense in the polar region and becomes less as the distance between this region and the transmission path increases. Thus the spread of this disturbed zone across the transmission path would be accompanied by the decrease and eventual disappearance of the normally propagated signals leaving a residue of southerly deviated signals caused by scattering.

In the map in Fig. 10 are shown a series of scattering zones such as might occur when energy is radiated from Daventry using an array directed toward South America. The location of these zones along the beam depends on the ionospheric height and the frequency used and those shown represent a possible distribution, based on the data obtained on multiple echoes. For the case shown, paths deviating approximately 20, 50, and 82 degrees south of the great circle are possible. It will be observed that for the more widely deviated directions, signal components from a large range of distances may be received within a relatively small azimuthal range as measured at the receiver. The poor quality generally observed on signals arriving via deviated paths is attributed to this large difference in delay between components scattered from widely separated portions of a zone. Which zones as well as which portions of a zone will contribute to the total received energy is, of course, materially influenced by transmission conditions between that zone, or portion thereof, and the receiver. On frequent occasions two deviated paths and, less often, three deviated paths have been observed to exist simultaneously on signals radiated from Daventry on an array directed toward South America. Their azimuthal distribution generally resembles that shown in Fig. 10 and thus it appears that they are the result of scattering from successive zones.

Southerly deviations have in the past been closely associated with transmission disturbances. However, some evidence has been obtained that deviated signals

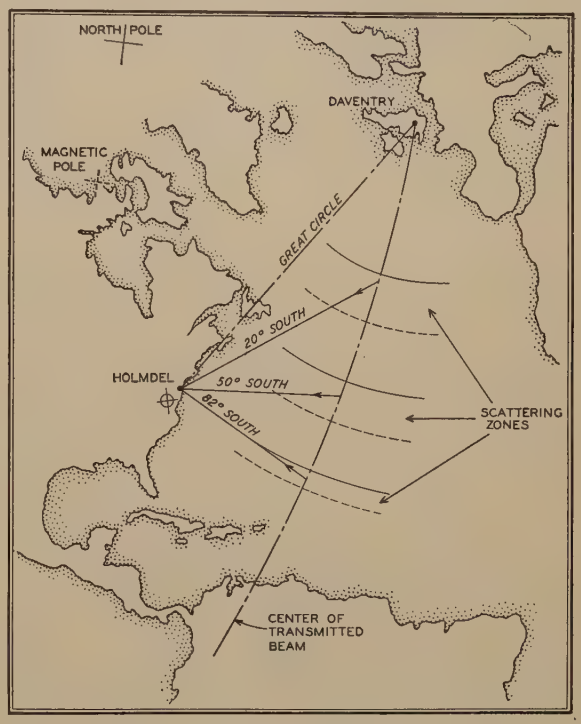

Fig. 10—Routes of southerly deviated waves caused by scattering.

of this type exist during periods of normal transmission conditions, particularly during the evening. When signals radiated from Daventry on the South American array are received at Holmdel with a rhombic antenna directed 70 or 90 degrees south of the great circle, the characteristic "hollow" quality caused by large delay differences is observed. Evidently the discrimination against signals propagated via the great circle occasioned by misdirecting both the transmitting and receiving arrays is sometimes sufficient to permit the weaker scattered energy to be detected.

The Response of Electrical Networks to Non-Sinusoidal Periodic Waves*

NATHAN MARCHAND†, ASSOCIATE, I.R.E.

Summary—*This paper presents a method of obtaining the steady-state solution for the current when a nonsinusoidal periodic voltage wave is applied to the circuit. The idea of obtaining an exponential equation for a nonsinusoidal steady-state current wave is not new, but the methods of obtaining it have been long and cumbersome. This paper shows a method of direct attack which yields the final result quickly and easily. One cycle of the steady-state voltage is all that is used and the solution follows the ordinary differential-equation method of obtaining the transient. However, the integration constants for the steady-state solution are obtained by equating the current at the end of one cycle, or part of a cycle, to the current at the beginning of the next part, and the final result is thus obtained.*

Introduction

NONSINUSOIDAL periodic waves have assumed much greater importance lately with the advent of television and facsimile. They are encountered in sweep circuits, synchronizing signals, and in the pictures themselves. In these instances, the actual shapes of the waves are important, not the harmonic content. When a nonsinusoidal periodic wave is applied to an electric network the steady-state current also assumes a nonsinusoidal periodic wave shape. The problem dealt with here is the solution for the equation of the current wave when the voltage wave is known.

One method of handling this problem which has received very wide attention is Fourier analysis. In this method the voltage wave is broken down into a series of sine waves, very often an infinite series. The steady-state current for each one of these sine waves is then obtained by the well-known solution for such waves. By means of superposition, the resultant steady-state current wave shape is then obtained. The only method of obtaining the actual shape of the resultant wave is by adding the series of sine waves graphically, and this is difficult to handle. The very fact that an infinite series of terms is usually obtained is also a great drawback.

Another method of handling this problem which is not very well known is the "transient-series" attack. In this method, each cycle of the voltage wave is considered to be a transient disturbance. At the beginning the switch is assumed to be closed at the instant that one of the cycles is just beginning and the transient current disturbance is solved for and obtained in an exponential form. The current at the end of the cycle is then obtained. This end current is used to obtain the integration constants for the transient wave of the next cycle. Thus, at the beginning, the integration constants are obtained from at-rest conditions, and for each new cycle whose solution is obtained, the integration constants are obtained from the final conditions of the last cycle. In this manner an infinite series of transient expressions displaced in time is obtained. In most cases, from inspection, these may be evaluated into a finite number of terms. This is still a laborious method and the final results depend upon the inspection of an infinite series of terms. However, the results are much better than those obtained with Fourier analysis, since a definite exponential expression for the resultant current shape is obtained in the final result.

* Decimal classification: R140. Original manuscript received by the Institute, November 14, 1940; revised manuscript received, April 17, 1941.

† Federal Telegraph Company, Newark, N. J.; formerly, Radio-Television Institute, Inc., New York, N. Y.

Description of the Method

In the method suggested by this paper, the result that would be obtained by the transient-series method is obtained by a much shorter and more direct means. The equations are set up to obtain the so-called complete solution for one of the intermediate cycles. A constant m in the equation is used to locate the cycle. This constant m may be any even integer. Thus the equation for the voltage is

$$e = f(\omega t) \text{ where } \pi(m-1) < \omega t < \pi(m+1). \quad (1)$$

The limits of variation of ωt confine the equation to the length 2π of one cycle of the periodic function. Applying Kirchhoff's law to the electric network, the general equation is obtained as follows:

$$L\frac{di}{dt} + Ri + \frac{1}{C}\int i\,dt = f(\omega t). \quad (2)$$

This equation is solved for i by the conventional means used in differential equations. Very often it is easier to solve for the charge q and then obtain i by differentiating q. Either way, however, the solution takes the same form. The solution for an equation like that shown in (2) has two parts, one of which may be called the particular solution, and the other the general solution. The particular solution is obtained by solving (2) as it stands, and this solution usually offers no difficulty. The general solution is obtained by equating the right-hand member of (2) to zero and then solving. A number of integration constants are obtained in the general solution which must be evaluated.

In order to understand the theory behind this evaluation it is necessary to review some of the fundamentals. When a periodic repeating voltage is applied to an electric network, the steady-state current also repeats itself in each period of the voltage wave. The very fact that Fourier analysis works is a definite proof of this. The equation of the current wave in any circuit is always continuous with time. By continuous is meant that the current has only one value at any one instant.

From this fact is obtained the material from which the integration constants of the general solution may be evaluated. At the time when t is equal to $\pi/\omega(m-1)$, which is at the beginning of the voltage cycle, the current there is equal to the current at t equal to $\pi/\omega(m+1)$ which is at the end of the voltage cycle. This means that at the beginning and end of each cycle the current must return to the same value for the solution to be the steady-state current. Thus by equating the currents of these two instances it is possible to obtain the integration constants of the general solution.

If the voltage wave should have a break in it necessitating the expression of the voltage equation as a series of functions which repeat every cycle, the added integration constants of the general solutions may be evaluated by equating the current at the end of one section of the voltage to the current at the beginning of the next.

Examples

An ideal saw-tooth voltage is shown in Fig. 1 where the voltage may be expressed by the equation

$$e = \frac{E\omega t}{\pi} - m \qquad E\pi(m-1) < \omega t < \pi(m+1). \quad (3)$$

The constant m may be taken equal to zero for sim-

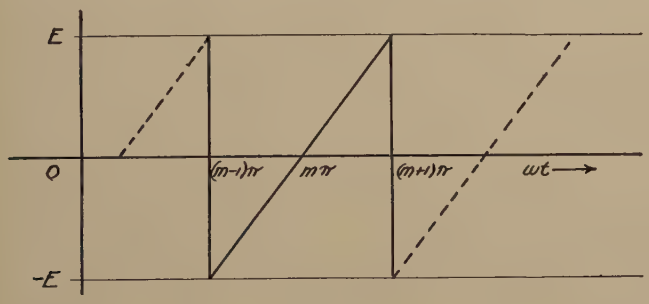

Fig. 1

plicity if it is remembered that at zero time, negative time, or at positive time the circuit is always at steady-state conditions. It shall be carried through in this solution in order to show its significance and in order to obtain a complete solution.

Applying the voltage shown in (3) to the circuit shown in Fig. 2, the following equation is obtained:

$$Ri + \frac{1}{C}\int idt = \frac{E\omega t}{\pi} - mE. \quad (4)$$

In order to remove the integration sign, (4) is expressed in charge q.

$$R\frac{dq}{dt} + \frac{q}{C} = \frac{E\omega t}{\pi} - mE. \quad (5)$$

Equation (5) is a homogeneous linear equation whose right-hand member is not equal to zero. This type of equation has been treated by Lyman M. Kells in his text on differential equations. The solution consists of two parts, one the general solution and the other, the particular solution, as stated previously.

$$q = q_g + q_p. \quad (6)$$

The general solution, from a previous knowledge of equations of this type is

$$q_g = A_1 \exp^{-(t/CR)} \quad (7)$$

where A_1 is an integration constant. The particular solution has the same form as the right-hand member

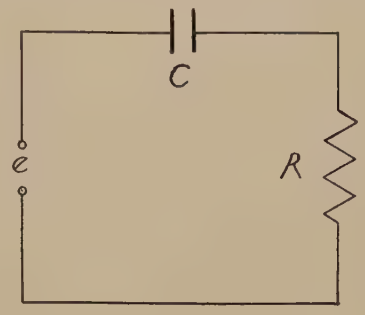

Fig. 2

plus all the forms that can be obtained by means of derivatives.

$$q_p = A_2 t + A_3 \quad (8)$$

where A_2 and A_3 are integration constants. These two integration constants, A_2 and A_3, are what may be called the steady-state integration constants of that cycle. They do not depend upon the initial conditions of the cycle but only upon the voltage applied to the circuit. Thus they may be evaluated by substituting (8) in (5).

$$RA_2 + \frac{A_2 t}{C} + \frac{A_3}{C} = \frac{E\omega t}{\pi} - mE. \quad (9)$$

Since (9) is an identity, the coefficients of like terms must be equal. Thus:

$$\frac{A_2}{C} = \frac{E\omega}{\pi} \quad (10)$$

and

$$RA_2 + \frac{A_3}{C} = -mE. \quad (11)$$

Solving (10) and (11) simultaneously for A_2 and A_3

$$A_2 = \frac{E\omega C}{\pi} \quad (12)$$

and

$$A_3 = -mCE - \frac{RE\omega C^2}{\pi}. \quad (13)$$

Substituting (12) and (13) in the particular solution

$$q_p = \frac{E\omega Ct}{\pi} - mCE - \frac{RE\omega C^2}{\pi}. \quad (14)$$

In order to evaluate the integration constant in q_g it is necessary to return now to the initial condition of the

cycle. First the equation for q is obtained by substituting (7) and (14) into (6)

$$q = A_1 \exp^{-(t/CR)} + \frac{E\omega C}{\pi} t - mCE - \frac{RE\omega C^2}{\pi} \cdot \quad (15)$$

So far the solution has followed the same general trend as the first solution of the transient-series method. In order to evaluate A_1 in the transient-series method, (15) is reapplied theoretically for an infinite number of times. However, this is not necessary if the principles stated in the description of the method are taken into consideration. The current and charge in any electrical circuit are uniformly continuous. This means that the q at the end of the voltage cycle will be equal to the q at the beginning of the voltage cycle. This results in the necessary equation needed to solve for the integration constant A_1. Equating the q at $\omega t = \pi\ (m-1)$ to the q at $\omega t = \pi\ (m+1)$, using (15)

$$A_1 \exp^{-[(m-1)\pi/\omega RC]} + \frac{E\omega C}{\pi} \frac{(m-1)\pi}{\omega} - LCE - \frac{RE\omega C^2}{\pi} \quad (16)$$

$$= A_1 \exp^{-[(m+1)\pi/\omega RC]} + \frac{E\omega C}{\pi} \frac{(m+1)\pi}{\omega} - LCE - \frac{RE\omega C^2}{\pi} \cdot$$

Solving (16) for A_1

$$A_1 = \frac{2EC \exp^{(m\pi/\omega RC)}}{\exp^{(\pi/\omega RC)} - \exp^{-(\pi/\omega RC)}} \cdot \quad (17)$$

Substituting this expression for A_1 in (15)

$$q = \frac{2EC \exp^{(m\pi/\omega RC)}}{\exp^{(\pi/\omega RC)} - \exp^{-(\pi/\omega RC)}} \exp^{-(t/RC)} + \frac{E\omega C}{\pi} t - mCE - \frac{RE\omega C^2}{\pi} \cdot \quad (18)$$

In order to obtain the expression for i, (18) is differentiated and the final result is

$$i = \frac{E\omega C}{\pi} - \frac{2E \exp^{[(m\pi-\omega t)/\omega RC]}}{R(\exp^{(\pi/\omega RC)} - \exp^{-(\pi/\omega RC)})} \quad (19)$$

between the limits $(m-1)\pi < \omega t < \pi(m+1)$ where m is any and all even integers.

Another example is the application of the square-wave voltage shown in Fig. 3 to the circuit shown in Fig. 4. Using the same symbols as in the above example

$$e = E \qquad \pi(m-1) < \omega t < \pi m \quad (20)$$

and

$$e = -E \qquad \pi m < \omega t < \pi(m+1). \quad (21)$$

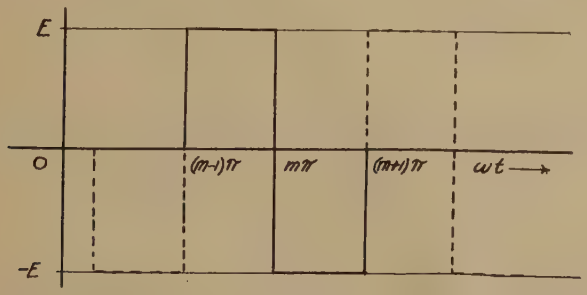

Fig. 3

Since the voltage applied is symmetrical it is evident that the current will also be symmetrical. This means that the solution obtained for the interval

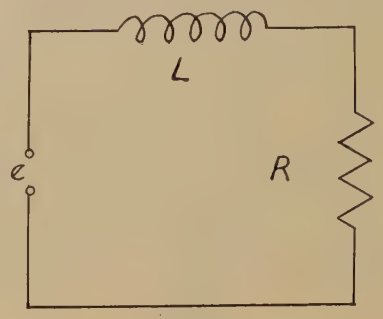

Fig. 4

$\pi(m-1) < \omega t < \pi m$ will be the same as that obtained for the interval $\pi m < \omega t < \pi(m+1)$ with only a change of sign.

Applying Kirchhoff's law to the circuit in Fig. 4,

$$Ri + L\frac{di}{dt} = E \qquad \pi(m-1) < \omega t < \pi m. \quad (22)$$

It is not necessary to use the negative part of the voltage cycle because of symmetry. Equation (22) is similar to the direct-current transient equation. This solution also takes the form

$$i = i_g + i_p \quad (23)$$

as explained earlier in the paper. i_g is obtained by equating the right-hand side of (22) to zero and solving the resultant differential equation. Thus,

$$i_g = A_1 \exp^{-(Rt/L)}. \quad (24)$$

The particular solution will have the same form as the voltage, or

$$i_p = A_2. \quad (25)$$

Substituting i_p for i in (22) and solving for A_2,

$$A_2 = \frac{E}{R} \quad (26)$$

or

$$i_p = \frac{E}{R} \cdot \quad (27)$$

Substituting (24) and (27) into (23),

$$i = \frac{E}{R} + A_1 \exp^{-(Rt/L)} \qquad \pi(m-1) < \omega t < \pi m. \quad (28)$$

In order that the current be symmetrical the current during the negative half of the voltage cycle will be

$$i = -\frac{E}{R} - A_1 \exp^{-(Rt/L)} \qquad \pi m < \omega t < \pi(m+1). \quad (29)$$

Using the theorem, now, that the current is continuous, and as stated before, the current at $\omega t = \pi(m+1)$ will be equal to the current at $\omega t = \pi(m-1)$ time.

$$\frac{E}{R} + A_1 \exp^{-R/L\ [\pi(m-1)/\omega]} = -\frac{E}{R} - A_1 \exp^{-R/L\ [\pi(m+1)/\omega]}. \tag{30}$$

Solving for A_1

$$A_1 = -\frac{2E}{R(\exp^{-R/L\ [\pi(m-1)/\omega]} + \exp^{-R/L\ [\pi(m+1)/\omega]})}. \tag{31}$$

Substituting this solution for A_1 into (29), the complete solution for i is

$$i = \frac{E}{R} - \frac{2E \exp^{-(Rt/L)}}{R(\exp^{-R/L\ [\pi(m-1)/\omega]} + \exp^{-R/L\ [\pi(m+1)/\omega]})}. \tag{32}$$

Conclusion

When this method of solution is used for the application of nonsinusoidal waves to electric circuits an accurate equation of the final current shape is obtained with not too much trouble. The same interpretations for exponential equations as applied to transients may be applied to the results obtained in this manner. The equations are not cumbersome, and the constant m may be equated to zero for still greater simplicity if care is taken to remember that the cycle is actually part of a steady-state condition.

Bibliography

(1) E. A. Guillemin, "Communication Networks," vol. 1, John Wiley and Sons, New York, N. Y., 1931.
(2) L. M. Kells, "Differential Equations," McGraw-Hill Book Co., New York, N. Y., 1935.
(3) R. R. Lawrence, "Principles of Alternating Current," McGraw-Hill Book Co., 1935.
(4) W. L. Everitt, "Communication Engineering," McGraw-Hill Book Co., New York, N. Y., 1937.
(5) E. A. Guillemin and P. T. Ramsey, "Frequency multiplication by shock excitation," Proc. I.R.E., vol. 17, pp. 629–651; April, 1929.

Theory and Application of Resistance Tuning*

CLEDO BRUNETTI†, associate, I.R.E., and ERIC WEISS‡, nonmember, I.R.E.

Summary—*The oscillation frequency of a resonant circuit can be adjusted over a wide range by inserting resistance in series with one or both of its capacitive and inductive arms. Series resistance in the capacitive arm tends to reduce the effective shunt capacitance and thereby to increase the frequency while series resistance in the inductive arm tends to increase the effective shunt inductance and thereby to decrease the frequency. A large variation in frequency requires so much resistance that the wave form becomes distorted. The nonlinear factors which influence the frequency are outlined in theory. Tests conducted with a pentode oscillator based on the reverse transconductance from the suppressor to the screen show that if good wave form is not essential a frequency variation in the ratio of 50 to 1 is possible. The simultaneous opposite variation of resistance in both arms permits a frequency variation of 20 to 1 with some distortion in wave form or 1.5 to 1 with very little distortion and uniform amplitude. In the latter case a linear relationship between resistance and frequency is possible. This device is useful in any applications where it is desired to convert a resistance variation to a frequency variation.*

Introduction

THE possibility of varying the frequency of an oscillator by means of variable resistances instead of the usual variable inductance or capacitance has already led to the development of practical resistance-tuned oscillators.[1–3] The successful designs of Scott and of Terman and his associates employ an amplifier in connection with an inverse-feedback or degeneration network. Resistance tuning is accomplished by varying the resistances in the degeneration network. Good wave form, good frequency stability, and fairly constant amplitude over the audio and ultrasonic tuning range are reported for these circuits.

The purpose of this paper is to point out the practicability of varying the frequency of a simple oscillator by varying the resistance in the conventional tuned oscillating circuit.

The General Circuit

Many of the common oscillators, including the usual triode feedback types, the dynatron, transitron, and diode oscillators, may be represented by the ideal circuit of Fig. 1. Here the two-terminal element to the left of A-B is a device having an operating current-

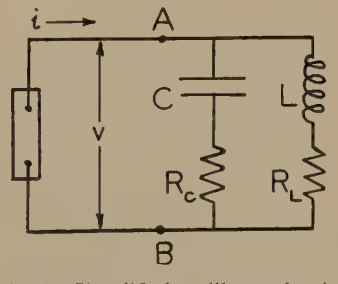

Fig. 1—Simplified oscillator circuit.

* Decimal classification: R141.2×R355.9. Original manuscript received by the Institute, November 1, 1940; revised manuscript received, March 31, 1941. Presented, Sixteenth Annual Convention, New York, N. Y., January 9, 1941.

† Assistant professor of electrical engineering, Lehigh University, Bethlehem, Pa.

‡ Naval Ordnance Laboratories, Washington, D. C.

[1] H. H. Scott, "A new type of selective circuit and some applications," Proc. I.R.E., vol. 26, pp. 226–236; February, 1938.

[2] F. E. Terman, R. R. Buss, W. R. Hewlett, and F. C. Cahill, "Some applications of negative feedback with particular reference to laboratory equipment," Proc. I.R.E., vol. 27, pp. 649–655; October, 1939.

[3] W. G. Gordon and R. E. B. Mackinson, "Resistance tuned oscillators," *Wireless Eng.*, vol. 14, pp. 467–471; September, 1937.

voltage characteristic of the type illustrated in Fig. 2 and represented by the equation.[4]

$$i = \phi(v) = \alpha v + \beta v^2 + \gamma v^3 + \delta v^4 + \epsilon v^5 + \cdots . \quad (1)$$

In general the device may be a vacuum tube or a vacuum tube and an associated circuit. One readily recalls the characteristic of Fig. 2 and its negative slope in connection with the dynatron and transitron oscillators. The "negative slope" or negative-resistance characteristic of the ordinary triode oscillator, though less familiar, has often been pointed out in the literature.[5] This negative-resistance effect exists between the instantaneous plate voltage and plate current during oscillation. Such circuits as those of the tuned plate, Hartley and Colpitts oscillators, and other similar types display this behavior. Thus with proper limitations[6] these oscillators may also be considered as tuned parallel circuits connected to a negative-resistance device.

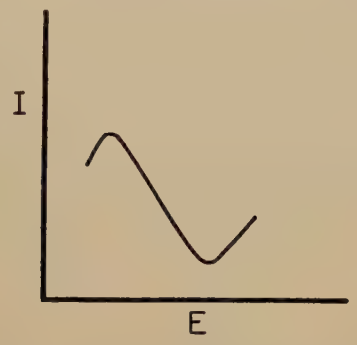

Fig. 2—Current-voltage characteristic of the transitron circuit.

Simple Resistance-Tuned Oscillator

Consider the case where the element to the left of terminals *A-B*, Fig. 1, is a negative resistance of constant value r_n. The admittance of the capacitive arm is

$$y_c = g_c + jb_c$$

$$y_c = \frac{1}{R_c + \frac{1}{j\omega C}} = \frac{1}{R_c} \cdot \frac{1}{1 + \frac{1}{j\omega C R_c}}$$

$$y_c = \frac{1}{R_c} \cdot \frac{1}{1 + \left(\frac{1}{\omega C R_c}\right)^2} + j \frac{1}{R_c} \cdot \frac{\frac{1}{\omega C R_c}}{1 + \left(\frac{1}{\omega C R_c}\right)^2} . \quad (2a)$$

The admittance of the inductive arm is

$$y_L = g_L + jb_L$$

$$y_L = \frac{1}{R_L + j\omega L} = \frac{1}{R_L} \cdot \frac{1}{1 + \frac{j\omega L}{R_L}}$$

$$y_L = \frac{1}{R_L} \cdot \frac{1}{1 + \left(\frac{\omega L}{R_L}\right)^2} - j \frac{1}{R_L} \cdot \frac{\frac{\omega L}{R_L}}{1 + \left(\frac{\omega L}{R_L}\right)^2} . \quad (2b)$$

Oscillations will occur in this circuit when

$$\frac{1}{r_n} + g_c + g_L = 0. \quad (3)$$

The frequency of oscillation will be that which makes

$$b_c + b_L = 0 \quad (4)$$

or

$$\frac{1}{R_c} \cdot \frac{\frac{1}{\omega C R_c}}{1 + \left(\frac{1}{\omega C R_c}\right)^2} - \frac{1}{R_L} \cdot \frac{\frac{\omega L}{R_L}}{1 + \left(\frac{\omega L}{R_L}\right)^2} = 0$$

yielding[7]

$$f = \frac{1}{2\pi\sqrt{LC}} \sqrt{\frac{1 - \frac{C}{L} R_L^2}{1 - \frac{C}{L} R_c^2}} . \quad (4')$$

If $R_L = 0$

$$f = \frac{1}{2\pi} \sqrt{\frac{1}{LC} - \frac{R_L^2}{L^2}} . \quad (4'')$$

If $R_c = 0$

$$f = \frac{1}{2\pi\sqrt{LC - C^2 R_c^2}} . \quad (4''')$$

Inserting (4′) and the real parts of (2a) and (2b) into (3) leads to

$$-r_n = \frac{L}{C(R_L + R_c)} + \frac{R_L R_c}{R_L + R_c} . \quad (3')$$

Thus, if either R_L or R_c or both are varied and r_n adjusted to maintain (3′) the frequency will vary in the manner given by (4′). The latter shows that there is no theoretical lower or upper limit for the frequency range. Equation (4) is shown plotted in Fig. 3 for four different cases.

Curve *A*, Fig. 3(a), shows how the frequency varies when R_c is made zero and R_L varied from $R_L = 0$ to $R_L = \sqrt{L/C}$. Curve *B* of this figure shows the frequency variation when R_L is zero and R_c is varied from $R_c = 0$

[4] In this equation the origin is taken at the center of the negative-sloped portion of the characteristic.

[5] B. van der Pol and E. V. Appleton, "On the form of free triode vibrations," *Phil. Mag.*, vol. 42, pp. 201–220; August, 1921.

[6] The flow of grid current, if present, acts to modify the effect of the tuned circuit in controlling the oscillations.

[7] Equation (4′) may also be arrived at directly by equating the two components of reactive energy in the tuned circuit since the oscillator selects that frequency at which the electrostatic and electromagnetic energies are equal.

to $R_c = \sqrt{L/C}$. Introducing resistance in the C branch would raise the point of intersection of curve A with the frequency axis but not change the value of R_L at which the frequency is zero. In like manner introducing resistance in the L branch would lower the point of intersection of curve B with the frequency axis but not alter the value of R_c required to make the frequency infinite. By varying both R_L and R_c successively it is theoretically possible to vary the frequency from zero to infinity proceeding along curve A, then along curve B.

By varying R_L and R_c simultaneously and keeping their sum constant, the variation of frequency with resistance shown by curves A and B may be combined to yield a result such as that shown in Fig. 3(b). In this case all the resistance is first placed in the C arm and then gradually transferred to the L arm. Reversing this procedure would cause the curves to slope the opposite way.

Curve D is plotted for a total value of resistance slightly less than $\sqrt{L/C}$. Curve E is plotted for a total value of resistance approximately one half that used for curve D. Curve E shows that an almost linear relationship between frequency and resistance is possible over a limited frequency range.

It is seen that by proper choice of L and C the frequency may theoretically be varied over any desired range for any predetermined range of variation of resistance. In practice, however, obvious limitations will prevent the complete attainment of the theoretical behavior.

Theory of the Practical Resistance-Tuned Oscillator

While the linear case treated above serves to give one an insight as to the behavior of a simple oscillator when the resistance is varied, it is not representative of conditions in a practical oscillator. As has been pointed out, the negative-resistance element to which the tuned circuit is connected (Fig. 1) is generally a vacuum tube whose operating current-voltage characteristic is illustrated by Fig. 2. Consequently, the average negative resistance appearing across the terminals of such a device depends on both the amplitude of the oscillations and the shape of the characteristic. It has been shown[8] that when a sinusoidal voltage $v = V \sin \omega t$ is maintained across the terminals of a device whose characteristic is given by (1), the average effective resistance presented by the device is

$$R_n = \frac{1}{\alpha + \frac{3}{4}\gamma V^2 + \frac{5}{8}\epsilon V^4 + \cdots}. \qquad (5)$$

If α is negative, γ positive, and if $\epsilon, \ldots$ etc., take on either positive or negative values then R_n will be negative when V is small. For larger values of V the device will operate over the bends of the characteristic of Fig. 2 and R_n will become increasingly negative, that is, it will remain negative but increase in absolute value. For still larger values of V it is possible for R_n to become infinite and even positive in value.

When such a device is connected to a tuned circuit, as in Fig. 1, to form an oscillator the amplitude of the oscillations will increase and with it the absolute magnitude of R_n until[8] (assuming $R_c = 0$)

$$R_n = -L/R_L C. \qquad (3'')$$

At this point the real energy supplied by the negative-resistance device equals that dissipated in the resistance R_L.

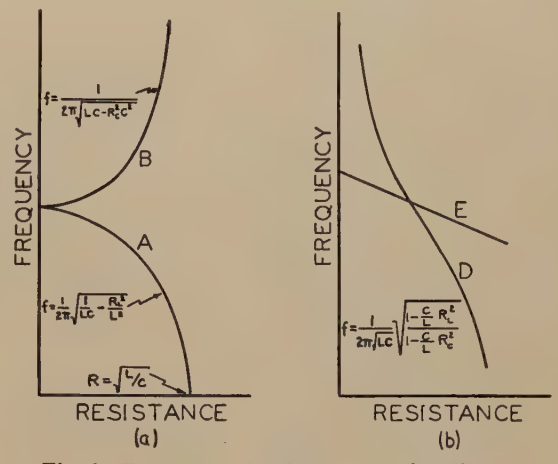

Fig. 3—Frequency of resistance-tuned oscillator.
Curve A: $R_c = 0$, R_L varied from 0 to $\sqrt{L/C}$
Curve B: $R_L = 0$, R_c varied from 0 to $\sqrt{L/C}$
Curve D: $R_L + R_c = k < \sqrt{L/C}$, R_L varied from 0 to k
Curve E: $R_L + R_c \leqq k/2$. R_L varied from 0 to $k/2$

If now R_L be increased, the amplitude of oscillation will decrease slightly, thus decreasing R_n in order to maintain (3″).

In this manner the nonlinear negative-resistance device automatically adjusts the amplitude of oscillation and the magnitude of its average negative resistance R_n so as to maintain a balance in the real energy of the system. By equating (5) and (3″) one may solve for the amplitude of oscillation V as a function of R_L, L, C, α, γ, ϵ, . . . etc. A simple experimental method of predicting the amplitude of oscillation from a set of R_n, V curves based on the above theory has been described in an earlier paper.[8]

It may be noted that (3″), which determines the amplitude of the oscillations, is the same as (3′) (when $R_c = 0$). The latter was derived for a constant negative resistance r_n. It will be interesting and of value to examine whether (4″) giving the frequency of the system when the negative resistance is constant also holds in practice where the negative resistance is the nonlinear quantity expressed by (5). The following treatment of this problem therefore will not only yield the frequency of oscillation but should lead to a better understanding of the theory of oscillations in circuits

[8] Cledo Brunetti, "The clarification of average negative resistance with extensions of its use," Proc. I.R.E., vol. 25, pp. 1595–1616; December, 1937.

in which the coil resistance may not be neglected.[9,10]

The differential equation representing the behavior of the circuit of Fig. 1 (with $R_c=0$) when the relationship between voltage and current in the element to the left of terminals A-B is given by (1) is

$$\frac{d^2v}{dt^2}+\left(\frac{R_L}{L}+\frac{\phi'(v)}{C}\right)\frac{dv}{dt}+\frac{v}{LC}+\frac{R_L}{LC}\phi(v)=0 \quad (6)$$

where

$$\phi(v)=\alpha v+\beta v^2+\gamma v^3+\delta v^4+\epsilon v^5+\cdots \quad (1)$$

and

$$\phi'(v)=\alpha+2\beta v+3\gamma v^2+4\delta v^3+5\epsilon v^4+\cdots. \quad (7)$$

It is possible to find an expression for the frequency by integrating (6) according to the method employed in the astronomical perturbation theory.[11] However, since the resulting voltage will be periodic the frequency may also be found by multiplying each term of (6) by v and then integrating over a complete period. It has been shown that this method of integrating such a differential equation, though much simpler, yields results which agree with the other more rigorous but more complex method.[12]

Proceeding in this manner one obtains

$$\int_0^T v\frac{d^2v}{dt^2}dt+\int_0^T\frac{vR_L}{L}\left(\frac{dv}{dt}\right)dt+\int_0^T\frac{v\phi'(v)}{C}\left(\frac{dv}{dt}\right)dt+\int_0^T\frac{v^2}{LC}dt+\int_0^T\frac{R_Lv\phi(v)}{LC}=0 \quad (8)$$

where $\phi(v)$ and $\phi'(v)$ have the values given by (1) and (7), and $T=2\pi/\omega$. Integrating the first integral by parts transforms it into

$$\int_0^T v\frac{d^2v}{dt^2}dt=-\int_0^T\left(\frac{dv}{dt}\right)^2dt.$$

As v is periodic it may readily be shown that the second and third integrals from the left of (8) are zero. We then have

$$-\int_0^T\left(\frac{dv}{dt}\right)^2dt+\frac{1+R_L\alpha}{LC}\int_0^T v^2dt+\frac{R_L\beta}{LC}\int_0^T v^3dt+\frac{R_L\gamma}{LC}\int_0^T v^4dt+\frac{R_L\delta}{LC}\int_0^T v^5dt+\frac{R_L\epsilon}{LC}\int_0^T v^6dt+\cdots=0. \quad (9)$$

In (9) the only restriction placed on v is that it be periodic. It should now be possible to find a solution for the frequency by assuming v to be made up of an infinite series of harmonic terms

$$v=\sum_{h=1}^{h=\infty}V_h\sin(h\omega t+\theta_h)$$

and inserting in (9). Such a procedure should yield a solution for ω as a function of R_L, L, C, α, γ, ϵ, . . . and the amplitudes of the fundamental and harmonic voltages. While of theoretical value such a solution is difficult to interpret and evaluate. In practice it is generally desirable that the voltage across the tuned circuit be as near a sinusoid as possible. The solution in which we are interested therefore is that which results when the voltage may be represented by $v=V\sin\omega t$. It will be shown later that a quasi-sinusoidal voltage does exist across the tuned circuit of a negative-resistance oscillator over the greater portion of the resistance-tuned frequency range. Inserting $v=V\sin\omega t$ in (9) and integrating, there results

$$\frac{-\omega^2V^2}{2}+\frac{V^2}{2LC}+\frac{1}{2}\left(\frac{R_L\alpha}{LC}\right)V^2+\frac{3}{8}\left(\frac{R_L\gamma}{LC}\right)V^4+\frac{5}{16}\left(\frac{R_L\epsilon}{LC}\right)V^6+\cdots=0$$

which leads to the desired expression for the frequency

$$\omega=2\pi f=\sqrt{\frac{1}{LC}\left[1+R_L\alpha+\tfrac{3}{4}R_L\gamma V^2+\tfrac{5}{8}R_L\epsilon V^4+\cdots\right]}. \quad (10)$$

From (10) it would appear that the frequency depends not only on the constants of the tuned circuit but also on the shape of the current-voltage characteristic of the tube to which it is connected and the amplitude of the oscillations.

However, (10) may be rearranged to yield

$$f=\frac{1}{2\pi}\sqrt{\frac{1}{LC}+\frac{R_L}{LC}\left[\alpha+\frac{3\gamma V^2}{4}+\frac{5\epsilon V^4}{8}+\cdots\right]}. \quad (11)$$

Inserting (5) in (11) leads to

$$f=(1/2\pi)\sqrt{(1/LC)\,(1+R_L/R_n)} \quad (11')$$

but by virtue of the fact that the amplitude of oscillation will be that value which makes $R_n=-L/R_LC$, there finally results

$$f=(1/2\pi)\sqrt{1/LC-R_L^2/L^2}. \quad (12)$$

Thus it is seen that (12) and (4″) are identical. So long as the voltage maintained across the tuned circuit is sinusoidal in shape the resulting frequency will be the same as that computed on the assumption that a linear operating characteristic is employed. The appearance of harmonics in the voltage will cause the frequency to be lower than that computed by (12). This follows in order that the system may maintain a balance between

[9] Since the effect of changing the load on an oscillator is to change the effective resistance of the tuned circuit, one can make use of this analysis to determine the effect of load on the frequency.

[10] The more general but more involved case in which $R_L\neq0$ and $R_c\neq0$ may be treated in a similar manner.

[11] E. V. Appleton and W. Greaves, "Solution of the representative equation of the triode oscillator," *Phil. Mag.*, vol. 45, pp. 401–414; March, 1923.

[12] Balth. van der Pol, "The nonlinear theory of electric oscillations," Proc. I.R.E., vol. 22, pp. 1051–1086; September, 1934.

the electrostatic and electromagnetic energy in the tuned circuit.[13,14] As indicated in (12) when the voltage is sinusoidal the frequency is determined entirely by the constants of the tuned circuit. The only way in which the shape of the operating characteristic affects the oscillations is in determining the amplitude. Since the latter adjusts itself so as to maintain $R_n = -L/R_L C$, no matter whether R_L, L, or C be varied, the second term under the radical in (11′) will always be equal to

$$\frac{1}{LC}\left[\frac{R_L}{-\frac{L}{R_L C}}\right] \text{ or } \frac{-R_L^2}{L^2}.$$

It is interesting to note that neither the frequency nor amplitude of oscillation depends on β, δ, . . . etc., the coefficients of the even terms of v in (1). Also if R_L is reduced to zero the resulting frequency will be

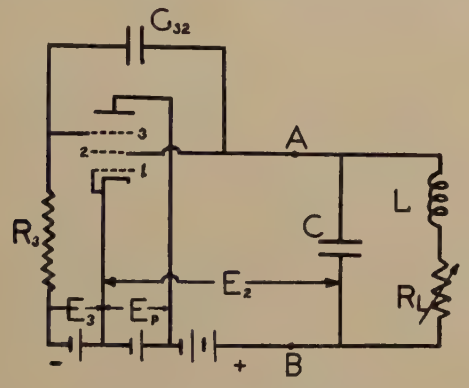

Fig. 4—Transitron oscillator.
Type '57 Tube

$E_3 = -10.4$ volts
$E_2 = 120$ volts
$E_p = 11.0$ volts
$I_{fil} = 0.92$ ampere
$C_{32} = 0.0012$ microfarad
$R_3 = 100{,}000$ ohms
$C = 0.00510$ microfarad
$L = 0.064$ henry
$R_{n\,min} = 3500$ ohms

$1/2\pi\sqrt{LC}$. In this case the tuned circuit will maintain a sinusoidal voltage regardless of the amplitude of oscillation or changes in shape of the tube characteristic.

Tuning by Means of a Variable Resistance in the Inductance Arm

While, as indicated previously, there are many devices which display a negative-resistance behavior, the transitron[15] or reverse-transconductance device is especially well suited to this purpose. The simplicity, good wave form, and other features of the transitron oscillator make it a desirable circuit with which to investigate the practical possibility of tuning an oscillator by varying the resistance in the conventional oscillating circuit. Fig. 4 shows the circuit employed. The device to the left of the terminals A-B has the current-voltage characteristic shown in Fig. 5.

The minimum negative resistance obtainable with the given operating voltages is determined by the reciprocal of the slope of the characteristic at the quiescent point 0, and, for the curve of Fig. 5, is found[16] to be 3500 ohms. The operation of this circuit has been amply described in the literature[8,15] and will not be treated in detail here. It is sufficient to point out that the negative-resistance behavior results from the action of grid 3 in combination with the resistance R_3 and the capacitance C_{32}. An instantaneous increase in voltage at point A (Fig. 4) is transmitted simultaneously by C_{32} to grid 3 causing it to draw more electrons away from the anode or grid 2 with a consequent reduction in the current at A. Thus an increase in voltage is followed by a decrease in current and vice versa.

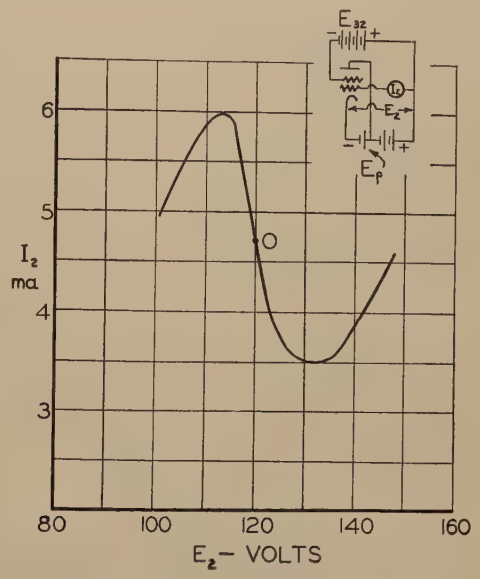

Fig. 5—Current-voltage characteristic of transitron oscillator showing quiescent point 0.
Type '57 Tube

$E_{32} = -130.4$ volts
$E_p = 11.0$ volts
$I_{fil} = 0.92$ ampere
Grid No. 2 is the anode

For a given setting of L, R_L, and C the circuit of Fig. 4 will oscillate at an amplitude which satisfies (3″) and (5). The effect of varying the resistance R_L on the frequency of oscillation is shown by curve A and on the amplitude of oscillation by the lower curve in Fig. 6. The amplitude is plotted in arbitrary units. The frequency computed from (12) for the same tuned circuit is shown in curve B. In Fig. 7 is reproduced the wave form of the voltage across the capacitance C as it appears on a cathode-ray oscilloscope for four different values of R_L.

It is seen that a quasi-sinusoidal wave form is maintained as the resistance R_L is increased from zero to 3000 ohms. The maintenance of good wave form for values of R_L up to 3000 ohms is due to an inherent

[13] E. B. Moullin, "The effect of the curvature of the characteristic on the frequency of the dynatron generator," *Jour. I.E.E.* (London), vol. 73, pp. 186–195; August, 1933.
[14] Janusz Groszkowski, "The interdependence of frequency variation and harmonic content, and the problem of constant frequency oscillators," Proc. I.R.E., vol. 21, pp. 958–981; July, 1933.
[15] Cledo Brunetti, "The transitron oscillator," Proc. I.R.E., vol. 27, pp. 88–94; February, 1939.
[16] In what follows the minimum negative resistance will be referred to as $|R_n|_{min}$.

property of the transitron oscillator. The pronounced bends of the operating characteristic act to decelerate the amplitude much faster than occurs in the ordinary feedback oscillator. Any pronounced harmonic introduced by the bends is therefore of a high order. Consequently its drop across the condenser C will be small in comparison to that of the fundamental. Thus, when R_L is small the voltage across the tuned circuit remains quasi sinusoidal even though large portions of the bends are traversed. As R_L increases, the oscillation over the characteristic decreases and as R_L approaches $|R_n|_{\min}$ the tube is operating for the most part over the

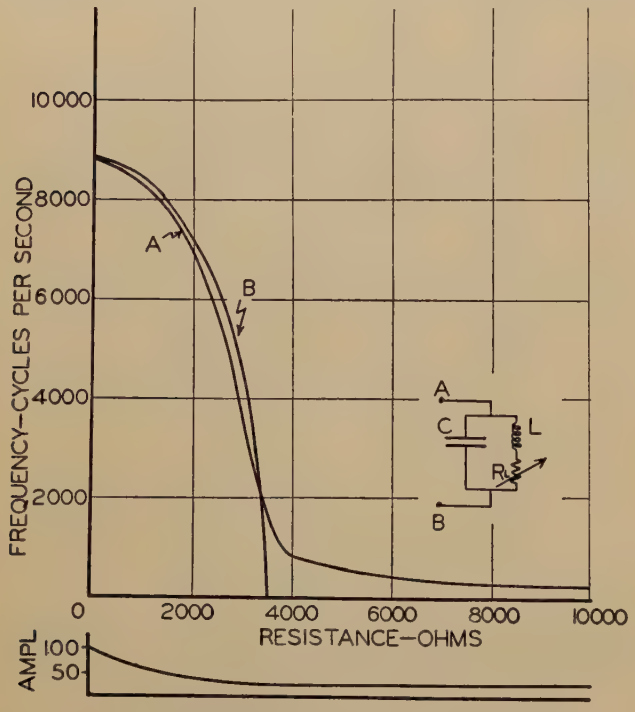

Fig. 6—Variation of frequency with R_L.
Curve A: $C = 0.00510$ microfarad, $L = 0.064$ henry
$E_2 = 120$ volts, $E_3 = -10.4$ volts, $E_p = 11$ volts.
Curve B: Theoretical curve from equation (12).
Lower curve: Amplitude of oscillations for curve A

negatively sloped linear portion of the characteristic. Thus again the harmonic content is small. If, however, R_L is made larger than $|R_n|_{\min}$ the oscillations cease to confine themselves to the characteristic of Fig. 5. For this reason the wave form no longer remains sinusoidal and, for example, when $R_L = 5000$ ohms takes on the form shown in Fig. 7. For still larger values of resistance the effect of the tuned-circuit inductance on the oscillations is decreased considerably and the circuit becomes essentially that of a relaxation oscillator with poor wave form.

The frequency is seen to follow the general variation predicted by (12) as long as the oscillations remain of a sinusoidal nature. The difference between the theoretical curve B and the actual curve A may be attributed to several factors not considered in deriving (12). It is found that the magnitude of the supply voltages influences the shape of the curve to some extent. Thus increasing E_2 or E_p raises the frequency slightly. Changing the supply voltages not only alters the shape of the operating characteristic but also changes the internal tube impedance, thus retuning the oscillator. Inspection of Fig. 4 will also show that the branch formed by R_3 and C_{32} in series appears in parallel with the tuned circuit. If C_{32} is increased, a slight lowering in the frequency will be noted.

A factor which might appear to alter conditions as R_L is varied is the drop in R_L produced by the steady component of anode current. This drop increases with R_L, thus changing the quiescent point by as much as 5 volts per thousand ohms. In order to determine the effect of this factor on the frequency, a constant resistance of 4000 ohms was inserted in series with L and by-passed with a 20-microfarad capacitor. By varying the portion of this resistance by-passed by the large capacitor it was possible to vary the effective series resistance in the tuned circuit while maintaining constant the drop due to the steady component of anode current. The result was a new curve falling between curves A and B of Fig. 6. Such a result shows that little improvement is obtained by maintaining a fixed quiescent point in this manner. The reason is that actually the drop in the direct anode voltage does not cause the quiescent point to shift rapidly towards the left bend of the characteristic (Fig. 5). It may be shown that the effect of lowering the direct anode voltage E_2 is to shift to an entirely new operating characteristic. As long as the bias E_3 is held fixed and R_L is not too large the new quiescent point will, as desired,

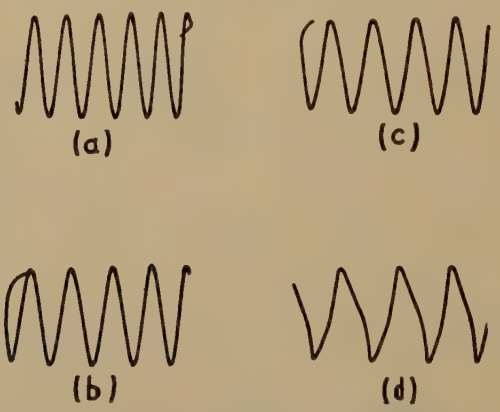

Fig. 7—Wave forms of resistance-tuned oscillator. (Using circuit of Fig. 4.) (Cathode-ray oscillograms, retouched.)
(a) $R = 0$ frequency = 8760 cycles per second
(b) $R = 1000$ " = 8300 " " "
(c) $R = 3000$ " = 3800 " " "
(d) $R = 5000$ " = 590 " " "

remain sufficiently near the center of the new characteristic to maintain conditions approximately as before. If, however, R_L is made large (of the order of two or three times $|R_n|_{\min}$) the direct-current drop in R_L may ultimately shift the quiescent point towards the left bend of the new characteristic. The result will be a marked decrease in the amplitude of oscillation and an increase in the harmonic content of the voltage.

It should also be pointed out that as the quiescent point is shifted to a new characteristic the value of

$|R_n|_{min}$ will increase. If the direct-current drop in R_L should be large enough to shift the quiescent point near the left bend of the new characteristic, $|R_n|_{min}$ may increase manyfold. In this way the oscillations may be quenched for failure to maintain the requirements imposed by (3″).

The persistence of oscillations for values of R_L greater than $\sqrt{L/C}$ (greater than 3540 ohms in Fig. 6) though not predicted by (12) may also be shown to be possible analytically.[12,17] If the tuned circuit to the right of terminals A-B in Fig. 4 be replaced by a resistance R', greater than $|R_n|_{min}$, relaxation oscillations will occur. Van der Pol[12,18] has shown that the frequency will vary with resistance in a manner similar to that shown in Fig. 8. The general wave form of the resulting voltage across R_L is also shown in Fig. 8.[19,20] It bears some resemblance to the wave form shown for $R_L = 5000$ ohms in Fig. 7.

In Fig. 6, as the resistance R_L is increased from 3000 ohms the wave form of the voltage across C gradually changes from a quasi-sinusoidal form to a form approaching the relaxation type. There occurs a gradual transition from the conditions yielding curve B of Fig. 6 to those yielding the curve of Fig. 8. For this reason the frequency does not go to zero at $R_L = \sqrt{L/C}$ as predicted by (12). The latter, as derived holds only as long as the oscillations are of a sinusoidal nature. The behavior in the transition region is modified somewhat by the presence of L and C.[17,21] The magnitude of R_3 and C_{32} also influences the frequency in the relaxation-oscillation region. By increasing C_{32} it is possible in some cases to reduce the frequency several hundred cycles. A more detailed treatment of the oscillations in the transition region is contained in a recent report by Carrara and Budini.[17,21]

In designing a resistance-tuned oscillator of this type care must be exercised to see that the ratio L/C be of such value that the criterion expressed by (3″) be maintained over the range of quasi-sinusoidal operation. As R_L is increased from zero, the amplitude of oscillations decreases thus decreasing the absolute value of R_n to maintain the balance required by (3″). However for a given set of supply voltages the absolute value cannot fall below the value $|R_n|_{min}$. If L/C is large enough to maintain the ratio L/R_LC equal to or greater than $|R_n|_{min}$ for values of R_L from zero to $|R_n|_{min}$ the oscillations will continue for any value of R_L within this range. For values of R_L larger than $|R_n|_{min}$ the condition for the maintenance of relaxations[17] is satisfied and the latter appear. The minimum value of L/C to sustain oscillations throughout the complete range of variation of R_L is $L/C = |R_n|^2_{min}$. If L/C is less than this, condition (3″) will no longer be satisfied for values of R_L equal to or greater than $L/|R_n|_{min}C$ and oscillation will cease until R_L is increased to the value at which oscillations of the relaxation type set in. This behavior is shown in Fig. 9. In curve A, $L/|R_n|_{min}C = 1540$ ohms while in curve B it is 1220 ohms. Above the point x, steady oscillations of good wave form occur. Between x and x' no steady oscillations occur. Below x' relaxation oscillations set in. This is further exemplified by the lower curve of this figure which shows the amplitude as the resistance is varied.

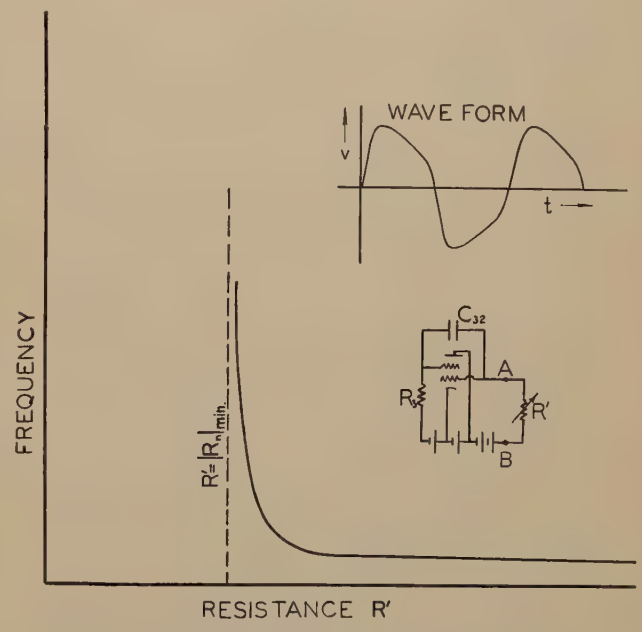

Fig. 8—Relaxation oscillations. (Circuit to left of terminals A-B same as in Fig. 4).

By the simple expedient of plotting L/R_LC against R_L as in Fig. 10 one may determine in advance whether or not oscillations will stop and the approximate value of R_L at which this will occur. The three curves in this figure are for the data of curve A, Fig. 6, and curves A and B, Fig. 9, respectively. The shaded area represents that region for which both L/R_LC and R_L are less than $|R_n|_{min}$. When R_L is less than $|R_n|_{min}$ oscillations of a quasi-sinusoidal nature will persist provided L/R_LC is greater than $|R_n|_{min}$. For R_L greater than $|R_n|_{min}$ relaxation oscillations occur. In the region represented by the shaded area neither the quasi-sinusoidal nor the relaxation conditions are met and the oscillations are extinguished. Thus, if a curve enters the shaded area oscillations will not be maintained for values of R_L within this region. If a curve does not enter the area, oscillations will persist for all values

[17] N. Carrara, "A systematic study of dipoles with negative differential resistance," *Alta Frequenza*, vol. 8, pp. 683–695; November, 1939.

[18] B. van der Pol, "Relaxation oscillations," *Phil. Mag.*, seventh series, vol. 2, pp. 978–992; November, 1926.

[19] In case the wave form is not important the circuit of Fig. 8 presents a handy and simple resistance-tuned oscillator. An interesting application of this circuit to a radio meteorograph has been reported.[20]

[20] H. Diamond, W. S. Hinman, and F. W. Dunmore, "A method for the investigation of upper-air phenomena and its application to radio meteorography," *Jour. Nat. Bur. Stand.*, vol. 20, pp. 369–392; June, 1938. Also PROC. I.R.E. vol. 26, 1938, pp. 1235–1265; October, 1938.

[21] P. Budini, "Experimental research on circuits containing dipoles of the N type with negative differential resistance," *Alta Frequenza*, vol. 8, pp. 696–706; November, 1939.

of R_L. This is seen to be the case by comparing curve A', Fig. 10, with curve A, Fig. 6. Here, as noted previously, there is a gradual transition from quasi-sinusoidal to relaxation oscillations within the vicinity of the region where $R_L = |R_n|_{min}$.

Since, as observed before, the shift in quiescent point as R_L increases is accompanied by an increase in $|R_n|_{min}$, the position of the upper boundary of the shaded area will shift upward slightly (as much as 5 per cent). The right-hand boundary will also shift, to

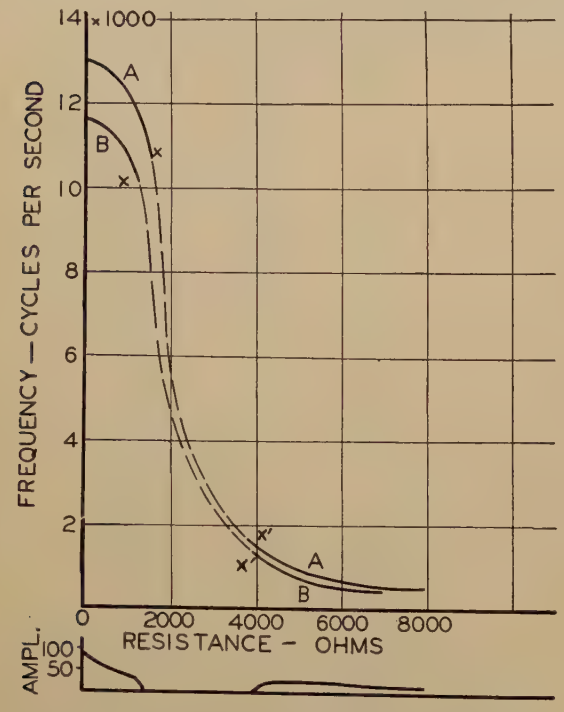

Fig. 9—Extinction of oscillations with too low L/C ratio.
Curve A: $C = 0.00510$ microfarad, $L = 0.0285$ henry
Curve B: $C = 0.00650$ microfarad, $L = 0.0285$ henry
Lower curve: Amplitude of oscillations for curve A
For all curves $E_2 = 120$ volts, $E_3 = -10.4$ volts, $E_p = 11.0$ volts
$|R_n|_{min} = 3500$ ohms when $R = 0$

the right. For this reason the above method is approximate but of sufficient accuracy for practical design purposes. In the case of curve A, Fig. 10, it is seen that when $R_L = 1630$ ohms the oscillations should cease. Curve A of Fig. 9 shows the oscillations to cease when $R_L = 1540$ ohms. The discrepancy is brought about by the increase in $|R_n|_{min}$ from 3500 to 3630 ohms. Curve A, Fig. 10, leaves the shaded area at $R_L = 3500$ ohms indicating that relaxation oscillations should start at this value of R_L. From curve A, Fig. 9, relaxation oscillations are seen to start at $R_L = 3880$ ohms showing that $|R_n|_{min}$ has increased 380 ohms from the value it had at $R_L = 0$.

If one desires, one may extend the range of oscillation into the shaded area of Fig. 10 by connecting a resistance R_x in series with the tuned circuit and the negative-resistance device, as at point A in Fig. 4. In this case the criterion for oscillation will be

$$(L/R_LC) + R_x \geqq |R_n|_{min}.$$

It is seen that the presence of R_x allows oscillations to continue for larger values of R_L than would be possible without it. However R_x must be kept small ($< |R_n|_{min}/4$) if good wave form is essential.

By proper selection of supply voltages it is possible to obtain values of $|R_n|_{min}$ as low as 1300 ohms with the ordinary type '57 or '58 tubes[14] so that one may reduce the shaded area to minimum in this manner. Further reduction may be had by employing hexode or octode tubes[22] in place of the pentode. By amplifying the variations in voltage between the anode (grid No. 2) and grid No. 3 values of $|R_n|_{min}$ as low as 100 ohms have been reported.[21]

With a circuit of the type of Fig. 4 it is possible by using several combinations of L and C to obtain a resistance-tuned oscillator of fairly good wave form extending from the ultrasonic range down through the audio range. Table I shows a typical set of combinations obtained.[23] The general shape of the curves of frequency against resistance over the frequency range indicated is the same as that of curve A, Fig. 6. The

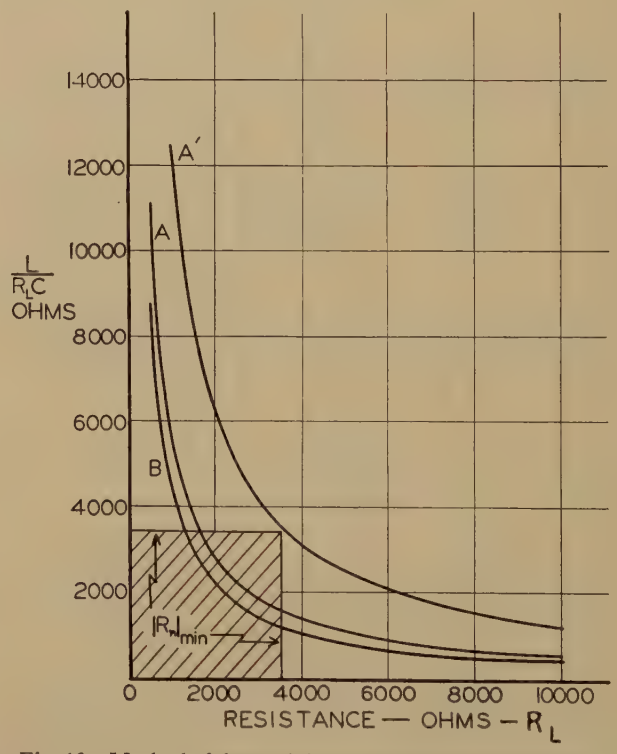

Fig. 10—Method of determining continuity of oscillations in the resistance-tuned oscillator of Fig. 4.
Curve A': $C = 0.00510$ microfarad, $L = 0.064$ henry
Curve A : $C = 0.00510$ microfarad, $L = 0.0285$ henry
Curve B : $C = 0.00650$ microfarad, $L = 0.0285$ henry

upper frequency limit of the oscillator is not completely explored in the data of this table. It may be extended into the broadcast band if desired. Lower frequencies than observed in Table I may be obtained with good wave form by using larger values of L and

[22] E. Viti, "Valori particolarmente bassi di resistenze negative," *Alta Frequenza*, vol. 5, pp. 1–2; November, 1936.
[23] In some cases E_2 and C_{32} were changed from the values given for Fig. 4.

C. With the values of L and C of Table I lower frequencies are also readily obtained but at the expense of increased harmonics in the voltage.

As recorded in a previous paper[15] it is possible to apply automatic amplitude control to the transitron oscillator to maintain the amplitude fairly constant and to improve the wave form over a considerable portion of the tuning range. This is accomplished by impressing a small portion of rectified output voltage across grid No. 1 of Fig. 4. As a result, operation is restricted primarily to the linear portion of an operating characteristic which varies with the amount of amplitude-control voltage fed to grid No. 1.

TABLE I
RESISTANCE-TUNED OSCILLATOR DATA
(Quasi-Sinusoidal Wave Form)

L (henry)	C (microfarad)	Range of Variation of Tuning Resistance in Series with L (ohms)	Corresponding Variation in Frequency (cycles per second)
0.143	0.0100	0–9000	4200– 1000
0.080	0.0083	0–3000	6200– 1500
0.064	0.0051	0–3000	8760– 3800
0.0285	0.0051	0–1540	13000–10700
0.0200	0.0022	0–2400	23700–15800
0.0200	0.0013	0–3300	30300–18700
0.0200	0.0009	0–3200	37000–30000
0.0100	0.0008	0–2400	54500–40000
0.0054	0.0008	0–1200	75000–67600
0.0054	0.00035	0–2800	112200–80000

TUNING BY MEANS OF A VARIABLE RESISTANCE IN THE CAPACITANCE ARM

If the tuned circuit to the right of terminals A-B of Fig. 4 be replaced with the circuit of Fig. 11 the resulting frequency will be that given by (4‴).

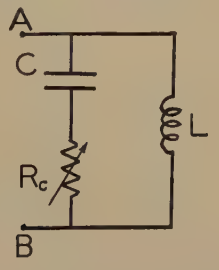

Fig. 11—Tuning by means of a variable resistance in the capacitance arm.

The balance of real energy in the system requires that L/R_cC be equal to or greater than $-R_n$. Fig. 12 shows the experimental results obtained for a circuit of this type. Though (4‴) yields an infinite frequency when $R_c=\sqrt{L/C}$ this evidently cannot be the case. Factors unaccounted for in the derivation of (4‴) cause the frequency to taper off and approach a limiting value. The influence of one of these factors, the R_3, C_{32} branch, is shown by curve D. In this case the conditions are the same as for curve A with the exception that C_{32} is increased from 0.0012 to 0.1080 microfarad. A somewhat similar effect occurs when R_3 is reduced. From this it is clear that the R_3, C_{32} branch is also a part of the effective resonant circuit which determines the frequency of oscillation. Another important component of this resonant circuit is the tube impedance.

Thus, when R_c is small the frequency is determined primarily by the L, C, R_c circuit. As R_c is increased the tube impedance and the R_3, C_{32} branch exert an increasingly greater influence on the frequency. When $R_c>\sqrt{L/C}$ the R_c, C arm gradually loses control over the frequency, the latter approaching the limiting value determined by the inductance L, the tube impedance, and the R_3, C_{32} branch. The effect of the inductance L is shown by comparing curves A and E, Fig. 12. A similar tapering off of both curves occurs for large values of R_c. The two limiting frequencies are found to be inversely proportional to $\sqrt{L}$.

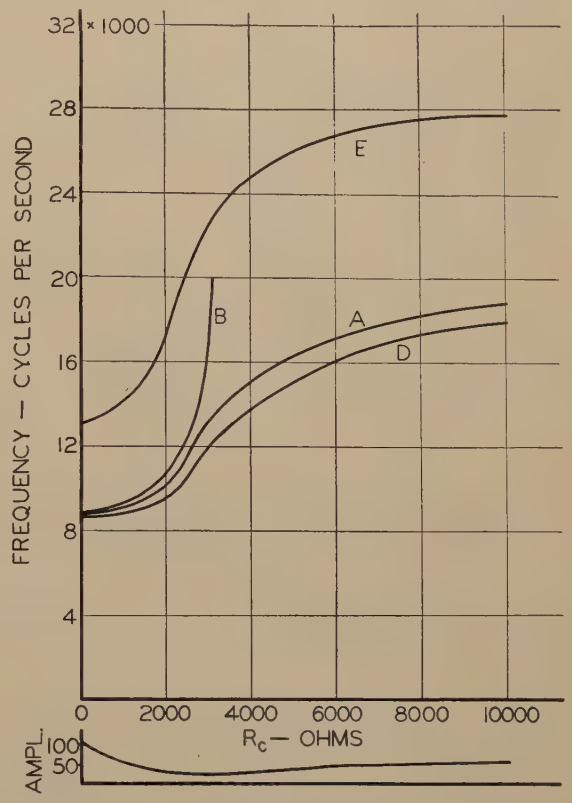

Fig. 12—Variation of frequency with R_c.
Curve A: $C=0.0051$ microfarad, $L=0.064$ henry, $C_{32}=0.0012$ microfarad
Curve B: Theoretical curve from equation (4‴)
Curve D: $C=0.0051$ microfarad, $L=0.064$ henry, $C_{32}=0.1080$ microfarad
Curve E: $C=0.0051$ microfarad, $L=0.0285$ henry, $C_{32}=0.0012$ microfarad
Lower curve: Amplitude of oscillations for curve A
For all curves $E_2=120$ volts, $E_3=-10.4$ volts, $E_p=11$ volts.

Further evidence of the gradually increasing influence of the tube impedance and the R_3, C_{32} branch on the behavior of the oscillator as R_c is increased is found in the fact that for curve E, oscillations are maintained for all values of R_c. The values of L and C for curve E are the same as those used in obtaining curve A, Fig. 9, in which the tuning resistance is in the inductance arm. In the latter case the oscillations cease when the resistance exceeds 1540 ohms. Regardless of whether $R_c=0$ and R_L is varied, or $R_L=0$ and R_c is varied, (3′) shows that the criterion $L/RC\geqq -R_n$ must be maintained. Therefore, it would be expected that oscillations would

cease when the resistance in the capacitance arm reaches the neighborhood of 1540 ohms, (approximately the same value of $|R_n|_{min}$ was maintained in both cases). Though the L, R_c, C circuit acting alone cannot sustain oscillations when R_c exceeds 1540 ohms, the circuit consisting of the inductance L, the tube impedance, and the R_3, C_{32} branch maintains a sufficiently high impedance to continue the oscillations.

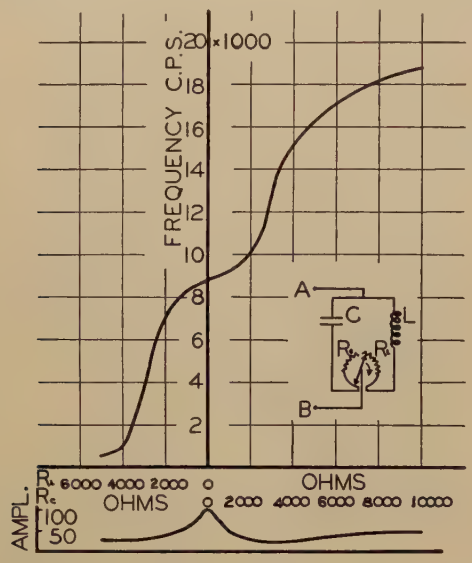

Fig. 13—Extended-range tuning varying both R_L and R_c successively (obtained by combining results of curve A, Fig. 6, with curve A, Fig. 12).

Ultimately, as seen by the curves of Fig. 12, the latter combination assumes complete control. This behavior does not occur in the cases illustrated by Fig. 9 where the tuning resistance is in series with the inductance L. In these cases as the resistance increases the effect of the inductance L on the oscillations gradually diminishes and the remainder of the circuit, external to the R_L, L arm, does not maintain a sufficiently high impedance to sustain oscillations.

Since the steady component of the anode current does not pass through R_c no shift occurs in the quiescent point as the resistance is increased. Consequently the tube works on the same operating characteristic for all values of R_c. The quiescent point, if chosen at the center of the characteristic, will remain there. For this reason R_c may be increased to any value without shifting the quiescent point to the left bend of a new characteristic when R_c is large, thus avoiding increased distortion and perhaps quenching of the oscillations for failure to maintain a sufficiently low value of $|R_n|_{min}$. Observation of the wave form obtained by tuning with R_c shows it to be much better at high values of tuning resistance than that resulting when the tuning resistance is in the inductance arm.

Extended-Range Tuning

By adding variable resistances to both the L and C arms of the tuned circuit as shown in Fig. 13 and varying first one and then the other it is possible to tune the oscillator over an extended range of frequency. The effect may be seen by combining curves A of Fig. 6 and Fig. 12 as in Fig. 13. A frequency variation from 590 to 18,800 cycles is obtained with a total resistance variation of 15,000 ohms. While the result in this case is not a desirable linear relationship between resistance and frequency, by proper selection of voltages and circuit components some of the curvature near the vicinity of zero resistance may be eliminated. (Another method of eliminating the curvature will be described shortly.) In any case, the oscillator should be calibrated. By selecting different combinations of L and C an extended-range resistance-tuned oscillator operating over various portions of the audio- and ultrasonic-frequency ranges may be obtained. At the center of the range shown in Fig. 13 the wave form is good. The harmonic content increases with resistance being greatly augmented for large values of R_L.

Straight-Line Tuning

If the resistance in both the L and C arms is varied keeping their sum constant, as in Fig. 3(b), it is possible to obtain a more linear relationship between resistance and frequency. In this method, as the resistance is removed from one arm, it is added to the other with the result that a good portion of the curvature of Fig. 13 is eliminated. Fig. 14 shows the frequency variation attained with this system using a total resistance of 5000 ohms. While a wide range of variation

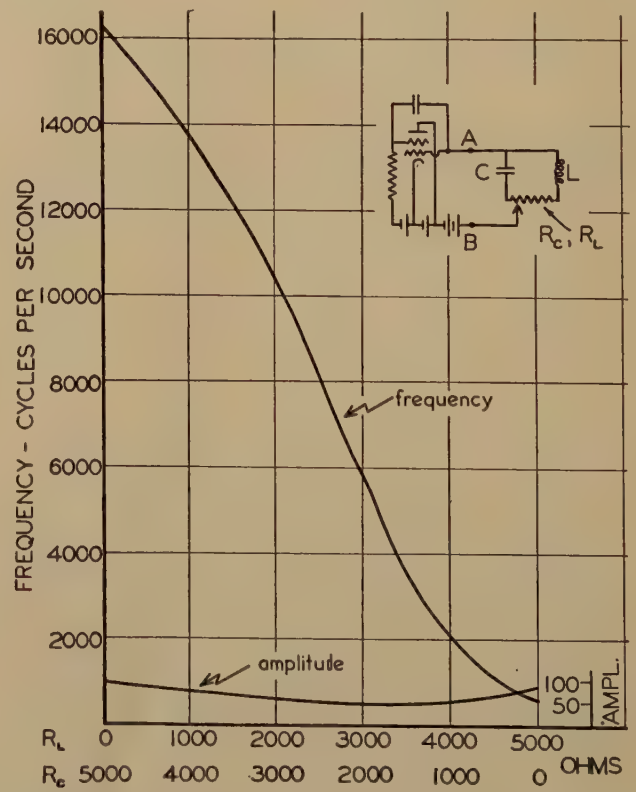

Fig. 14—Extended-range tuning varying both R_L and R_c simultaneously.
$C = 0.0051$ microfarad, $L = 0.064$ henry
$E_2 = 120$ volts, $E_3 = -10.4$ volts, $E_p = 11.0$ volts

is obtained the wave shape is not sinusoidal throughout the range.

If, however, the total resistance is made only 2000 ohms, a much more favorable result is obtained as shown in Fig. 15. In this case the wave form is practically sinusoidal throughout the range of variation and, as observed, the amplitude remains fairly constant. By proper selection of L and C a sine-wave resistance-tuned oscillator of this type having a fairly constant amplitude, and with approximately 30 per cent variation in frequency, may be constructed to operate over various desired portions of the audio- and ultrasonic-frequency ranges.

Effect of Supply Voltages on Frequency

Measurements made with 1000 ohms in series with L, using the circuit of Fig. 4, showed that for a simultaneous variation of ± 10 per cent in all the supply voltages the frequency varied ± 0.03 per cent. This is a variation of 30 parts in a million per per cent variation in the supply voltages. This value increases rapidly as R_L is made greater than 1000 ohms. Thus, while the oscillator is reasonably stable against normal changes in supply voltages when the tuning resistance is 1000 ohms or less, some form of supply-voltage regulation is necessary when it is desired to vary the resistance over a wider range. Since the total current taken by the oscillator is small, the voltage regulator need not be elaborate. In this connection a simple well-regulated power supply described by Bousquet[24] has been found very successful. With this type of supply a variation of over ± 10 per cent in line voltage produced no perceptible changes in the voltages supplied to the tube elements, and consequently no variation in the frequency or amplitude of oscillations for any setting of the tuning resistor.

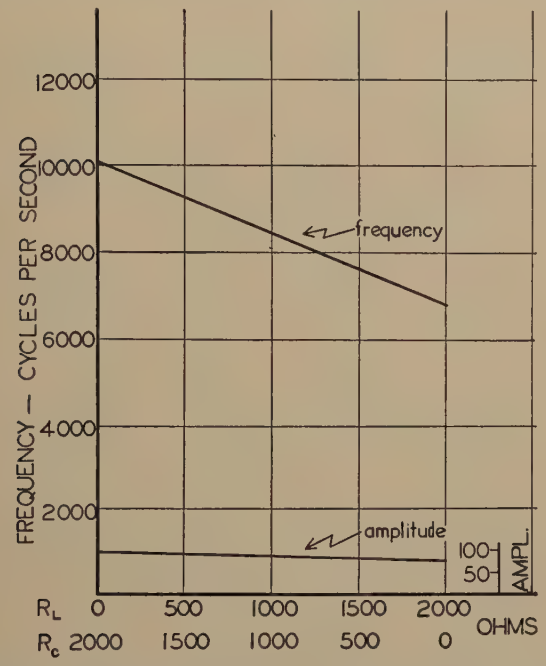

Fig. 15—Straight-line frequency variation with resistance. Sinusoidal wave form maintained throughout the range.
$C = 0.0051$ microfarad, $L = 0.064$ henry
$E_2 = 120$ volts, $E_3 = -10.4$ volts, $E_p = 11.0$ volts

Further Considerations

The thermal drift of a direct-tuned audio oscillator is normally much smaller than that of the beat-frequency type. In the latter, because of the necessity of operating at high frequencies with respect to the audio beat frequency, any small thermal drift is greatly magnified. In addition to being free of this disadvantage, the resistance-tuned transitron oscillator may be designed to have a very small thermal drift by the selection of low-temperature-coefficient components for the circuit. Perhaps the most important factor in this consideration is the tuning resistor. Since in the transitron oscillator the current in the tuned circuit is small the heating of the tuning resistor will also be small. A rheostat of low wattage rating may be employed as the maximum power dissipated in this unit is of the order of 25 milliwatts per thousand ohms. This occurs when the tuning rheostat is in the inductance arm and carries the direct anode current. When the tuning rheostat is in series with the capacitance arm the power dissipated in it is much less. As it is possible to construct rheostats of alloys whose change of resistance with temperature is extremely small, the thermal frequency drift with only 25 milliwatts of power dissipated per thousand ohms is negligible at audio and even at ultrasonic frequencies. If a case should arise where this small drift is not negligible, rheostats of manganin are available with not only small positive but also negative temperature coefficients over the range of temperatures encountered in this application.[25] At audio frequencies a wire-wound rheostat has proved very satisfactory, the inductance of the unit being negligible.

If it is desired to operate at lower audio frequencies than included in the data of this paper coils of larger inductance should be used. As there are now available alloyed-cored coils of high inductance and fairly high Q this problem is easily met. These coils occupy little space and are light in weight. For applications in portable units this feature is of great value. The advent of low-drain and miniature-type vacuum tubes and batteries of reduced size and weight makes it a simple task to construct a small, compact, and lightweight portable resistance-tuned oscillator.

In general, any ordinary two-grid tube may be employed in the negative-resistance device. Using a type '57 or '58 tube a voltage as high as 20 volts root-mean-square may be obtained across the tuned circuit. Since the device is inherently of low power some amplification will be necessary if appreciable loads are imposed on the oscillator. This presents no serious difficulties. If the load is not large the output may be taken from

[24] A. G. Bousquet, "Improving regulator performance," *Electronics*, p. 26; July, 1938.

[25] Bulletin R-36, Driver-Harris Co., Harrison, N. J., 1936, p. 36.

the tuned circuit either by direct coupling or transformer coupling. In the latter case, one winding of the transformer may serve as the inductance of the tuned circuit. Another means of coupling a load to the oscillator is across R_3 or a variable portion of it.

It might properly be re-emphasized that if the frequency is to be controlled by a resistance in series with the inductance of the tuned circuit the L/C ratio must be chosen so as to prevent the oscillations from being extinguished over part of the tuning range. The manner of doing this has already been described.

Since circuit elements other than those of the tuned circuit influence the circuit, the oscillator should be calibrated before using. If supplied by a regulated source of voltage the oscillator, once calibrated, should hold its calibration over long periods of time and use.

As in the case of the ordinary transitron oscillator[15] great freedom is possible in the selection of the supply voltages E_2, E_3, and E_p. With some manipulation it is possible to find a large number of combinations that will work satisfactorily with any given circuit. In many cases E_3 may be made zero. It is possible to build a resistance-tuned transitron oscillator that will function satisfactorily with values of E_2, E_3, and E_p, of 4, 0, and 2 volts, respectively, over a limited range of operation.

Applications

The practicability of varying the frequency of an oscillator by means of a variable resistance in the tuned circuit has been shown by the results obtained. It is possible, by a suitable arrangement of the circuit, to obtain a linear relationship between frequency and resistance over a limited range.

The following table summarizes the results attainable with a resistance-tuned transitron oscillator.

TABLE II

Summary of Resistance-Tuned Transitron Oscillator Performance

Tuning Resistance in	Ratio of Frequency Variation	Wave Form
L arm	25 to 1	+++variable
L arm	5 to 1	good
C arm	2 to 1	good
both L and C arms	50 to 1	variable
both L and C arms	+20 to 1	variable
both L and C arms	++1.5 to 1	good

+ Near-linear relationship between frequency and resistance.
++ True linear relationship between frequency and resistance.
+++ Wave form good over large portion of range; approaches relaxation oscillations over remainder of range.

The simplicity, compactness, and light weight of the resistance-tuned transitron oscillator lends itself to many applications. As an inexpensive ordinary general-purpose laboratory oscillator it should find much usefulness. Also, since it is possible to vary the plate resistance of a vacuum tube by varying the grid voltage, one may construct a voltage-tuned oscillator or frequency modulator. All that is necessary is to connect the plate resistance in parallel with either tuned-circuit resistor of Fig. 1. By the proper selection of the parameters, the oscillator frequency may be made proportional to the instantaneous voltage impressed on the grid of the tube in parallel with the tuned-circuit resistor. This method of frequency modulation in connection with a tuned-grid type of feedback oscillator has been employed to some extent in automatic-frequency-control circuits.[26] When used with a resistance-tuned transitron oscillator the method is particularly effective and should find many other applications.

The resistance-tuned oscillator may be used for measuring temperature, pressure, humidity, light intensity, and other physical quantities. In this application the variation of the quantity being measured is converted into a variation in frequency and the magnitude read on a properly calibrated frequency meter. It is necessary to obtain units whose resistance is a function of the quantity being measured. This unit is then connected either in series with, in parallel with, or in place of the ordinary tuning resistor as the situation may require.

For recording temperature, either a wire resistor or a proper electrolytic solution may be used.[20] For recording pressure, a pressure diaphragm connected to a rocker arm making either a rolling or sliding contact with a resistance card is useful.[20] The new electric hygrometer[27] developed at the National Bureau of Standards should serve well as a humidity unit to use with a resistance-tuned oscillator. This hygrometer consists of an insulated tube supporting chemically coated bifilar windings of palladium wire. The resistance across the windings varies with humidity. Because of the attendant difficulties of polarization of devices of this type, they operate best when subjected to alternating instead of direct current. The unit should, therefore, be connected in the capacitance arm of the tuned circuit which carries no direct component of current. The frequency of the oscillator will then vary with the humidity.

In the field of chemistry the resistance-tuned oscillator should be useful in measurements such as that of the conductivity of solutions. In addition to its compactness and versatility the simplicity of construction should appeal to investigators not versed in the problems of oscillator design. It should find favor in such fields of research as medicine, biology, psychology, agriculture, and others in addition to engineering, chemistry, and physics.

Acknowledgment

The authors are indebted to Joseph A. Waldschmitt, former Packard Research Fellow in Electrical Engineering at Lehigh University for supplying experimental data for Fig. 8.

[26] Charles Travis, "Automatic frequency control," Proc. I.R.E., vol. 23, pp. 1125–1141; October, 1935.

[27] F. W. Dunmore, "An improved electric hygrometer," *Jour. Nat. Bur. Stand.*, vol. 23, pp. 701–714; December, 1939.

On the Induced Current and Energy Balance in Electronics*

C. K. JEN†, ASSOCIATE, I.R.E.

Summary—*With a given specification of the space-charge density and velocity functions for a general electron-tube system, the balance of instantaneous rates of energy change between the space and the external circuits has been derived here from Green's theorem. It is shown that the external currents can be completely accounted for by the changes brought about by moving charges and changing field intensity in space. The ordinary concept of current as the rate of direct transfer of charges represents the limiting case of this theory at low frequencies. The induced current for steady fields can be calculated simply by knowing the electrostatic field caused by a given electrode at unit potential, with all the other electrodes grounded, and the space-current density function. It is also shown that a direct-current source can supply power only when there is a direct flow of charges between the space and the electrode to which the source is connected. Net alternating-current power, however, can be exchanged between the space and the external circuits even in the absence of direct transfer of charges. A number of ultra-high-frequency phenomena can be qualitatively explained by the theory.*

Introduction

BY THE conventional concept, the current on any electrode in an electron-tube system has been regarded by some as measured by the instantaneous rate of transfer of charges between the electrode and its surrounding space. This concept applies very well for steady or low-frequency fields and holds approximately true for high-frequency fields where the transit time of the moving charges is negligible as compared with the fundamental period of variation. For ultra-high-frequency fields, this transit time is usually of very great importance and under such conditions the above concept is definitely inapplicable. One finds, for instance, there may be a considerable power loss on the grid even in the absence of actual charge transfer from the space to the grid.[1] Also, in the velocity-modulated tubes developed during recent years, considerable ultra-high-frequency power can be drawn from a certain combination of electrodes where there is no actual collection of space charges.[2–4] These evidences together with other general considerations point to the necessity of a fundamental revision of the earlier and incomplete concept of current.

It has already been suggested at several places in the literature[1–3,5] that a generalized concept of current must be based upon the instantaneous rate of change of the electrostatic flux terminating on an electrode. The movement of any space charge must be accompanied by a change in the terminating electrostatic flux which in turn calls for a flow of charges in the external circuit. Thus the current flowing to an electrode from its external connection is a necessary consequence of electrostatic induction. This notion of current coincides with the conventional one for steady or low-frequency fields, but has the merit of being also applicable to very high-frequency variations.

The above generalized concept of current turns out to be rigorously correct and promises to be very useful for ultra-high-frequency work. But the arguments in the literature have been so far mostly qualitative with the exception of Ramo's work,[5] which gives a formula for the current induced by a single electron motion for a unit applied potential. The effects of space charge and changing electrode potentials have not been considered. Further, it remains to verify that the induced current is the only possible current flowing to an electrode from its external connection and that the transfer of charges between the electrode and its immediate surrounding space does not constitute an external current at all. Finally, one has to show that the energy (or power) relations at different portions of the system are exactly balanced. This paper attempts to demonstrate such reasonings on an elementary mathematical basis.

General Formulation of Instantaneous Induced Current and Power Relations

Let there be N electrodes of arbitrary shapes oriented arbitrarily in a common evacuated enclosure. The electrodes themselves are assumed to have zero resistance and negligible effects of magnetic induction. Some of the electrodes (usually only one) have the property of emitting charges (usually negative electrons) to the space, while the others may serve as collectors of charges from the space. Let $\Phi_1, \Phi_2, \ldots, \Phi_N$ be the potentials on the individual electrodes, referred to a common ground potential. Each potential may be an arbitrary function of time. In the space there is given a continuous distribution of charges defined by the space-charge density function $\rho(x, y, z, t)$. These charges move in the space, subject to the laws of motion. This part of the problem is assumed to be already solved and we are given a velocity function defined by $v(x, y, z, t)$. The charge density and velocity functions must of course be related by the equation of continuity, $\partial\rho/\partial t + \mathrm{div}(\rho v) = 0$.

As a preliminary we face the problem of finding the electric intensity defined by $\boldsymbol{E}(x, y, z, t)$, which in the electrostatic case is always derivable from a scalar potential function defined by $\phi(x, y, z, t)$ from the relation, $\boldsymbol{E} = -\mathrm{grad}\ \phi$. Now the potential function must

* Decimal classification: R139. Original manuscript received by the Institute, March 3, 1941.

† Radio Research Institute, National Tsing Hua University, Kunming, China.

[1] W. R. Ferris, "Input resistance of vacuum tubes as ultra-high-frequency amplifiers," PROC. I.R.E., vol. 24, pp. 82–107; January, 1936.

[2] W. C. Hahn and G. F. Metcalf, "Velocity-modulated tubes," PROC. I.R.E., vol. 27, pp. 106–117; February, 1939.

[3] A. V. Haeff, "An ultra-high frequency power amplifier of novel design," *Electronics*, p. 30; February, 1939.

[4] R. H. Varian and S. F. Varian, "High frequency oscillators and amplifiers," *Jour. Appl. Phys.*, vol. 10, p. 321; May, 1939.

[5] Simon Ramo, "Currents induced by electron motion," PROC. I.R.E., vol. 27, pp. 584–586; September, 1939.

satisfy Poisson's equation,[6] $\nabla^2\phi=-4\pi\rho$, with the boundary condition that any electrode surface must represent an equipotential having the specified value of potential. It can be shown by the theory of boundary-value problems that there always exists a unique potential function which satisfies the given conditions. We shall assume here that this is true.

The relation between the electrode surface and the spatial quantities is expressed by Green's theorem, which may be written as

$$\int \phi \frac{\partial \phi}{\partial n} dS = \int \{\phi \nabla^2 \phi + |\operatorname{grad} \phi|^2\} d\tau. \tag{1}$$

Here the surface integration is extended over all electrode surfaces and the surface at infinity, and the volume integration is extended over the entire space bounded by all the surfaces. $\boldsymbol{n}$ is a unit normal vector drawn from the space to the surface. From Gauss's theorem, we have the relation

$$4\pi q_k = \int \left(\frac{\partial \phi}{\partial n}\right)_k dS_k \tag{2}$$

where q_k=total charge on the kth electrode. Noting the above relations and the fact that the surface integral at infinity vanishes, we have

$$\tfrac{1}{2}\sum_{k=1}^{N} \Phi_k q_k + \tfrac{1}{2}\int \rho\phi d\tau = \frac{1}{8\pi}\int E^2 d\tau. \tag{3}$$

The first term on the left-hand side of (3) represents the work required to bring all the electrode charges to their specified potentials and the second term represents the work for the space charges to be at their equilibrium potentials. The term on the right-hand side is the energy of the electrostatic field. Equation (3) therefore expresses the fact that the work done in establishing the surface and space charges to their equilibrium state is all stored up in the field.

In electronics problems we are more interested in the rate of change of energy (or power) rather than the energy itself. Differentiating (3) with respect to time, we get

$$\sum_{k=1}^{N} (\dot{\Phi}_k q_k + \Phi_k \dot{q}_k) + \int (\dot{\rho}\phi + \rho\dot{\phi}) d\tau = \frac{1}{2\pi}\int \boldsymbol{E}\dot{\boldsymbol{E}} d\tau \tag{4}$$

where the dot above a letter denotes differentiation with respect to time t and $\boldsymbol{E}\dot{\boldsymbol{E}}$ denotes the scaler product of $\boldsymbol{E}$ and its time derivative. (In what follows we shall deal only with scalar products of the vectors; hence, no special sign is needed.) Noting the following relations with the aid of the equation of continuity and the relation div $\boldsymbol{E}=4\pi\rho$,

$$\int \dot{\rho}\phi d\tau = -\sum_{k=1}^{N} \Phi_k \int (\rho v)_n dS_k - \int \rho \boldsymbol{v} \boldsymbol{E} d\tau \tag{4a}$$

$$\int \rho\dot{\phi} d\tau = -\sum_{k=1}^{N} \dot{\Phi}_k q_k + \frac{1}{4\pi}\int \boldsymbol{E}\dot{\boldsymbol{E}} d\tau. \tag{4b}$$

Equation (4) can now be reduced to

$$\sum_{k=1}^{N} \Phi_k \left\{ \dot{q}_k - \int (\rho v)_n dS_k \right\} = \int \left(\rho \boldsymbol{v} + \frac{\dot{\boldsymbol{E}}}{4\pi}\right) \boldsymbol{E} d\tau. \tag{5}$$

Now, the equation of continuity when applied to the surface of each electrode requires

$$\dot{q}_k = i_k + \int (\rho v)_n dS_k \tag{6}$$

where i_k is the conduction current flowing to the kth electrode from its external connections. Equation (6) expresses the fact that the rate of increase of the charge on the kth electrode is equal to the sum of the current from the external connection and the space current landing on the kth electrode (remembering that the unit normal is drawn toward the electrode). Combining (5) and (6), we obtain

$$\sum_{k=1}^{N} \Phi_k i_k = \int \left(\rho \boldsymbol{v} + \frac{\dot{\boldsymbol{E}}}{4\pi}\right) \boldsymbol{E} d\tau. \tag{7}$$

Equation (7) represents the final result of our general formulation. The presence of Maxwell's total current $\rho v+\boldsymbol{E}/4\pi$ in the integrand of the volume integral suggests that (7) can be derived much more easily by noting the fact $\operatorname{div}(\rho v+\dot{\boldsymbol{E}}/4\pi)=0$. Thus the relation, $\operatorname{div}\{(\rho v+\dot{\boldsymbol{E}}/4\pi)\phi\}=(\rho v+\dot{\boldsymbol{E}}/4\pi)\operatorname{grad}\phi$, gives (5) directly by the integration. In spite of its simplicity we still prefer to take it as a verification of (7) derived from a more general approach.

Equation (7) can be somewhat rewritten by using the following definitions:

$$\frac{dT}{dt} = \int \rho \boldsymbol{v} \boldsymbol{E} d\tau \tag{8a}$$

$$\frac{dU}{dt} = \frac{1}{4\pi}\int \boldsymbol{E}\dot{\boldsymbol{E}} d\tau \tag{8b}$$

where T is the kinetic energy of all the charged particles in space[7] and $U=\int E^2 d\tau/8\pi$, the electrostatic-field energy. Thus we can write

$$\sum_{k=1}^{N} \Phi_k i_k = \frac{d(T+U)}{dt}. \tag{9}$$

The formulation in (7) and (9) enables us to make the following statements:

1. The rate of change of the kinetic energy of all the charged particles in space plus the rate of change of the electrostatic-field energy[8] is equal to the sum of the instantaneous powers on all the electrodes.

[6] The fact that we use Poisson's equation instead of the general d'Alembert's equation means that we assume the electrostatic field propagates with infinite velocity. With the dimensions encountered in electronics, this assumption is quite accurately true, if the frequencies involved are not extraordinarily high. That is, the wavelengths should be long in comparison with the interelectrode spacing and the electron velocity considerably less than that of light.

[7] See for instance, W. Heitler, "The Quantum Theory of Radiation," Oxford Press, New York, N. Y., 1936, p. 6.

[8] It is interesting to remark here that the field energy plays the same part as the potential energy in ordinary mechanics. Refer for instance to M. Abraham and R. Becker, "The Classical Theory of Electricity and Magnetism," 1932 edition, p. 89.

2. All the electrodes are coupled to one another through the medium of total space current and the intensity field. Hence the electrodes can freely transfer power or energy among themselves.

3. The current flowing to any electrode from its external connection is entirely due to the effect of the total current (convection current plus displacement current) flowing in space. Consequently the external current is completely accounted for by the action of electrostatic induction.

4. The current flowing from any electrode to its immediate surrounding space or vice versa merely changes the total charge on the electrode and has nothing to do with the flow of external current. Thus an emitter may be considered as a source while a collector as a sink of charges.

Instantaneous Induced Current and Power Relations for Quasi-Steady Applied Fields

The relation given by (7) assumes a more readily manageable form if the applied field is steady or quasi steady (low frequency). Let $\phi=\phi_1+\phi_2$, where ϕ_1 and ϕ_2 satisfy the following relations:

$$\begin{aligned} &\nabla^2\phi_1 = 0 && (\phi_1)_k = \Phi_k \\ &\nabla^2\phi_2 = -4\pi\rho && (\phi_2)_k = 0 \quad k = 1, 2, \cdots, N. \end{aligned} \tag{10}$$

In effect we have by the above process considered the actual potential as a superposition of one part due to the electrode potentials and another due to the space charges. By applying either Green's theorem (a more generalized form than (1)) or the solenoidal property of the total current density, we obtain

$$\sum_{k=1}^{N} \Phi_k i_k = \int \left(\rho v + \frac{\dot{E}}{4\pi}\right) E_1 d\tau \tag{11a}$$

$$0 = \int \left(\rho v + \frac{E}{4\pi}\right) E_2 d\tau \tag{11b}$$

$$0 = \int E_1 E_2 d\tau. \tag{11c}$$

So far the relations expressed in (11) are perfectly general. Now in the steady applied field where $\dot{E}_1$, is zero, or in a quasi-steady field where $\dot{E}_1$, is negligible, we then have

$$\sum_{k=1}^{N} \Phi_k i_k = \int \rho v E_1 d\tau. \tag{12}$$

Equation (12) expresses the fact that if the applied field is steady or quasi steady, then the external electrodes combined have only to supply the power necessary to accelerate the charges by their own field. This is true when the integral on the right-hand side of (12) is positive. If it is negative, then the electrodes actually absorb power from the space. The effect of static interaction of the space charges does not come in here.

From (12) we get a simple means of calculating the induced current on any electrode for steady applied voltages. Since all the electrode potentials are arbitrary, suppose $\Phi_1=\Phi_2=\cdots=\Phi_N=0$, except that $\Phi_k=1$. We then have

$$i_k = \int \rho v \mathcal{E}(k) d\tau \tag{13}$$

where $\mathcal{E}(k)$ is the intensity vector at any point due to a unit potential on the kth electrode while all the other electrodes are grounded. In the case of a single electron, the volume integration may be supposed to be in a tiny sphere, where v and $\mathcal{E}(k)$ are sensibly constant (the electron itself is considered to be removed) and $e=\int\rho d\tau$, being the charge of the electron. Thus we obtain

$$i_k = ev\mathcal{E}(k). \tag{14}$$

This is exactly the result obtained by Ramo[5] by a different method. This result applies very readily to the case of two infinite parallel planes separated by a distance d with a charge e moving with a velocity v perpendicular to the two planes. Then (14) gives

$$i = \frac{ev}{d}. \tag{15}$$

Equation (15) can also be obtained by an infinite series of image charges on each side of the planes and the current is a consequence of the rate of change of the total induced charge on each plane.[9] The last method is naturally much too cumbersome as compared with the above-mentioned methods.

Lastly, if the applied field is steady, then the flow of space current would attain an equilibrium state at which $\dot{\rho}=0$. Then we have $\dot{E}=0$ and in (6), $\dot{q}_k=0$. Thus we get from (6)

$$i_k = -\int (\rho v)_n dS_k = \int (\rho v)_{n'} dS_k \tag{16}$$

where $n'=-n$. We draw from (16) the important conclusion that only when the external field is steady or quasi steady, the external current happens to be equal to the rate of transfer of charges. Thus the conventional concept of current represents the special case of the generalized concept at low frequencies.

Average Power Balance for Periodic Fields

For high-frequency (more particularly ultra-high-frequency) work where the transit time is not negligible, the instantaneous power relations must always be governed by (7). But we are really more interested in the time-average quantities of a periodic phenomenon rather than the instantaneous values. Defining the time average of a quantity $\psi(t)$ as $\overline{\psi(t)}=\int_0^T\psi(t)dt/T$, where $T=$period of variation, we have

$$\overline{\frac{dU}{dt}} = \frac{1}{T}\{U(t_0+T) - U(t_0)\}. \tag{17}$$

[9] See O. D. Kellogg, "Foundations of Potential Theory," 1929 edition. Ex. 7, p. 231.

Now since $\boldsymbol{E}$ is periodic, U must also be periodic; hence, $\overline{dU/dt}$ vanishes. We then have, from (7) and (8),

$$\sum_{k=1}^{N} \overline{\Phi_k i_k} = \overline{\int \rho v E d\tau}. \tag{18}$$

Let us consider $\overline{\Phi_k i_k}$ for the moment. There are in general two situations we often encounter in electronics:

(1) Φ_k is a constant. This is usually the case of a constant potential-energy source. Let the potential be represented by Φ_k^0. Then $\overline{\Phi_k i_k} = \Phi_k^0 \overline{i_k}$. From (6), noting that $\overline{\dot{q}_k} = 0$ for periodic variation, we have (also referring to the notation of (16))

$$\overline{i_k} = \overline{\int (\rho v)_{n'} dS_k}. \tag{19}$$

Thus we state from (19) that $\overline{i_k} \neq 0$ only when there is an actual transfer of charges between the electrode and the space. It is only under this condition that the source can deliver power (if $\overline{i_k} > 0$).

(2) Φ_k is a periodic function of t. Then $\overline{\Phi_k i_k}$ may not be zero even if $\overline{i_k} = 0$. If $\overline{\Phi_k i_k} > 0$, the electrode potential (for example, a high-frequency alternating-current source) delivers average power to the space charges, resulting in an increase of average kinetic energy. On the other hand, if $\overline{\Phi_k i_k} < 0$, average power is actually absorbed by the circuit associated with the electrode at the expense of retarding the space charges. Thus alternating-current power may be delivered to space charges or extracted therefrom even in the absence of direct transfer of charges.

The above two situations are in general simultaneously present in the entire electron-tube system. According to (18) the sum of the average external circuit powers is equal to the average rate of increase in kinetic energy of the charged particles. Some electrodes may have positive values for $\overline{\Phi_k i_k}$, while the other electrodes may have negative values for $\overline{\Phi_k i_k}$. Power may thus be transfered from one electrode to another with a simultaneous transformation from direct to alternating-current power. The transformation can in no case be complete as the average rate of increase in kinetic energy is degraded into heat energy when the charges strike the electrodes at considerable velocities.

Some Illustrative Applications

The theory presented above may serve to point out the nature of things, but in itself does not offer concrete solutions for a given problem, for the things we have assumed, the space-charge-density and velocity functions, are exactly those to be found for any actual solution. Nevertheless, the qualitative information derivable from this theory may often prove to be quite useful. We shall illustrate the point by taking up two special problems.

1. *Analysis of Parallel Plane Tubes at Ultra-High Frequencies*

Suppose we take two infinite parallel planes, one serving as the cathode at ground potential and the other serving as the anode. Both the convection current and the field will be in the direction perpendicular to the planes. Thus we have simply a one-dimensional problem. By the solenoidal property of the total current density, we see that it is purely a function of time, not a function of space. Let $J = \rho v + \dot{E}/4\pi$ and A = area of each plane. We have from (7)

$$i = JA. \tag{20}$$

Since, according to (20), the total external current is simply related to the space-current density, the latter should form a convenient tool for our analysis. This is in fact the fundamental starting point of some previous work on ultra-high-frequency electronics by Benham,[10] Llewellyn,[11,12] and Mueller.[13] To solve for the velocity function (or the space-charge function) one has to start from the equation of motion and apply appropriate boundary conditions. Following through this procedure and making extensions to triodes, one can actually derive the grid impedance at ultra-high frequencies,[14] which is in agreement with experiments.[1] We shall go no further here than to remark that our theory agrees in principle with what other workers have started.

2. *Analysis of a Klystron Amplifier or Oscillator*[4]

For the operation of this newly developed device, it is only necessary that a modulated space current be allowed to pass through the center holes of a pair of parallel plates, constructed as a part of a certain kind of resonator, sometimes designated as a rhumbatron. For simplicity, this setup may be regarded as equivalent to a pair of plates shunted by a parallel resonant circuit. As the space charges pass by, there is an induced current flowing between the plates which will support an alternating potential difference of the same fundamental frequency as the modulated space current. We see from (18) that the external circuit is able to extract power from the moving charges if we have

$$\overline{\phi i} = \overline{\int_{\tau_0} \rho v E d\tau} < 0 \tag{21}$$

where τ_0 is the volume between the plates and ϕ may be taken as the alternating potential of one plate while the other is at alternating-current ground. Neglecting

[10] W. E. Benham, "Theory of the internal action of thermionic systems at moderately high frequencies," Part I, *Phil. Mag.*, p. 641; March, 1928; Part II, *Phil. Mag.*, p. 457; February, 1931.

[11] F. B. Llewellyn, "Vacuum tube electronics at ultra-high frequencies," Proc. I.R.E., vol. 21, pp. 1532–1573; November, 1933.

[12] F. B. Llewellyn, "Note on vacuum tube electronics at ultra-high frequencies," Proc. I.R.E., vol. 23, pp. 112–127; February, 1935.

[13] J. Mueller, "Elektronenschwingungen in Hochvakuum," *Hochfrequenz. und Elektroakustik*, vol. 41, p. 158; May, 1933.

[14] D. O. North, "Analysis of the effects of space charge on grid impedance," Proc. I.R.E., vol. 24, pp. 108–136; January, 1936.

space-charge effect, E is just the field produced by the external potential. It is now clear that for (21) to be true there must be more charges flowing across the plates when the field retards than when the field accelerates the flow. That is to say, ρv has to be modulated. In a klystron the modulation is accomplished by imparting a velocity modulation by means of a buncher rhumbatron to a uniform electron stream and letting the modulated product drift along in a field-free space, acquiring naturally a space-current modulation. By finding the relation of the space current at the catcher rhumbatron (where power is to be extracted) and the original uniform current, one can readily write down the relations for power output and efficiency, which have already been treated by Webster[15] and Condon.[16]

[15] D. L. Webster, "Cathode-ray bunching," *Jour. Appl. Phys.*, vol. 10, p. 501; July, 1939.

[16] E. U. Condon, "Electronic generation of electromagnetic oscillations," *Jour. Appl. Phys.*, vol. 11, p. 502; July, 1940.

High-Frequency Radio Transmission Conditions, May, 1941, with Predictions for August, 1941*

NATIONAL BUREAU OF STANDARDS, WASHINGTON D. C.

THE radio transmission data herein are based on observations at Washington, D.C., of long-distance reception and of the ionosphere. Fig. 1 gives the May average values of maximum usable frequencies, for undisturbed days, for radio transmission by way of the regular layers of the ionosphere. The maximum usable frequencies were determined by the F layer at night and by the E, F_1, and F_2 layers during the day. Fig. 2 gives the expected values of the maximum usable frequencies for radio transmission by way of the regular layers, average for undisturbed days, for August, 1941. Average critical frequencies and virtual heights of the ionospheric layers as observed at Washington, D.C., during May are given in Fig. 3. Critical frequencies for each day of the month are given in Fig. 4.

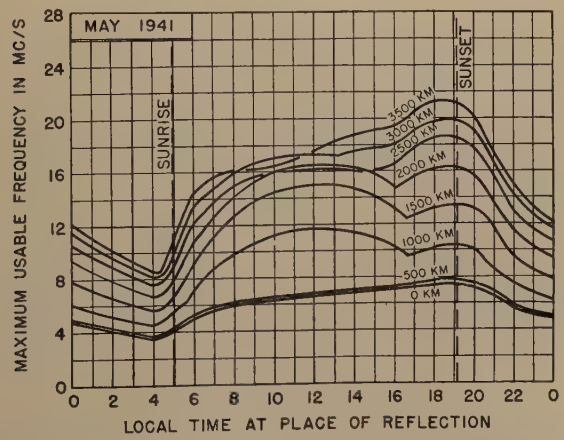

Fig. 1—Maximum usable frequencies for dependable radio transmission via the regular layers, average for undisturbed days, for May, 1941. These curves and those of Fig. 2 also give skip distances, since the maximum usable frequency for a given distance is the frequency for which that distance is the skip distance. The values shown were considerably exceeded during irregular periods by reflections from clouds of sporadic E layer (see Table III).

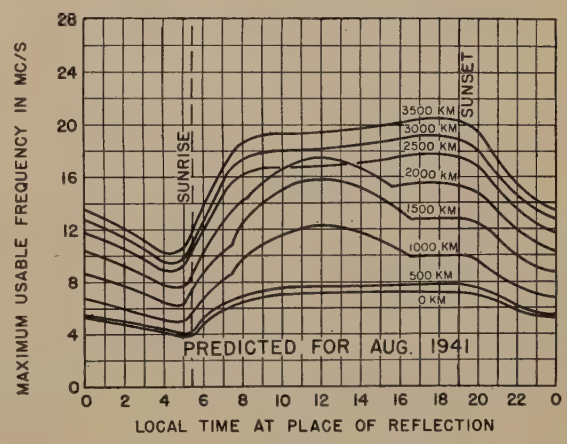

Fig. 2—Predicted maximum usable frequencies for dependable radio transmission via the regular layers, average for undisturbed days, for August, 1941. The values shown will be considerably exceeded during irregular periods by reflections from clouds of sporadic E layer. For information on use in practical radio transmission problems, see Letter Circulars on radio transmission obtainable from the National Bureau of Standards, Washington, D. C., on request.

Ionospheric storms are listed in Table I. A change has been made this month in the scales used for the ionospheric and magnetic character figures. In this and subsequent reports, both scales run from 0 to 9 instead of 0 to 2 as hitherto. The magnetic character figures given in Table I are averages, for each Greenwich half day, of the 3-hour magnetic K figures determined by the seven American-operated magnetic observatories. The change was made because the new magnetic character figure is a more quantitative measure of the storminess. The scale of the ionospheric character figure was changed in order to conform with that of the magnetic character figure.

The details of the ionospheric storm day of May 10 are shown in Fig. 3. The open circles in Fig. 4 indicate

* Decimal classification: R113.61. Original manuscript received by the Institute June 16, 1941. These reports have appeared monthly in the PROCEEDINGS starting in vol. 25, September, 1937. See also vol. 25, pp. 823–840: July, 1937. Report prepared by T. R. Gilliland, N. Smith, and C. O. Marsh.

the noon and midnight critical frequencies observed during the ionospheric storms listed in Table I. The sizes of the circles roughly represent the severity of the storm. Like April, May was characterized by much sustained, although not very severe, ionosphere storminess.

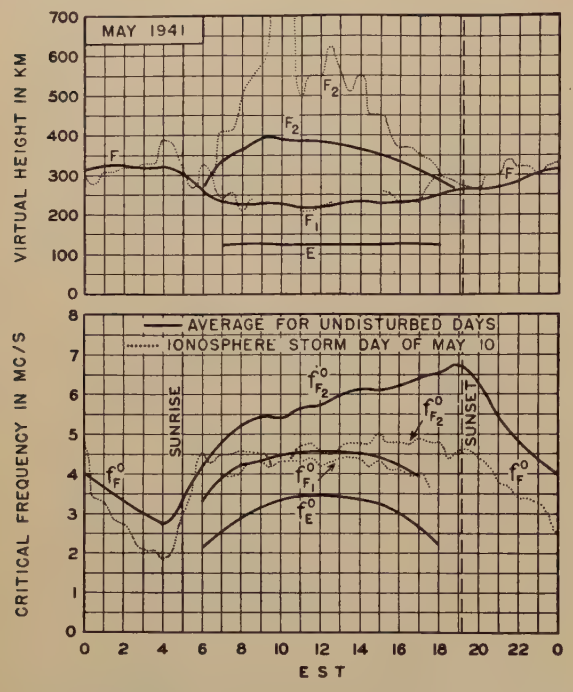

Fig. 3—Virtual heights and critical frequencies of the ionospheric layers, observed at Washington, D. C., May, 1941.

Sudden ionospheric disturbances are listed in Table II.

Table III gives the approximate maximum usable frequencies for good radio transmission via sporadic-E reflections.

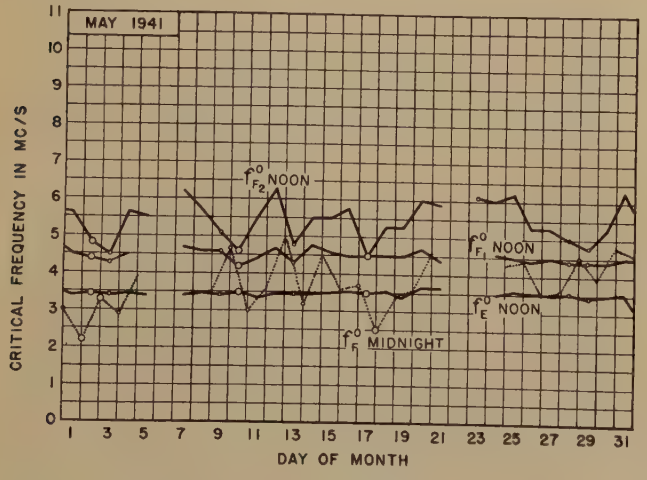

Fig. 4—Midnight and noon critical frequencies, for each day of May. Open circles indicate critical frequencies observed during ionospheric storms; size of circle represents approximate severity of storm.

TABLE I

IONOSPHERIC STORMS (APPROXIMATELY IN ORDER OF SEVERITY)

Day and hour E.S.T.	hF before sunrise (km)	Minimum fF^2 before sunrise (Mc)	Noon fF_2^0 (Mc)	Magnetic character[1] 00–12 G.M.T.	Magnetic character[1] 12–24 G.M.T.	Ionospheric character[2]
May						
1 (from 2100)	—	—	—	0.5	2.2	2
2	400	2.2	4.8	1.5	1.5	4
3	380	2.0	4.4	1.6	1.1	4
4 (through 0500)	383	1.5	—	3.0	1.8	1
9 (from 0700)	—	—	5.1	2.6	1.8	2
10	330	1.9	4.6	2.1	1.9	3
11 (through 0400)	325	1.9	—	1.6	0.8	1
17	372	2.7	4.5	3.6	2.4	3
18 (through 0500)	343	2.2	—	1.9	1.6	1
27 (from 2200)	—	—	—	1.8	1.5	2
28	312	2.4	5.0	1.9	2.0	2
29 (through 1600)	324	2.3	4.8	2.6	1.6	1
13 (from 0600)	—	—	4.8	2.2	1.6	2
14 (through 0500)	324	2.3	—	1.0	1.6	1
21 (from 1800)	—	—	—	2.1	3.0	[3]
22	[3]	[3]	[3]	3.9	3.0	[3]
23	[3]	[3]	[3]	2.9	3.2	[3]
24 (through 0500)	[3]	[3]	—	3.1	2.5	[3]
1 (through 0500)	350	2.2	—	0.5	2.2	1
For comparison: average for undisturbed days	322	2.78	5.70	1.8	1.6	0

[1] Average for 12 hours of American magnetic K figure determined by seven observatories, on an arbitrary scale of 0 to 9, 9 representing the most severe disturbance.
[2] An estimate of the ionospheric storminess at Washington, on an arbitrary scale of 0 to 9, 9 representing the most severe disturbance.
[3] Recorder not in operation.

TABLE II

SUDDEN IONOSPHERIC DISTURBANCES

Day	G.M.T. Beginning	G.M.T. End	Locations of transmitters	Relative intensity at minimum[1]
May				
8	1250	1310	Ohio, Ont., D.C.	0.05
8	1315	1410	Ohio, Ont., D.C.	0.00

[1] Ratio of received field intensity during fade-out to average field intensity before and after, for station W8XAL, 6080 kilocycles, 650 kilometers distant.

TABLE III

APPROXIMATE MAXIMUM USABLE FREQUENCIES IN MEGACYCLES, FOR RADIO TRANSMISSION VIA STRONG SPORADIC-E REFLECTIONS

Day	Hour, E.S.T. 00	01	02	03	04	05	06	07	08	09	10	11	12	13	14	15	16	17	18	19	20	21	22	23
May																								
1															19	19			21			14	20	16
2		14	15	14	15	18			22		22	22				22	21	24	19					
3			14		14													19	22	23	21	25	16	21
4	18	17																	16	16	16	17	15	16
5	15			18	15	17	18																	
7																			19	15	16	19		15
8		14	16	16		16	16											22	18	16	16	14	15	
9																	24			22				
10									24				22	23					28		16	15	17	
11				16							27											13	16	14
12	16	18	15														24	21	19	16				
13					15											33					22	22	16	17
14	15	15				16	18	22																
15										24								33	16	16				
16												22	40				28		22	15	18	14		
17																20				17	18			
18			15	15	18	16									21			23	20	22	25	18		
19			15	17																	19	45	19	19
20	18	23	24	22	22	18	20																	
21															22									
23												22	40											
25			24	19																				
26							22	26	32	34				25	40		33	29						
27	18																							
28																		22	21					
29																		24			22	21	23	
30											28	22			40	50	46	45	45	28				
31								22									23	23	19		18	16	15	

Institute News and Radio Notes

THE EXECUTIVE COMMITTEE

In managing the affairs of the Institute, the Board of Directors has found it necessary to adopt a practice followed by many other societies, that of establishing an Executive Committee. Our constitution places the responsibility of managing the Institute upon the Board of Directors. The President is assigned no duties or responsibilities beyond that of presiding at meetings. The Treasurer is assigned general supervision of the fiscal affairs of the Institute. The Secretary, besides being Secretary to the Board of Directors, is directed to attend principal meetings of the Institute and to prepare the business and to record the proceedings thereof. He is placed in charge of the books of account in the Institute and of the handling of correspondence and records. The Institute therefore is not provided with officers having all the powers and duties of officers with the corresponding names which are found in business organizations. Most of these powers and duties are reserved to the Board itself.

It has become evident in the last few years that a group of men, twenty-one in number, acting as a unit cannot properly exercise duties of management as charged in the constitution and that such a group as a whole may fail to exercise leadership at those vital times when leadership is essential. To remedy this situation the Board has appointed an Executive Committee from its membership consisting of the President, Treasurer, Secretary, Editor and two or more (three at present) other members to exercise the duties of executive management under policies laid down by the Board. In addition, these members are charged with certain duties. It is believed that by specifically assigning certain duties to certain members on this Committee that these various affairs of the Institute will get more attention than is given by the Board as a whole and that when problems arise and leadership is essential such members will be in a position to exercise leadership by suggesting appropriate action.

The powers delegated to the Executive Committee are outlined in bylaws which have just been adopted by the Board. These powers concern only matters which would fall under the category of management powers. The Board has reserved to itself all powers over elections, awards, budget, constitution and bylaws, and full authority to overrule the Executive Committee on any matter at any time. All policies of the Institute will continue to be determined by the Board itself. The Committee is definitely an instrument of the Board to facilitate the handling of management affairs in the Institute in what is hoped to be a better manner than has obtained in the past.

The Board as a rule holds eight to ten meetings a year, each meeting occupying a full afternoon. Under the new arrangement it is believed the Board will be relieved of much routine matter and can spend more time discussing problems and policies than it has been able to do in the past. Members on the Executive Committee will of necessity not only attend the Board meetings but will spend extra time in Executive Committee meetings and in other ways carrying out their assigned duties.

The present Executive Committee and the divisions of responsibility are given in the following table:

President (Dr. F. E. Terman)
- Chairman
- Supervisor of Executive Committee and General Supervision of Institute Affairs
- Prepare Board Agenda

Secretary (H. P. Westman)
- Secretary to the Executive Committee
- Assists President with Agenda
- Executive Management of Institute Affairs under the Supervision of Executive Committee and Members
- Managing Editor, News Writer

Treasurer (Haraden Pratt)
- Vice Chairman of Executive Committee
- Supervision of Office, Publications

Editor (Dr. A. N. Goldsmith)
- Board of Editors
- Papers Committee
- Papers Solicitation Committee
- Co-ordinating Committee
- Editorial Supervision of all Publications

Mr. A. (B. J. Thompson)
- Standardization and Other Technical Committees

Mr. B. (R. A. Heising)
- Advertising
- Nontechnical Committees (Conventions and Conferences, Public Relations, Admissions, Membership, Sections)

Mr. C. (M. Eastham)
- None assigned as yet

Since the Executive Committee is specifically charged to exert leadership its appointment opens a channel through which improvements in service to membership may be rendered and communications and suggestions on appropriate subjects are invited. It is hoped that the membership will take advantage of the division in responsibility and write their suggestions directly to that member of the Executive Committee responsible for the matter that interests them. Conversely complaints are also in order. In fact, the Executive Committee is inclined to quote the old advertising slogan, "If you like our product, tell your friends; if you don't, tell us."

R. A. Heising

Seattle and the omnipresent Mount Ranier.

PACIFIC COAST CONVENTION
August 20, 21, and 22, 1941
Seattle, Washington

The holding of four Pacific Coast conventions has established these annual meetings as high spots in the radio activities of our western membership. That the meetings are not exclusively of the Pacific Coast is indicated by the number who travel from other parts of the country to attend and to present papers.

The previous four meetings were held coincidently with the Pacific Coast conventions of the American Institute of Electrical Engineers. The headquarters hotels of the two conventions were adjacent and a free interchange of attendance at meetings occurred. It will not be possible to do this in 1941.

Our fifth Pacific Coast Convention will be held with headquarters at the Olympic Hotel in Seattle, Washington. The American Institute of Electrical Engineers will hold its summer convention on August 27, 28, and 29 at Yellowstone Park. Adequate time is available to permit those interested in both conventions to go from Seattle to Yellowstone Park in the interim between the conventions. Those making this trip may detour about 20 miles off the direct route and visit the Grand Coulee Dam. This is the biggest concrete structure in the world and when completed will develop large quantities of electricity, part of which will be used to pump water from the Columbia River to Grand Coulee to transform many thousand acres of arid wasteland into farms.

Seattle is located on Puget Sound and in its 70 square miles are located about half a million persons. On the west are the Olympic Mountains and the Cascade Range is to its east. Lake Union and Green Lake are of fresh water and are entirely within the city. Lake Washington, which forms the eastern boundary, is 26 miles long.

A shipping and transportation center, the city has a water front of almost 200 miles. Seattle is the gateway to Alaska and the western transcontinental terminus of four railroad lines and three airlines. It has a large lumber industry, which is second in importance only to its production and processing of food.

The convention program which follows is considered final and no important changes are anticipated. Papers are not available in preprint form and may not be published in the PROCEEDINGS.

PROGRAM

(Pacific Standard Time)

Wednesday, August 20

9:00 A.M.

Registration

10:00 A.M.–12:00 NOON

Presidential Address by F. E. Terman and technical session.

1. "Measurement of the Slope and Duration of Television Synchronizing Impulses," by R. A. Monfort and F. J. Somers, National Broadcasting Company, Inc., New York, N. Y.
2. "Practical Studio Speech-Input Systems and System Objectives for Radio Broadcast Service," by H. F. Scarr, Western Electric Company, Inc., Kearny, N. J.
3. "Relaxation Response of Video Amplifiers," by W. H. Huggins, Oregon State College, Corvallis, Ore.

12:30 P.M.–2:30 P.M.

Official Luncheon. Motion pictures and demonstration of disk recording.

8:00 P.M.–10:00 P.M.

Technical Session

4. "Impedance Measurements on Aircraft Antennas," by Frederick Ireland and Paul Holmes, General Radio Company and Stoddart Aircraft Radio Company, respectively, Los Angeles, Calif.
5. "Development of an Ultra-High-Frequency Aural Radio Range," by J. C. Hromada, Civil Aeronautics Administration, Washington, D. C.
6. "A Method for Calculating the Performance of Self-Biased Plate-Modulated Amplifiers," by R. I. Sarbacher, Illinois Institute of Technology, Chicago, Ill.
7. "Notes on Electrical Indicating Instruments," by H. E. Held, Weston Electrical Instrument Corporation, San Francisco, Calif.

Thursday, August 21

9:00 A.M.

Registration

9:30 A.M.–12:00 NOON

Technical Session

8. "The Determination of Field-Strength Patterns of Antenna Systems by Graphical Methods," by E.A. Yunker, Oregon State College, Corvallis, Ore.
9. "Horizontal-Polar-Pattern Calculator for Directional Broadcast Antennas," by F. A. Everest and W. S. Pritchett, Oregon State College, Corvallis, Ore.
10. "A Mechanical Device To Aid in the Calculation of Class B and C Power-Tube Performance," by R. I. Sarbacher, Illinois Institute of Technology, Chicago, Ill.
11. "Some Observations on Interruptions to Radio Communication over Short Distances in High Northern Latitudes," by R. J. Gleason, Pan American Airways, Seattle, Wash.
12. "Concentric-Section Resonant Transmission Lines," by L. M. Hollingsworth, San Francisco Junior College, San Francisco, Calif.

1:30 P.M.–4:30 P.M.

Trip to Lake Washington Floating Bridge

6:30 P.M.

Official Dinner. Color motion pictures of the collapse of the Tacoma Narrows Suspension Bridge taken by Professor Farquharson will be shown.

Friday, August 22

9:00 A.M.

Registration

9:30 A.M.–12:00 NOON

Technical Session

13. "Some Simplified Methods of Determining the Optical Characteristics of Electron Lenses," by Karl Spangenberg and L. M. Field, Stanford University, Stanford University, Calif.
14. "Theory of Radial Direct-Current Space-Charge Flow Between Concentric Cylinders," by W. G. Dow and A. B. Bronwell, University of Michigan, Ann Arbor, Mich., and Northwestern Technological Institute, Evanston, Ill., respectively.
15. "Factors Encountered in Frequency-Modulation-Sideband Limitation," by H. J. Scott and L. J. Black, University of California, Berkeley, Calif.
16. "A Frequency-Modulation Station Monitor," by H. R. Summerhayes, Jr., General Electric Company, Schenectady, N. Y.
17. "Application of Conducting Rubber to the Shielding of Flexible Leads," by T. F. Peterson and W. Lewis, American Steel and Wire Company, Worcester, Mass.

1:30 P.M.–6:00 P.M.

Trip to KIRO

8:30 P.M.–11:00 P.M.

University of Washington Penthouse Theater

LUNCHEON AND DINNER

The official luncheon scheduled for Wednesday will be informal. It will be held at the Olympic Hotel. Tickets will be $1.25 each.

Motion pictures of the laboratory and shop of the Presto Recording Corporation will be projected. Enlarged views of cutting and playing needles and of the record grooves will be included. Sound accompaniment will be by disk recordings. In addition, recordings made at the University of Washington will be played.

The official dinner which is scheduled for Thursday evening is also informal and will be at the Olympic Hotel. Tickets will be $1.60 each.

The Tacoma Narrows Suspension Bridge which collapsed some months ago had previously shown weaknesses which demanded engineering attention. F. B. Farquharson, professor of civl engineering at the University of Washington, was consulted and built a model of the structure for testing methods of strengthening the bridge. Professor Farquharson took colored motion pictures of the bridge at the time of its destruction. These pictures will be shown at the dinner.

TRIPS

Thursday, August 21

LAKE WASHINGTON FLOATING BRIDGE

On Thursday afternoon, a trip will be taken to see the Lake Washington Floating Bridge. This unusual bridge, which was opened to traffic last year, is 1.3 miles long. It is the largest floating structure in the world and crosses Lake Washington on 25 concrete pontoons. One section of the bridge may be moved to permit boats to pass through.

Friday, August 22

KIRO

On Friday afternoon, an inspection trip will be taken to the transmitter of KIRO which is located on Vashon Island in Puget Sound. It is about 10 miles from Seattle by ferry. KIRO has recently placed a new 50-kilowatt transmitter in operation.

The Olympic, headquarters hotel for the convention.

PENTHOUSE THEATER

Arrangements have been made for reserving tickets for the Friday evening performance at the University of Washington Penthouse Theater. This unique theater has the stage located in the center of the room with the audience surrounding it. New production techniques have been successfully evolved during several years of operation. The theater is housed in a new modernistic structure located on the campus and is operated by the division of drama of the University. Tickets are fifty-five cents each.

WOMEN'S PROGRAM

Wednesday, August 20

9:00 A.M.

Registration

12:30 P.M.–5:00 P.M.

Luncheon, followed by a visit to the Seattle Art Museum and to the Northwest Indian Exhibit at the University of Washington

8:00 P.M.–11:00 P.M.

Showboat Theater

Thursday, August 21

1:30 P.M.–5:00 P.M.

Trip on Steamer *Sightseer*

6:30 P.M.

Official Dinner

Friday, August 22

1:00 P.M.–6:00 P.M.

Trip to KIRO

8:30 P.M.–11:00 P.M.

Penthouse Theater

SEATTLE ART MUSEUM

The Seattle Art Museum is located in Volunteer Park and is noted for its collection of Chinese art, included in which is an outstanding exhibition of jade carvings.

NORTHWEST INDIAN EXHIBIT

This exhibition of clothing, tools, pottery, and other equipment used by the Northwest Indians depicts the life and conditions of their times. It is located at the University of Washington.

SHOWBOAT THEATER

The Showboat Theater is operated by the division of drama of the University of Washington. It is built in the form of a ship on the shore of Lake Union, and is on the campus of the University. During intermission, one may promenade on the balcony overhanging the lake. A large revolving stage permits rapid changes in scenes. Admission is seventy-five cents.

SIGHTSEEING TRIP

From Puget Sound, the Steamer *Sightseer* will pass through the second largest locks in North America to Lake Union and Lake Washington. Unlike most boat trips, this one is through the heart of a city. Tickets are $1.25 each.

Trans-Pacific liner going through one of the locks.

OTHER EVENTS

The dinner on Thursday evening, the Friday trip to KIRO, and attendance at the Penthouse Theater are arranged for both the men and women and details are given under the men's program.

TECHNICAL PAPERS

Copies of the technical papers will not be available from the Institute either before or after the convention. In some cases the authors may be able to supply copies.

Summaries of the papers follow and are arranged alphabetically by the names of the authors. Papers are numbered in the order in which they are to be presented and this permits ready cross reference between the program and the summaries.

SUMMARIES OF TECHNICAL PAPERS

14. THEORY OF RADIAL DIRECT-CURRENT SPACE-CHARGE FLOW BETWEEN CONCENTRIC CYLINDERS

W. G. Dow and A. B. Bronwell
(University of Michigan, Ann Arbor, Mich., and Northwestern Technological Institute, Evanston, Ill., respectively)

A general differential equation is set up governing the unidirectional direct-current and alternating-current flow of space charge wherever the lines of electric flux and space-charge flow are coincident and straight, thus including normally directed flow between parallel planes, radial flow between concentric cylinders, and radial flow between concentric spheres. It is shown that a simple form of these equations is obtained by the introduction of a parameter which measures transit time in terms of an electronic time unit of 2.38×10^{-8} second duration. Direct-current boundary conditions are classified as follows, for purposes of solution: Case I, involving a minimum in the potential distribution; Case II, in which the potential distribution curve rises from zero with a finite slope; and Case III, the complete space-charge condition. Numerically useful solutions for all of these three general types of direct-current flow between parallel planes and concentric cylinders are obtained, and presented in the form of parametric families of curves describing potential distribution and transit-time relations for useful ranges of currents, voltages, and geometries.

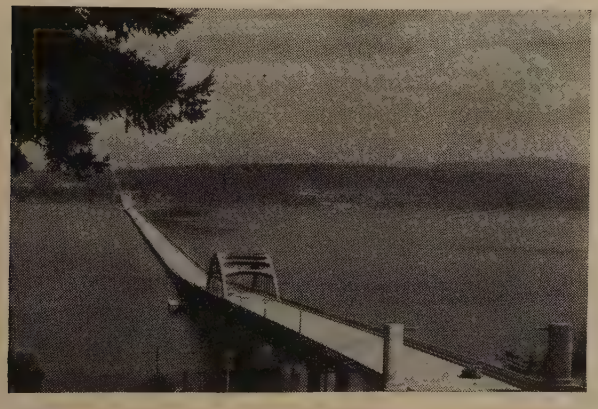

The Floating Bridge across Lake Washington.

9. HORIZONTAL-POLAR-PATTERN CALCULATOR FOR DIRECTIONAL BROADCAST ANTENNAS

F. A. Everest and W. S. Pritchett
(Oregon State College, Corvallis, Ore.)

While a working understanding of the functioning of arrays is quite easily attained through vector and geometrical concepts, the actual determination of space patterns may become exceedingly laborious. For instance, the determination of a suitable horizontal polar pattern of a 2-element array to solve certain definite interference or coverage problems may consume many hours or even days of painstaking calculations and plotting in exploring the promising regions. The calculations for the nonsymmetrical, 3-element case are much more involved. The number of possible combinations is also very great. For instance, for element spacings up to 1 wavelength in 20-degree steps, current ratios in 10 per cent steps, and element phasings up to 360 degrees in 20-degree steps, there are several thousand possible symmetrical patterns for the 2-element array, and many million nonsymmetrical patterns for the 3-element array. The desirability of a device which will automatically plot the horizontal polar pattern, once the adjustments for element spacing, phasing, and current ratios are made, is obvious.

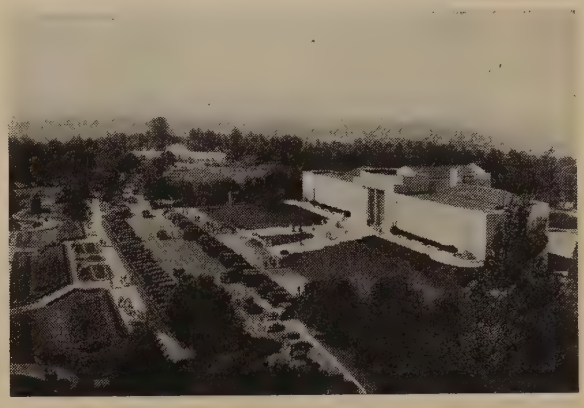

The Seattle Art Museum in Volunteer Park.

Methods of accomplishing this task by electrical and mechanical means will be described. A mechanical calculator intended primarily for 2- and 3-element broadcast arrays is described in detail and a model demonstrated.

At any point P on a horizontal plane passing through the base of a vertical tower antenna, the field strength is directly proportional to the current in the antenna. In an array, the resultant field strength is the vector sum of the voltages from each element. These vectors have lengths proportional to the currents in their respective elements and angular relationships determined by the relative phasings of the elements and the differences in path length. The mechanical array calculator combines these vectors automatically and utilizes the resultant vector length to drive a recording pen which

traces the horizontal polar pattern on a table revolving with the horizontal-angle disk.

Olympic Mountains.

11. SOME OBSERVATIONS ON INTERRUPTIONS TO RADIO COMMUNICATION OVER SHORT DISTANCES IN HIGH NORTHERN LATITUDES

R. J. Gleason
(Pan American Airways, Seattle, Wash.)

Communication on short waves is often interrupted for periods of hours and even for days in the more northern latitudes. This paper presents, in summarized form, the results of hundreds of observations of this phenomenon made in Alaska and the Yukon.

7. NOTES ON ELECTRICAL INDICATING INSTRUMENTS

H. E. Held
(Weston Electrical Instrument Corporation, San Francisco, Calif.)

This paper deals with the fundamental principles of basic electrical-indicating-instrument mechanisms; permanent-magnet and moving-coil, iron-vane, and dynamometer types. Improvements in manufacturing processes and newer materials enable instrument designers to make available instruments of improved sensitivity performance and other characteristics. A review of the fundamental theory of operation of the basic instrument mechanisms covers the development of torque and damping in an instrument and the effect of the weight of the moving parts.

The effect of temperature on portions of the mechanisms and on the completed devices is covered.

The use of direct-current mechanisms to measure other than unidirectional currents; for example, the use of thermal converters and copper-oxide rectifiers for measurement of alternating current of extended frequencies, is treated together with a description of recent improvements in their design.

12. CONCENTRIC-SECTION RESONANT TRANSMISSION LINES

L. M. Hollingsworth
(San Francisco Junior College, San Francisco, Calif.)

A new method of shortening the physical length of concentric resonant transmission lines which are used as resonant circuits and as circuit elements at high radio frequencies has been developed. Usual resonant transmission lines must have a physical length equivalent to 90 electrical degrees at their resonant frequency. They have been shortened in the past by coiling or folding them and by condenser loading. This new method of shortening the required length of line consists in dividing the necessary length of line into sections and by properly proportioning their diameters to arrange all of the sections inside of the outer conductor of the first section. In this way conductors with the exception of the outermost and the innermost conductor are utilized as inner conductors of one section and outer conductors of the following section. The first and outermost section is the one with the short-circuited end. It is chosen thus, so that the highest current will occur where the diameters are the greatest.

Using the same b/a value for each section, the total length of sections must equal 90 degrees. So a 2-section line will have a physical length corresponding to 45 degrees; a 3-section line, a length corresponding to 30 degrees; etc. It is found that while the Q does decrease from that of a straight line, the length decreases faster so that when one considers Q divided by length, a significant gain is noted.

Using different values of b/a ratio in the different sections introduces a load angle at their junction. This has the effect of making the needed total length of sections either more or less than 90 degrees. If the first section has a high value of b/a ratio and the second section a low value, the length needed may be greatly reduced. At the same time Q is reduced only a slight amount so that on a basis of Q/length this type of concentric-section line surpasses both the straight line and the concentric-section line with constant b/a ratio.

A line of each type was constructed and values of Q measured by the frequency-variation method. Both lines were 8 inches in diameter, about 20 inches long and resonant at a frequency of 56 megacycles. The theoretical values of Q were 3520 and 4600 and the measured values were 2430 and 3100 which are 69 per cent and 67.7 per cent of the theoretical values. This difference was anticipated since it was known that the surface of the commercial copper forms would not be perfect and that this would decrease the value of Q.

Equations for calculating the Q of these lines were developed. Charts and curves for use in the calculation of Q are included.

5. DEVELOPMENT OF AN ULTRA-HIGH-FREQUENCY AURAL RADIO RANGE

J. C. Hromada
(Civil Aeronautics Administration, Washington, D. C.)

This paper describes a series of aural radio range experiments conducted at Indianapolis, Indiana; Pittsburgh, Pennsylvania; Washington, D. C.; and Van Nuys, California, at frequencies of 63 and 125 megacycles. The results of numerous ground and flight tests using vertical and horizontal antennas are discussed with particular reference to the frequency, multiple courses, cone-of-silence characteristics, polarization effects, reflections, noise, atmospherics, distance range, ionospheric reflections, and aircraft antennas. The paper shows the progression of development from vertical polarization to horizontal polarization, using crossed dipoles, to the finally adopted horizontally polarized array using horizontal loops which have substantially pure polarization. The adopted array possesses two very desirable characteristics; namely, a field pattern having a considerable increase in field strength on-course and a reduction of field strength off-course. These characteristics are not available with the conventional crossed figure-of-eight radio range pattern.

In the early part of the development it is shown that the 63-megacycle vertically polarized range was somewhat superior to the 125-megacycle range using either vertical or horizontal crossed dipole antennas particularly as regards multiple courses and polarization effects. Through the use of new developments made available by the rapidly progressing art of applying ultra-high frequencies to the radio range problem, it is shown conclusively that a radio range operating on 125 megacycles and using pure horizontal polarization is superior to any of the other ultra-high-frequency facilities previously developed.

3. RELAXATION RESPONSE OF VIDEO AMPLIFIERS

W. H. Huggins
(Oregon State College, Corvallis, Ore.)

Because of the close similarity existing between the television video signal and a square-topped voltage wave, a fundamental approach to the problem of the design of a video amplifier is through the response of the amplifier to a square-wave signal. It is obvious that any signal may do only two things: it may change or it may remain constant. A square wave does both of these things to the extreme. The manner in which the amplifier responds to an instantaneous unit change in signal voltage is the "impulse" response and is closely related to the high-frequency characteristics of the amplifier. The "relaxation" response is the manner in which the response returns to zero after the unit change in signal voltage has been applied. It is related to the low-frequency characteristics of the amplifier.

The impulse response of the video amplifier, as measured by its ability to amplify a high-frequency square wave, has already been investigated by other writers. They have shown that this high-frequency analysis is most easily accomplished by replacing the square wave with its equivalent Fourier series. This is true when the fundamental frequency of the square wave is high because then the amplifier acts essentially as a low-pass filter and only the first few harmonics of the Fourier series need be considered.

However, in the case of the low-frequency square wave, the amplifier acts as a high-pass filter, and many of the harmonics must be included in the Fourier series if the response is to be accurately represented. For this reason, it is more convenient to discard all such concepts as sine waves and impedances, and, returning to the fundamental differential equations for the network, derive equations for an applied square wave of any frequency by properly determining the constants of integration so that they satisfy certain "conditions of continuity."

Since the relaxation distortion occurring in a square wave is of a definite general type, it is convenient to define a "distortion index" which is proportional to the amount of distortion in the wave shape. Then, since the analytic response equations to a square-wave signal are known, it is possible to obtain the relation between the values of the various circuit components and the distortion index. The circuit constants required to produce a response of any desired distortion value are thereby readily determined.

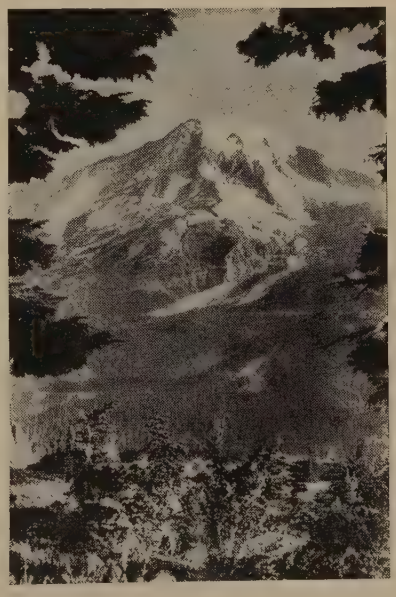

Mount Ranier.

4. IMPEDANCE MEASUREMENTS ON AIRCRAFT ANTENNAS

Frederick Ireland and Paul Holmes
(General Radio Company and Stoddart Aircraft Radio Company, respectively, Los Angeles, Calif.)

This paper reports a brief comparison of aircraft-antenna characteristics as measured directly by (a) a radio-frequency bridge, and (b) a bridged-T impedance-measuring circuit, as contrasted with the usual substitution methods. The purpose of the paper is therefore to show that consistent measurements of aircraft antennas are practicable by several methods.

1. MEASUREMENT OF THE SLOPE AND DURATION OF TELEVISION SYNCHRONIZING IMPULSES

R. A. Monfort and F. J. Somers
(National Broadcasting Company, New York, N.Y.)

The operation of a television broadcasting system on a regular public-service schedule over a period of years has shown the need for various auxiliary monitoring and measuring equipment. Suitable equipment and technique for insuring that the synchronizing signals transmitted shall at all times correspond to the prescribed standards is one important requirement in maintaining a high-quality service.

In order to be useful, equipment for making measurements on synchronizing signals must not only be capable of the required accuracy, but must at the same time be simple and easy to use under actual operating conditions. The tolerances prescribed for the steepness of the wave-fronts of television synchronizing impulses, as well as their duration times, require measurement equipment and techniques capable of precision measurement of fractional microsecond time intervals.

Owing to the complicated wave shapes and wide band of frequency components represented by television synchronizing signals, visual methods of measurement utilizing a suitable cathode-ray oscilloscope, or its equivalent, are used in making synchronizing-pulse measurements.

Errors arising from the use of the usual saw-tooth sweep oscillator in measuring impulse widths and slopes are described in the paper. An accurate and satisfactory method for making these measurements utilizing a sine-wave horizontal sweep of either power-supply frequency or scanning-line frequency, depending on the portion of the signal under consideration, is described in detail. Equipment for deriving the sine-wave directly from the main synchronizing generator for measuring local signals, as well as equipment for generating a suitable sine wave for making measurements on remotely generated signals, is described. It is also shown that the sine-wave technique is useful in measuring transmission times in television studio delay networks and for making useful checks on the synchronizing generator.

An alternative method of measuring impulse slopes utilizes a high harmonic of the scanning-line frequency to modulate the grid of the oscilloscope.

Equipment for checking the number of vertical sections and other features of the synchronizing signal, utilizing a video monitor, is also described.

17. APPLICATION OF CONDUCTING RUBBER TO THE SHIELDING OF FLEXIBLE LEADS

T. F. Peterson and W. Lewis
(American Steel and Wire Company, Worcester, Mass.)

Many forms of shielding have been applied to cables and wiring of power, measurement, and radio circuits. Generally speaking most requirements are met by full metallic coverings or wire braids.

Tinned-copper-wire shielding may be more difficult and costly to obtain in the future. To meet this situation the authors have expanded their development of "conducting-rubber" shielded power cables to include its application to high-frequency circuits and leads.

Characteristics of the flexible rubber shielding in combination with "wire drains" are given and suggested uses are discussed.

6. A METHOD FOR CALCULATING THE PERFORMANCE OF SELF-BIASED PLATE-MODULATED AMPLIFIERS

R. I. Sarbacher
(Illinois Institute of Technology, Chicago, Ill.)

A method has been developed by means of which it is possible to calculate the performance of a plate-modulated amplifier with a resistance bias. This method permits the accurate determination of the path followed by the quiescent point during the modulation cycle when the bias for the amplifier is obtained either from grid current alone or from grid and plate current together.

Dynamic characteristics showing the performance of a triode operating as a plate-modulated amplifier have been obtained for generator bias, resistance bias, and a combination of both. The improvement in linearity of the amplifier and in the reduction in driving power required when resistance bias in the grid circuit gradually replaces generator bias is clearly shown on these dynamic characteristics. A large reduction in peak driving power is also plainly evident when grid-resistance bias is employed. The gains and sacrifices made in the transition from one type of grid polarization to the other are brought out. An experimental confirmation of the calculated characteristics shows an agreement everywhere within 3 per cent.

A calculating device has been developed which aids materially in the calculation of the operating char-

acteristics of amplifiers operating in class B or C. This device, employed in the calculation of the material discussed above, greatly simplied the procedure and speeded the progress of the work.

10. A MECHANICAL DEVICE TO AID IN THE CALCULATION OF CLASS B AND C POWER-TUBE PERFORMANCE

R. I. Sarbacher
(Illinois Institute of Technology, Chicago, Ill.)

When it is desired to make graphical calculations of the complete dynamic characteristics of power tubes in various classes or conditions of service, it is often found advantageous to have available a mechanical device to aid in the preparation of the data. Such a device has been developed and is easy to construct and use. The principle employed may be applied to any type of harmonic analysis and is especially adaptable to E. L. Chaffee's 13-point harmonic analysis. A number of these devices have been made up for the students at the Illinois Institute of Technology and have proved extremely valuable in their work.

2. PRACTICAL STUDIO SPEECH-INPUT SYSTEMS AND SYSTEM OBJECTIVES FOR RADIO BROADCAST SERVICE

Henry F. Scarr
(Western Electric Company, Inc., Hearny, N. J.)

In the early days the audio system was a simple accessory—necessary to drive the broadcast transmitter, but not important in its own right. To attract clients and listeners under present-day competitive conditions, the technical side of program production becomes a complex and more important function, and requires audio facilities which have flexibility, operating simplicity, and reliability, and provide noise-free life-like transmission. This is necessary even though audio frequencies now reach well into the "long-wave" radio region. Broadcasting has "come of age" commercially. Appearance of equipment must be considered. Investment in facilities must be economically proportioned to earning power. Experimentation is costly. It is, therefore, timely to set down for the guidance of the studio engineer some typical systems which have proved themselves and to point to the objectives which have served as a basis for their design.

15. FACTORS ENCOUNTERED IN FREQUENCY-MODULATED-SIDEBAND LIMITATION

H. J. Scott and L. J. Black
(University of California, Berkeley, Calif.)

The spectral width of a frequency-modulated wave and, consequently, adjacent-channel interference, depends upon the amplitude as well as upon the frequency of the modulating signal. The maximum width which this spectrum may have has been tentatively specified by the Federal Communications Commission as 200 kilocycles. This limitation may be attained by restricting the amplitude of the modulating signal, or it may be attained by the use of radio-frequency filters.

Limitation of the frequency spectrum is most logically controlled by limiting the amplitude of the modulating signal. By this means, the magnitude of the sideband at the edge of the transmitted band may be made to have any desired value below that of the unmodulated carrier. With this type of band-width limitation, no distortion is introduced into the system by the process of limitation.

It is at all times desirable to modulate as completely as possible within the limits placed upon the resulting spectral width. A universal family of curves relating the maximum permissible frequency deviation to the audio modulating signal has been prepared. Other curves which show the distribution of the energy in normal speech and music have been prepared along with a curve showing the use of these in setting modulation limits.

Limitation of the frequency spectrum may also be accomplished by the use of radio-frequency filters designed to pass the desired band of frequencies and to reject all other frequency components lying outside of this band. When spectrum limitation is accomplished in this manner, however, serious distortion results and the received signal is no longer a true reproduction of the original modulating signal. An analysis has been made and expressions have been derived to show the type and the extent of this distortion. Wave forms showing the received signal resulting from the removal of sidebands have been prepared and the distortion in each case has been calculated. In general it may be stated that within the practical limits of operation, the distortion introduced by sideband clipping is of the order of $2J_n(m)$ where n is the order of the lowest sideband removed.

13. SOME SIMPLIFIED METHODS OF DETERMINING THE OPTICAL CHARACTERISTICS OF ELECTRON LENSES

Karl Spangenberg and L. M. Field
(Stanford University, Stanford University, Calif.)

Some new methods of calculating electron paths are proposed and their limitations discussed. A new experimental method of determining focal lengths of lenses has also been developed. This makes use of angular magnifications measured from shadows cast by object screens illuminated by a point source of electrons. The method does not require screens movable in a vacuum nor the generation of rays parallel to the axis. Measurements were made with a demountable vacuum system. Results are more accurate than those obtained by previous investigators and cover a greater range of voltage ratios. Results are presented for various types

of cylinder and aperture lenses and combinations thereof. The field has been covered extensively enough so that interpolations between different lenses are possible and trends for all important cases can be determined. In addition to presenting the characteristics in the standard form showing the variation of focal lengths with voltage ratio, the results are presented in a new and simplified form in which associated object and image distances and corresponding magnification are immediately given for the extended range of voltage ratios. Observations on the relative aberrations of different types of lenses are made.

10. A FREQUENCY-MODULATION STATION MONITOR

Harry R. Summerhayes, Jr.
(General Electric Company, Schenectady, N. Y.)

This is a nonmathematical paper which describes the development, theory, and characteristics of a frequency-modulation station monitor developed in the general engineering laboratory of the General Electric Company. The monitor measures center frequency with and without modulation and the percentage of frequency modulation as a per cent of 75-kilocycle deviation. In addition, it provides a flasher and alarm circuit for overmodulation adjustable from 50 to 120 per cent and an audio-frequency fidelity monitoring circuit. The paper begins with a discussion of the requirements for frequency-modulation monitors and compares the problems involved with those involved in standard broadcast monitors. Several schemes which were examined for use as a frequency-modulation monitor are briefly described, including counter and frequency-division systems. The principles and design of the final monitor are discussed. In these monitors, precision crystal oscillators are employed to provide for both accurate calibration and the intermediate frequency.

The last part of the paper is devoted to a discussion of the salient development problems encountered, to a detailed description of the circuit, and to a discussion of the over-all specifications of the commercial sample.

8. THE DETERMINATION OF FIELD-STRENGTH PATTERNS OF ANTENNA SYSTEMS BY GRAPHICAL METHODS

E. A. Yunker
(Oregon State College, Corvallis, Ore.)

The general problem of the determination of antenna directivity by graphical vector addition rather than by the use of analytical expressions is discussed and an example worked out. The method is applicable to the most general combination of known factors which completely determine field-strength patterns and has several advantages over analytical methods.

Board of Directors

A regular meeting of the Board of Directors was held on June 4 and those present were Haraden Pratt, chairman; A. B. Chamberlain, I. S. Coggeshall, Melville Eastham, Alfred N. Goldsmith, Virgil M. Graham, O. B. Hanson, R. A. Heising, L. C. F. Horle, C. M. Jansky, Jr., F. B. Llewellyn, B. J. Thompson, H. M. Turner, A. F. Van Dyck, H. A. Wheeler, L. P. Wheeler, and H. P. Westman, secretary.

Several proposals to amend the Institute constitution were approved for submission to the membership for ballotting. They concerned provisions for admitting into the Institute as Members, those in work closely allied to radio, equalization of the admission fee for Member and Fellow grade at $5.00 each in view of the fact that the dues for these grades are identical, and procedures for the appointment of committees and directors.

A number of bylaws were adopted and concerned the holding of meetings of the Board of Directors, the listing of the standing committees, and provisions for the Appointments Committee and the Executive Committee.

The Awards Committee voted the Morris Liebmann Memorial Prize for 1941 to Philo T. Farnsworth for his contributions in the field of applied electronics.

Executive Committee

The Executive Committee met on June 4 and those present were Haraden Pratt, chairman; Melville Eastham, Alfred N. Goldsmith, R. A. Heising, B. J. Thompson, and H. P. Westman, secretary.

During the month of May, 83 applications for Associate, 4 for Junior, and 69 for Student grade were received. These were approved.

The Secretary was authorized to continue work on the publication of a cumulative index for the Proceedings.

Sections

Atlanta

"Practical Studio Construction" was the subject of a presentation by H. J. Sabine of the Celotex Company. It was divided into two parts. There was treated first the elimination of undesired sound from the studio and then the control of the desired sound.

The elimination of undesired sound, which is the result of vibration of the studio by conduction, is one of the most difficult problems. Most cases of this kind are remedied either by the use of resilient mountings for the machine creating the disturbance or by mounting the studio on springs, or both. The next major problem is the transmission of noise through the air and the most advantageous way to overcome this is by the use of double-wall construction.

Some acoustic phenomena were described by electrical analogies. It was pointed out that sound attenuation through walls is a function of the type of construction. Attenuation of sound by the use of mass was referred to as the reactive method and resilient mountings were called high-frequency shunts.

A minimum loss between studios of 45 decibels was considered necessary for good results.

Sectional illustrations were shown of several types of wall construction and the attentuation factor in decibels for each was noted. The use of doors and windows in studios was given detailed attention and the necessity of avoiding air leaks around microphone outlets and similar fittings was stressed.

Information was provided on the velocity of air used for air conditioning. It was recommended that air ducts be lined with sound-absorbing material and that grillwork be used at the air vents to reduce noise.

An example of good door construction was given as an extra-heavy door or a door of double construction, the panels of which

float in gaskets or are backed with a damping material. Sound locks were described.

The use of inclined walls and zig-zag ceilings was considered. An obvious fault is the placing of windows opposite each other at the microphone level.

Reverberation time was defined as the time required for a sound to diminish to a level 60 decibels below its original level. The Sabine reverberation-time formula was given and an explanation of its use in practical studio construction was provided.

At the conclusion of the meeting, members were invited to attend a demonstration of reverberation-time measurements made at the WGST studios by the speaker.

May 16, 1941, A. W. Shropshire, chairman, presiding.

Boston

F. V. Hunt and J. A. Pierce of the Cruft Laboratory of Harvard University presented a paper on "High-Fidelity Sound Reproduction." A paper on their lightweight pickup was presented before the Boston section over two years before this meeting. That device has been improved so that it is no longer the limiting mechanism in the system and at this meeting the emphasis was on the loud speaker.

A number of demonstrations were made using practical material drawn from radio and other sources. Ten different loudspeaker systems were employed varying from the inexpensive midget dynamic speaker to a theater-type "reference system" constructed by the authors. Products of various manufacturers were included.

By using wave filters, the effects of eliminating different parts of the audio-frequency spectrum were demonstrated. It was shown that the sibilant "*s*" is present when the high-frequency range extends to 4000 cycles but disappears when the cutoff occurs at 3500 cycles.

A number of records of widely differing types of music were played and the voices of various speakers were used for reproduction. Ballots were distributed among the audience and each hearer indicated which speaker he preferred. Fairly good agreement was obtained as to which was the best speaker although there was considerable diversity of opinion. The authors intend to correlate these data with similar information previously secured.

This was the annual meeting and W. L. Barrow of Massachusetts Institute of Technology, was elected chairman; J. M. Henry of the New England Telephone Company, was named vice chairman; and P. K. McElroy of the General Radio Company was designated secretary-treasurer.

May 31, 1940, P. K. McElroy, secretary-treasurer, presiding.

J. A. Worcester of the radio and television department of the General Electric Company (Bridgeport) presented a paper on "Frequency-Modulation-Receiver Design."

The characteristics of an ideal frequency-modulation receiver were described and the difficulties of attaining it were pointed out. The gain ahead of the audio-frequency system should be about 4 million. An analysis was then presented of the theoretical gain which could be achieved in each section of the receiver. Practical gains are lower because of production tolerances and stray couplings. The necessary gain cannot be provided with the ordinary superheterodyne system and an ingenious double-heterodyne scheme using only one oscillator was devised to solve the problem.

A new type of limiter circuit employing two tubes is incorporated in the receiver and improves limiter performance substantially. The results obtained with these receivers were described and compared with what would be expected of an ideal receiver.

January 31, 1941, W. L. Barrow, chairman, presiding.

K. K. Darrow of Bell Telephone Laboratories presented a paper on "The Ionosphere."

Dr. Darrow presented first a brief historical sketch of investigations of the ionosphere starting with the independent work of Kennelly and Heaviside around 1904. About 1925, methods for investigating the ionosphere were devised and those used by Breit and Tuve and by Appleton were described.

The broad constitution of the ionosphere was then discussed. The so-called E and F layers were considered and the critical frequency of each for transmission and reflection of electromagnetic waves was indicated.

The paper closed with a qualitative demonstration of the mathematical procedure of interpreting the echo-method records of virtual height of the ionospheric layers into the true height of those layers.

February 28, 1941, W. L. Barrow, chairman, presiding.

Buenos Aires

A paper on "Loud Speakers" was presented by Adolfo Di Marzo.

The application of electric circuit treatment, both qualitatively and quantitatively, to the acoustical and mechanical elements of a loud speaker was first presented. Fundamental formulas for the performance of direct-radiating cone loud speakers under ideal conditions for both the high- and low-frequency region were then developed.

Several practical limitations were discussed and included those affecting the high-frequency region such as the relatively large mass of the voice coil. The fact that the cone does not act as a rigid piston at the higher frequencies was also discussed and these effects were demonstrated.

Systems for obtaining wide-range response were described. The double-voice-coil speaker was considered in detail. The practical impossibility of obtaining large acoustic output and wide frequency range in a single direct-radiating cone speaker was demonstrated.

The application of extremely wide-range loud speakers for ordinary broadcast reception was shown to be generally undesirable. The elimination of the distortion products produced both in the receiver and in the transmission medium was shown to be possible by designing the speaker to act as its own low-pass filter.

May 30, 1941, P. J. Noizeux, chairman, presiding.

Cincinnati

"The Design of Feedback Amplifier Systems" was the subject of a paper by F. E. Terman, president of the Institute and head of the electrical engineering department of Stanford University.

The advantages of hum reduction, lower distortion, better frequency response, less cross modulation, and higher stability that may be obtained through the use of negative feedback in radio- and audio-frequency amplifiers were pointed out. These advantages are obtained at the price of more accurate design, some complication in circuits, and the provision for greater amplification because of the reduction in over-all gain resulting from negative feedback.

The phase shift of the ordinary resistance-coupled audio-frequency amplifier without any allowance for bias or screen-grid networks is 90 degrees on either end of the response curve. With bias- and screen-grid networks, these shifts are usually greater than 90 degrees and a two-stage amplifier tends to oscillate. Two stages can be used if care is taken in regard to these phase-shifting elements. If distributed constants and lattice networks are avoided, a minimum phase shift can be expected for a specified transmission characteristic.

To prevent oscillation up to a certain frequency, special attenuating networks must be placed in the feedback loop to make the actual response curve of a number of stages in a transmitter approach the calculated curve. This means that to utilize feedback in any number of stages without oscillation requires an extension of the response curve beyond its normal useful range.

Circuits and methods of producing a desired attenuation or response characteristic were shown.

June 9, 1941, J. M. McDonald, chairman, presiding.

Los Angeles

The chief engineer of Walt Disney Productions, W. E. Garity, and J. N. A. Hawkins, chief transmission engineer of that organization, presented a paper on "Fantasound Recording and Reproducing Equipment."

Mr. Garity discussed the factors which affected the studio's decision to engage in the development of new methods of sound reproduction. The symphonic nature of the program material to be used in "Fantasia" was particularly unfitted for the limitations of monaural reproduction.

As the problems of picture perspective had been an important research project for many years in the Disney studios, it was logical that some thought should be given to sound perspective. The initial research produced such interesting possibilities that finally several hundred thousand dollars were spent in developing equipment and operating procedure for twelve "Fantasia" road shows.

Mr. Hawkins presented a description of the "Fantasia" recording and reproducing equipment. The deficiencies of commercial monaural sound systems were first presented. The differential-function network used to feed single-channel program material to one, two, or three reproducing channels with a constant level and smooth transitions was then described. A block diagram of the Fantasound reproducer was then discussed briefly. The variable-gain amplifier, a bias-controlled variolosser capable of a 50-decibel transmission change, was discussed. The log-log tone rectifier also was described together with the quad film phonograph and the quad optical printer.

This meeting was held jointly with the Pacific Coast section of the Society of Motion Picture Engineers, and was presided over by J. G. Frayne, chairman of that group. The speakers were introduced by W. W. Lindsay, Jr., chairman of the Institute section.

April 10, 1941.

Pittsburgh

The annual meeting of the Pittsburgh Section was in the form of a banquet. As a result of the election of officers, P. N. Bossart of the Union Switch and Signal Company was named chairman; J. G. O'Shea of the Midwest Radio Corporation was elected vice chairman; and Ralph Overholt, Jr., of the Union Switch and Signal Company was named secretary-treasurer.

Rochester

"Television Today" was the subject of a paper by D. G. Fink, associate editor of *Electronics* at a meeting held jointly by the Buffalo-Niagara, Emporium, and Rochester Sections of the Institute at Olean, N. Y.

April 25, 1941, L. C. F. Horle, presiding.

"The Electron Microscope" was the subject of a paper by A. L. Schoen, physicist of the research laboratories of the Eastman Kodak Company.

This development has extended the range of magnification and resolution considerably beyond that attainable with the optical microscope. A few electron microscopes are in operation in this country, and pictures showing magnifications of 100,000 times and a resolution of 100 Angstroms are appearing in the literature. The principle of operation and general constructional details were described. Some of the recent discoveries resulting from use of the electron microscope in the fields of photography, biology, and industrial research were described.

This was the annual meeting and H. J. Klumb of the Rochester Gas and Electric Company was elected chairman; A. L. Schoen of the Eastman Kodak Company was made vice chairman; and O. L. Angevine, Jr., of the Stromberg-Carlson Telephone Manufacturing Company was designated secretary-treasurer.

May 15, 1941, H. C. Sheve, chairman, presiding.

Washington

F. M. Ryan of the department of operation and engineering of the American Telephone and Telegraph Company presented a paper on "Coastal-Harbor Stations of the Bell System."

A history of the coastal-harbor service development was first presented and was concluded with a description of the present-day installations and their operating characteristics. Descriptions were given of stations on both coasts of the United States and the Gulf of Mexico and included the installation in the telephone exchange. Methods of handling communications between ships and receiving points were described.

The codan relay (carrier-operated device, antinoise) which is a vital part of the system was clearly shown and its operation described. Although the paper dealt principally with the land transmitting and receiving stations, in the discussion which followed it, much information on ship installations was presented.

The licensing and functions of these stations under the present regulations of the Federal Communications Commission were described by E. M. Webster, who is in charge of this work on the Commission staff.

June 9, 1941, M. H. Biser, chairman, presiding.

Membership

The following admissions to Associate grade were approved by the Board of Directors.

Ahmed, W., 11 Tiljala Rd., Circus, Calcutta, India

Barnard, R. E., 1055 S. Plymouth Blvd., Los Angeles, Calif.

Bauer, J. A., 23 Central Ave., Cheltenham, Pa.

Bechtold, I. C., 3445 Oakwood Ter. N.W., Washington, D. C.

Beitman, M. N., 3727 W. 13th St., Chicago, Ill.

Benham, T. A., 33 Simpson Rd., Ardmore, Pa.

Bereskin, A. B., University of Cincinnati, Cincinnati, Ohio

Breeden, W., 2281 Moreno Dr., Los Angeles, Calif.

Brown, S. H., Radio Station WRAL, Raleigh, N. C.

Buckbee, J. A., Farnsworth Television & Radio Corp., Fort Wayne, Ind.

Buehler, M. E., 309 W. 14th St., Marion, Ind.

Cary, H. H., 815 N. Hidalgo Ave., Alhambra, Calif.

Chow, B., 131 Hudson Ave., Red Bank, N. J.

Doyle, W. J., 742 Kentucky, Vallejo, Calif.

Easley, R. B., 2467 Olive St., Huntington Park, Calif.

Epperson, W., 35 Seaford Ave., Essex, Baltimore, Md.

Frederick, J. R., Physics Department, University of Michigan, Ann Arbor, Mich.

Fredine, E. L., 207-23rd St. Dr., S.E., Cedar Rapids, Iowa

Geddes, B. B., 111 Allen Rd., Yorktowne Village, Md.

Gorman, D. P., c/o KGEZ, Kalispell, Mont.

Hammann, W. A., RCA Manufacturing Company, Bloomington, Ind.

Herweh, A. C., Swift Hall, University of Cincinnati, Cincinnati, Ohio

Howell, A. H., 349 Harvard St., Cambridge, Mass.

Hudson, C., 1215 Mahanoy Ave., Mahanoy City, Pa.

Ingalls, C. E., 19 E. Park Ave., Pittsford, N. Y.

Jones, W. G., Vanderbilt University, Nashville, Tenn.

Kahl, E., 220 W. 4th St., Emporium, Pa.

Katzoff, P., 424 Pulaski St., Brooklyn, N. Y.

Kent, R. C., Electrical Engineering Building, Iowa City, Iowa

Kesecker, K. S., 2828 Myrtle Ave., Washington, D. C.

Levitt, H. J., Federal Telegraph Company, 200 Mt. Pleasant Ave., Newark, N. J.

Libby, L. L., 10 Summit St., East Orange, N. J.

McLoughlin, R. P., 9-772 La Plata, F.C.S., Argentina

McWhan, B., Bell Telephone Laboratories, Inc., 463 West St., New York, N. Y.

Miller, G. N., Hq. Det., 2nd Battalion, 69th A.R., Fort Knox, Ky.

Mins, L. E., Murray Hill Hotel, 112 Park Ave., New York, N. Y.

Mori-Casucci, A. T., c/o Radio Club Argentino, Rivadavia 2170, Buenos Aires, Argentina

Morris, I., Tucuman 569, General Roca, Rio Negro, Argentina

Murray, C. W., Eastern Air Command, Hq. R.C.A.F., Halifax, N. S., Canada

Neitzert, C., Stevens Institute of Technology, Hoboken, N. J.

Osborn, R. E., 1420 E. Rudisill Blvd., Fort Wayne, Ind.

Page, C. H., 9209 Saybrook Ave., Silver Spring, Md.

Porteous, J. W., University of Alberta, Edmonton, Alta., Canada

Quilty, H. E., 50 Brighton Blvd., Bondi Beach, Sydney, N.S.W., Australia

Rabinoff, C. V., 5612 Sunset Blvd., Hollywood, Calif.

Root, C. S., General Electric Company, Bridgeport, Conn.

Sanders, M. A., Allen B. DuMont Laboratories, Inc., 2 Main Ave., Passaic, N. J.

Schlaudecker, R. A., 3127 West Ridge Rd., Erie, Pa.

Seal, P. M., R.R. 10, Lafayette, Ind.

Spong, D. C., Signal Office, Fort Snelling, Minn.

Starr, E. C., 2730 Arnold Way, Corvallis, Ore.

Stephenson, H. R., 229 N. Grey St., Indianapolis, Ind.

Wentworth, A. M., 89 Johnswood Rd., Roslindale, Mass.

Westcott, V. C., Raytheon Manufacturing Company, 190 Willow St., Waltham, Mass.

Works, A., 2701—14th St. N.W., Washington, D. C.

Wroblewski, W. L., 1067 Davis Ter., Schenectady, N. Y.

Contributors

John E. Benson* (A'39) was born at Sydney, Australia, on March 7, 1911. He received the B.Sc. degree from the University of Sydney in 1932, the B.E. degree in mechanical and electrical engineering in 1934, and Dip.Ed. in 1935. In December, 1934, he joined the staff of Amalgamated Wireless (Australasia) Ltd., in charge of frequency-measuring equipment in the research laboratories. From 1936 to the present he has been engaged on development and production of piezoelectric crystals and associated equipment for frequency measurement and control. He is an Associate Member of the Institution of Engineers (Australia) and a Graduate of the Institution of Electrical Engineers (London).

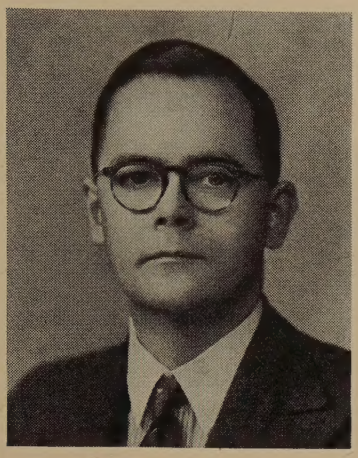

JOHN E. BENSON

* Paper appeared in the April, 1941, issue of the PROCEEDINGS.

❖

Cledo Brunetti (A'37) was born on April 1, 1910, at Virginia, Minnesota. He received the B.E.E. degree from the University of Minnesota in 1932 and the Ph.D. degree in 1937. From 1932 to 1936 he was a Teaching Fellow in the department of electrical engineering at the University of Minnesota and from 1936 to 1937, an instructor. From 1937 to 1939 Dr. Brunetti was an instructor in electrical engineering at Lehigh University; since 1939 he has been assistant professor of electrical engineering. During the summers of 1939 and of 1940 he was a research associate at the radio laboratory, National Bureau of Standards, Washington, D. C. Since May, 1941, he has been on leave of absence from Lehigh University and is a radio physicist at the National Bureau of Standards, Washington, D. C. He is a member of Tau Beta Pi, Eta Kappa Nu, and Sigma Xi.

CLEDO BRUNETTI

❖

Geoffrey Builder* (A'32) was born at Cue, Western Australia, on June 21, 1906. He received the B.Sc. degree from the University of Western Australia in 1928, and the Ph.D. degree from London University in 1933. From 1928 to 1930 he was an observer at the Watheroo, Western Australia, Magnetic Observatory of the Carnegie Institution of Washington. During 1931 and 1932 he was engaged in research work in radio physics at the University of London, and during 1933 and 1934 was a research physicist of the Australian Radio Research Board. From 1934 to date he has been in charge of the research and development laboratories of Amalgamated Wireless (Australasia) Ltd. Dr. Builder is a Fellow of the Institute of Physics, London, a Fellow of the Institution of Radio Engineers (Australia), and an Associate member of the Institution of Engineers (Australia).

GEOFFREY BUILDER

* Paper appeared in the April, 1941, issue of the PROCEEDINGS.

❖

C. F. Edwards was born at Greenfield, Ohio, on April 21, 1906. He received the B.A. degree in physics from Ohio State University in 1929 and the M.A. degree from the same university in 1930. From 1930 to 1934 he was with the American Telephone and Telegraph Company engaged in short-wave transoceanic transmission studies. Since 1934 Mr. Edwards has been at the Holmdel radio laboratory of the Bell Telephone Laboratories where these studies have been continued.

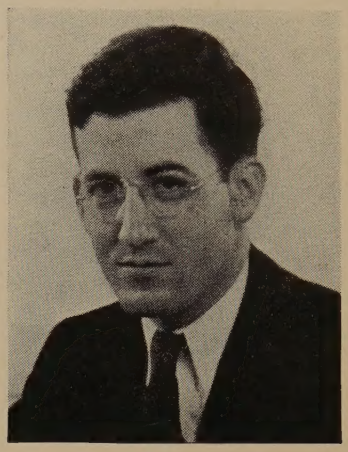

C. F. EDWARDS

❖

Donald G. Fink (A'35) was born at Englewood, New Jersey, on November 8, 1911. He received the B.Sc. degree in electrical engineering (communications) in 1933 from the Massachusetts Institute of Technology. During 1933–1934 he served as a member of the staff of the electrical engineering and geology departments at M.I.T. In 1934 Mr. Fink joined the editorial staff

DONALD G. FINK

❖

of *Electronics*, where, in 1937, he was made managing editor. At the present time he is on leave of absence from *Electronics* and is a research associate at the radiation laboratory of Massachusetts Institute of Technology. Mr. Fink is a member of Tau Beta Pi, Sigma Xi, and Eta Kappa Nu, and a Fellow of the Radio Club of America.

KARL G. JANSKY

❖

Harry F. French was born on November 7, 1886, at Plymouth, New Hampshire. He received the B.S. degree in chemical engineering from the University of New Hampshire in 1908. Since 1910 he has been research chemist with the National Carbon Company, Inc.

❖

Karl G. Jansky (A'28-M'34) was born on October 22, 1905, at Norman, Oklahoma. He received the A.B. degree in 1927, and the M.A. degree in 1936 from the University of Wisconsin. Since 1928 he has been with the Bell Telephone Laboratories.

❖

C. K. JEN

C. K. Jen (A'29) was born on August 15, 1906, in China. He received the B.S. degree in electrical engineering in 1928 from the Massachusetts Institute of Technology, the M.S. degree in 1929 from the University of Pennsylvania, and the Ph.D. degree in physics in 1931 from Harvard University. He was an assistant in physics from 1930 to 1932 and an instructor from 1932 to 1933 at Harvard University. Dr. Jen was a professor in physics from 1933 to 1934 at the National Shantung University, China. From 1934 to 1937 he was a professor in physics and electrical engineering at the National Tsing Hua University, China. From 1937 to date he has been a professor and the director of the Radio Research Institute, National Tsing Hua University, Kunming, China.

❖

Nathan Marchand (A'39) was born in Canada on June 20, 1916. In 1937 he received the B.E.E. degree from the College of the City of New York and the M.S. degree in electrical engineering from Columbia University in 1941. From 1937 to 1938 Mr. Marchand was service engineer for the eastern district of the Knapp-Monarch

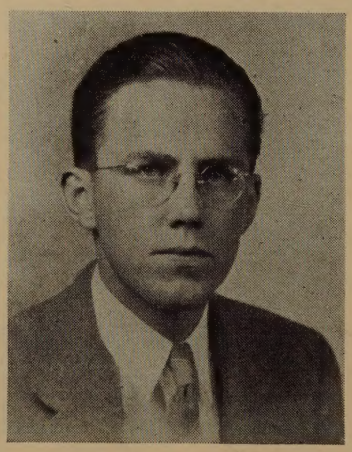

ERIC WEISS

Corporation. In 1938 he became associated with the National Television Corporation while the Radio Television Institute was being formed. From 1939 to 1941 Mr. Marchand was chief instructor of the Radio-Television Institute. Since May, 1941, he has been with the research group of the Federal Telegraph Company. He is a member of Tau Beta Pi.

❖

Eric Weiss received the B.S. degree in electrical engineering from Lehigh University in 1939 and the M.S. degree from the same school in 1940. He was employed by the RCA Manufacturing Company until the end of 1940 and since then has been with the Naval Ordnance laboratory in Washington, D. C. He is a member of Tau Beta Pi and Phi Beta Kappa and an associate member of Sigma Xi.

❖

J. D. Schantz (S'33–A'35) was born at Schaefferstown, Pennsylvania, on August

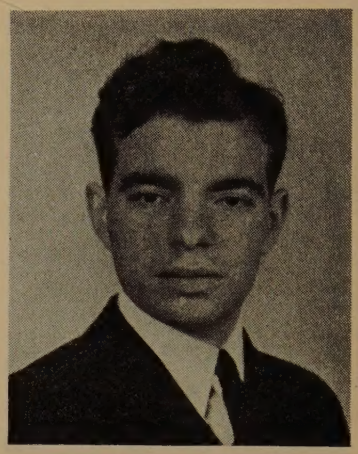

NATHAN MARCHAND

10, 1910. After attending the United States Naval Academy for one and one-half years, he enrolled at Gettysburg College where he received the B.S. degree in electrical engineering in 1932. There followed a year of graduate work at Stanford University and another at the University of Michigan where he received the M.S.E. degree in 1934. In 1934 he entered the research division of the RCA Manufacturing Company in Camden, N. J. Since 1936 he has been a member of the engineering staff of Farnsworth Television & Radio Corporation, where he is engineer in charge of the television terminal equipment section. He has also pursued graduate studies at the University of Pennsylvania and is an associate member of Sigma Xi.

❖

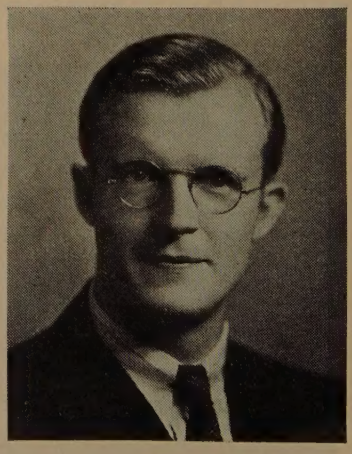

J. D. SCHANTZ